OPTIMISATION ON XYLNASE PRODUCTION FROM *Aspergillus niger* VIA STATISTICAL TOOL

TAN CHIA ZHI

MASTER OF ENGINEERING SCIENCE

FACULTY OF ENGINEERING AND GREEN TECHNOLOGY
UNIVERDITI TUNKU ABDUL RAHMAN
JANUARY 2026

OPTIMISATION ON XYLANASE PRODUCTION FROM *Aspergillus niger* VIA STATISTICAL TOOL

By

TAN CHIA ZHI

A dissertation to the Department of Petrochemical Engineering,
Faculty of Engineering and Green Technology,
Universiti Tunku Abdul Rahman,
in partial fulfilment of the requirements for the degree of
Master of Engineering Science
January 2026

ABSTRACT

OPTMISATION ON XYLANASE PRODUCTION FROM *Aspergillus niger* VIA STATISTICAL TOOL

TAN CHIA ZHI

Nowadays, the biotechnology potential of xylanase enzyme in a range of industrial processes has drawn increasing attention. In the present study, the filamentous fungus *Aspergillus niger* was utilized for xylanase production inder submerged fermentation conditions. There are three main primary phases that will be discussed in the discussion section. Initial time-course analysis revealed that both optimum mycelial dry cell weight and xylanase activity peaked between Day 3 and Day 5, establishing this as the optimal fermentation period for enzyme productivity. To further enhance xylanase yield, ten variables were selected for screening using Plackett-Burman Design (PBD). Results from the PBD screening revealed that pH, temperature, xylan, NH_4NO_3, and K_2HPO_4 positively influenced xylanase production, while incubation time and $CaCl_2$ had negative effects. The significance of each variable was further verified using a Pareto chart, which graphically represented the standardized effects of different parameters on xylanase activity at a significance level of $p < 0.05$. According to the analysis, pH and $CaCl_2$ emerged as the most significant variables affecting xylanase production by *A. niger*. Therefore, optimisation via Central Composite Design (CCD) focused on these two key variables. Statistical analysis using ANOVA confirmed the robustness of the quadratic model generated, with a

model F-value of 27.13 and a p-value of 0.0002, signifying strong model significance. The model also demonstrated excellent predictive accuracy, evidenced by an adjusted R^2 of 0.9159 and a predicted R^2 of 0.7198. Furthermore, the lack-of-fit test yielded a non-significant p-value of 0.3160, validating the model's adequacy. Optimised conditions for maximum xylanase production were determined to be pH 6.5 and a $CaCl_2$ concentration of 0.931 g/L, with other parameters maintained at central levels. Validation experiments under these conditions yielded a maximum xylanase activity of 1.7569 U/mL, closely matching the model prediction.

ABSTRAK

OPTIMISASI PENGHASILAN XILANASE DARIPADA *Aspergillus niger* MELALUI ALAT STATISTIK

TAN CHIA ZHI

Pada masa kini, potensi bioteknologi enzim xilanase dalam pelbagai proses perindustrian telah menarik perhatian yang semakin meningkat. Dalam kajian ini, kulat berbenang *Aspergillus niger* telah digunakan untuk pengeluaran xilanase di bawah keadaan fermentasi terendam. Terdapat tiga fasa utama yang akan dibincangkan dalam bahagian perbincangan. Analisis masa awal mendedahkan bahawa berat sel kering miselium optimum dan aktiviti xilanase mencapai kemuncak antara Hari ke-3 dan Hari ke-5, menetapkan tempoh penapaian ini sebagai tempoh optimum untuk produktiviti enzim. Untuk meningkatkan hasil xilanase, sepuluh pembolehubah telah dipilih untuk saringan menggunakan Reka Bentuk Plackett-Burman (PBD). Keputusan saringan PBD mendedahkan bahawa pH, suhu, xilan, NH_4NO_3, dan K_2HPO_4 memberi kesan positif terhadap pengeluaran xilanase, manakala masa inkubasi dan $CaCl_2$ memberi kesan negatif. Kepentingan setiap pembolehubah disahkan lagi menggunakan carta Pareto, yang menggambarkan secara grafik kesan standardisasi pelbagai parameter terhadap aktiviti xilanase pada tahap kepentingan $p < 0.05$. Menurut analisis, pH dan $CaCl_2$ muncul sebagai pembolehubah paling penting yang mempengaruhi pengeluaran xilanase oleh *A. niger*. Oleh itu, pengoptimuman melalui Reka Bentuk Komposit Pusat (CCD)

memberi tumpuan kepada dua pembolehubah utama ini. Analisis statistik menggunakan ANOVA mengesahkan keteguhan model kuadratik yang dijana, dengan nilai F model 27.13 dan nilai p 0.0002, menandakan kepentingan model yang tinggi. Model ini juga menunjukkan ketepatan ramalan yang cemerlang, dibuktikan oleh R^2 disesuaikan sebanyak 0.9159 dan R^2 diramalkan sebanyak 0.7198. Selain itu, ujian ketidakcocokan menunjukkan nilai p tidak signifikan iaitu 0.3160, mengesahkan kecukupan model tersebut. Kondisi optimum untuk pengeluaran xilanase maksimum ditentukan pada pH 6.5 dan kepekatan $CaCl_2$ sebanyak 0.931 g/L, dengan parameter lain dikekalkan pada tahap tengah. Eksperimen pengesahan di bawah kondisi ini menghasilkan aktiviti xilanase maksimum 1.7569 U/mL, yang hampir menepati ramalan model.

ACKNOWLEDGEMENT

I would like to give millions of thanks and appreciation to everyone who had contributed to the successful completion of this project. Firstly, I would like to express my gratitude to my research, Ts. Dr. Teoh Yi Peng, Dr. Lee Kok Chang and Ts. Dr. Kunasundari Balakrishnan (Universiti Malayisa Perlis, UniMAP) for giving me physically and mentally supports that helped me get through all this difficult time and completed my study. Besides, I would like to thank my parents who love me and always support me unconditionally in doing what I like. I would like to thank all the lab staffs in department of biological science for helping me when I needed helps in anytime. I would like to thanks to all my seniors and friends who had helped and given me encouragement, advice and guidance in completing the research. I am glad to study in UTAR, met all the people that are so kind. It is my pleasure to have all of you in my life. Lastly, I would like to thank UTAR for providing financial support (UTARRF) and Research Scheme Scholarship (RSS) to let me finish my master study.

DECLARATION

I hereby declare that the dissertation is based on my original work except for quotations and citations which have been duly acknowledged. I also declare that it has not been previously or concurrently submitted for any other degree at UTAR or other institutions.

Tan Chia Zhi

Date: 5/1/2026

APPROVAL SHEET

This dissertation entitled "**OPTIMISATION ON XYLANASE PRODUCTION FROM *Aspergillus niger* VIA STATISTICAL TOOL**" was prepared by TAN CHIA ZHI and submitted as partial fulfilment of the requirements for the Master of Engineering Science at Universiti Tunku Abdul Rahman.

Approved by:

(Ts. Dr. Teoh Yi Peng)
Date: 5/1/2026
Supervisor
Department of Petrochemical Engineering
Faculty of Engineering and Green Technology
Universiti Tunku Abdul Rahman

(Dr. Lee Kok Chang)
Date: 5/1/2026
Co-supervisor
Department of Biological Science
Faculty of Science
Universiti Tunku Abdul Rahman

(Ts. Dr. Kunasundari Balakrishnan)
Date: 5/1/2026
Co-supervisor
Faculty of Chemical Engineering and Technology
Universiti Malaysia Perlis

FACULTY OF ENGINEERING AND GREEN TECHNOLOGY

UNIVERSITI TUNKU ABDUL RAHMAN

Date: 5/1/2026

PERMISSION SHEET

It is hereby certified that TAN CHIA ZHI (ID No: 20AGM00800) has completed this thesis entitled "OPTIMISATION ON XYLANASE PRODUCTION FROM *Aspergillus niger* VIA STATISTICAL TOOL" under the supervision of Ts. Dr. Teoh Yi Peng (Supervisor) from the Department of Chemical Science, Faculty of Science, Dr. Lee Kok Chang (Co-Supervisor)* from the Department of Biological Science, Faculty of Science and Dr. Kunasundari Balakrishnan (Co-Supervisor)* from the Faculty of Faculty of Chemical Engineering and Technology (UniMAP). I hereby give permission to the University to upload the softcopy of my thesis in pdf format into the UTAR Institutional Repository, which may be made accessible to the UTAR community and public.

Your truly,

(Tan Chia Zhi)

TABLE OF CONTENTS

LIST OF TABLES

LIST OF FIGURES

LIST OF SYMBOLS

R^2	Coefficient of determination
°C	Degree celcius
U	Enzyme unit
g	Gram
L	Litre
mg	Milligram
mL	Millilitre
M	Molarity
%	Percentage
rpm	Round per minute
v/v	Volume to volume
w/v	Weight to volume
%wt	Weightage
M	Molarity
nm	Nanometer

LIST OF ABBREVIATIONS AND NOMENCLATURE

A. awamori	*Aspergillus awamori*
A. niger	*Aspergillus niger*
A. niveus	*Aspergillus niveus*
A. ochraceus	*Aspergillus ochraceus*
A. oryzae	*Aspergillus oryzae*
A. foetidus	*Aspergillus foetidus*
DoE	Design of Experiment
PBD	Plackett-Burman Design
RSM	Response Surface Methodology
CCD	Central Composite Design
BBD	Box-Behnken Design
et al.	(*et alia*): and others
etc	(*etceteros*): and other things
OFAT	One-Factor-At-a-Time
PDA	Potato Dextrose Agar
RSM	Response Surface Methodology
S. cerevisiae	*Saccharomyces Cerevisiae*
SmF	Submerged Fermentation
SSF	Solid State Fermentation
sp.	species
SD	Standard Deviation
$CaCl_2$	Calcium chloride
$CoCl_2•6H_2O$	Cobalt chloride hexahydrate
DNS	3,5-dinitrosalicylic acid
$FeSO_4•7H_2O$	Ferrous sulpate heptahydrate
HCl	Dilute hydrochloric acid
K_2HPO_4	Dipotassium hydrogen phosphate
$KNaC_4H_4O_6•4H_2O$	Sodium potassium tartrate solution
$MgSO_4•7H_2O$	Magnesium sulphate heptahydrate
$MnSO_4•4H_2O$	Manganese (II) sulfate tetrahydrate
Na_2SO_3	Sodium sulphite

NaOH	Dilute sodium hydroxide
NH_4NO_3	Ammonium nitrate
$ZnSO_4•7H_2O$	Zinc sulfate heptahydrate
2D	2-dimensional
3D	3-dimensional
UV-vis	UV – Visible Spectrophotometer

CHAPTER 1

INTRODUCTION

1.1. Background of Study

Xylanase, also known as endo-1,4-xylanohydrolase (EC 3.2.1.8), is a hydrolytic enzyme that catalyzes the hydrolysis of xylan to the monomeric unit, such as xylo-oligosaccharides and pentose sugar. In the plant cell, xylan is a major constituent as the second most abundant polysaccharide after the cellulase in the lignocellulosic wastes (Bajpai, 2014a; Basit *et al*., 2021). Hence, xylanase enzymes have wide industrial applications, for example, biobleaching of wood pulp, papermaking, food and beverage manufacture, animal nutrition, and production of bioethanol. Due to their biotechnology applications, the interest has increased and has grown tremendously in recent years. Moreover, they can avoid the need for chemical use, lowering production costs and minimizing environmental pollution. In the production of xylanase enzymes, microorganisms, such as bacteria, fungi, actinomycetes, and yeast, are chosen as the best option since they possess the rich sources of xylanases (Bajar *et al*., 2020; Bajpai, 2014a; Mujtaba *et al*., 2023).

In recent years, filamentous fungi have been employed for xylanase production. From the research, there is evidence that the filamentous fungal species, especially the *Aspergillus* species, are excellent producers of xylanases

compared with bacteria and other microbes. This is because filamentous fungi can produce a high level of xylanase enzyme in the culture medium compared with other microorganisms. In this study, one of the objectives is to use the filamentous fungi, which is *Aspergillus niger* (*A. niger*) as the producer to produce the xylanase. There was evidence that proves the *A. niger* can degrade the lignocelluloses efficiently in the previous study. It can also grow effectively in a culture medium (Zhang *et al*., 2024). The culture medium, which is the Mandels and Sterburg's basal salt (MSBS) medium was used in this study.

Due to the xylanase enzyme used in variety of the industrial application, it has been increased the interest of researchers in the lab and the industrial field. There are many studies about the large-scale production of the xylanase enzymes were carried out through the cultivation systems. Commonly, there are two types of cultivation systems used to produce the xylanase enzymes, such as submerged fermentation (SmF) and solid-state fermentation (SSF) (Jonathan *et al*., 2021). SmF is defined as the growth of microorganism in liquid substrate, such as mineral salt medium, while the SSF involves solid substrate that act as the energy source, with no free-flowing water. SSF has many advantages over the SmF, for example, such as a higher production rate, simple fermentation equipment, less effluent generation, etc.(Renge *et al*., 2012). However, SSF is still not recommended in industrial uses due to its complex product purification process, long fermentation period, heterogeneity of fermentation media, and enzyme loss in the solid residues during process. Therefore, SmF method is more widely practiced due to its shorter fermentation period, easy of process control and parameter measurement, low production cost, higher enzyme production yield,

etc. Moreover, SmF also provides lower contamination risk for enzyme production (Martínez-Mira *et al*., 2025).

The production of xylanase can be screened and optimised using an experimental design statistical approach using a response surface methodology (RSM) to reduce the production cost. In the previous study, there has been stated that the cost of enzyme production is the basic goal in the research on the industrial application (Cao *et al*., 2008). Several factors, including incubation temperature, medium pH, agitation speed, incubation time, and the nutritive components of the medium, can affect the production of xylanase enzyme during the fermentation (Cunha *et al*., 2018). In the present study, a design of experiment (DOE) including screening step and optimisation, is used to determine the MSBS medium and to evaluate selected factors under submerged fermentation for optimal xylanase production.

To achieve the optimal parameters for xylanase production effectively, the screening of factors is necessary by using Plackett-Burman Design (PBD). PBD is a statistical tool to screen 'n' variables in just 'n+1' experiment as a preliminary step in optimisation process since the interaction effect cannot be determined (Cunha *et al*., 2018; Maan *et al*., 2016). Consequently, the selected factors were further optimised for the planned statistical optimisation of xylanase production of an *A. niger* under submerged fermentation with a Central Composite Design (CCD) based response surface methodology (RSM) (Bhardwaj *et al*., 2017; Cunha *et al*., 2018).

In this study, we used the Central Composite Design (CCD), acts as a statistical method to characterize the xylanase enzyme from the *A. niger* which is cultivated in the liquid medium. CCD is used to optimise the process by controlling the optimal conditions for the enzyme production. The CCD method has been proven that it is an efficient way to evaluate the effect of independent variables without performing time- and labor-intensive one-factor-at-a-time experiments (Siwach *et al*., 2024; Rashid *et al*., 2024).

1.2. Problem Statement

Xylanase enzyme is an important hydrolytic enzyme that is used for hydrolysis of xylan to xylose or xylo-oligosaccharides (Sohpal *et al*., 2010). For example, the xylanase enzyme is used to eliminate the hemicellulose in the plant cell wall since it is one of the major structural components (Kalpana and Devi Rajeswari, 2015). However, there is a problem that the massive production cost for the xylanase is one of the factors that can limits the uses of the enzyme in industrial application and determining the economics of a process (Kalpana and Devi Rajeswari, 2015; Cao *et al*., 2008; Betini *et al*., 2009). This is because the enzyme production requires the high cost invested, the expensive media, the processes of purification, and low selectivity. In order to reduce the production cost, optimisation was implemented to create an ideal condition which can decrease the production cost for the enzyme (El-Gendi *et al*., 2023; Patel and Amaresan, 2022).

Microbes, such as bacteria, fungi, actinomycetes and yeast can produce the xylanase enzyme. By comparing among the microbial sources, filamentous fungi are more suitable and applied in the production of xylanase due to its level of xylanase enzyme is higher than the bacteria and yeasts (Bajpai, 2014b). In this study, the fungi, which is *A. niger* will be used as the microbial source since it is an excellent producer of extracellular xylanase enzyme. Also, it can be used for debranching of the substituted xylan by using several auxiliary enzymes which is produced by itself (Modi *et al*., 2011).

Besides, the parameters of culture conditions such as temperature, pH, moisture content, inoculum size, the period of incubation, and rate of agitation can affect the production of xylanases strongly. Furthermore, the nutritive components can also affect the xylanase production since the growth of microorganisms mostly dependent on the nutrient substrate, such as carbon and nitrogen source (Kalpana and Devi Rajeswari, 2015). Therefore, the screening and optimisation of the process is vital to improve both activity of xylanase and volumetric productivity of the general metabolites (Uday *et al*., 2016). But there is a limitation for development of best cultural conditions and nutritive components due to the microorganism used. The optimisation condition of *A. niger* to produce the xylanase is limited. Therefore, in order to improve the xylanase production, several parameters are needed to study and improve the process for build a friendly environment for good fermentation (Cao *et al*., 2008). In this study, several parameters including temperature, pH, and incubation time and agitation rate are concentrated in optimisation process.

On the other hand, screening of culture conditions and nutritive components is very important step in this study since they can influnce the xylanase production. Therefore, in the screening part, the determination of the optimal parameters is required by using a statistical tool, which is Plackett-Burman Design (PBD) for efficient production. This statistical tool can be used for the intial step of optimisation process. Thus, several parameters including cultural conditions and nutritive components were be screened for maximum production of xylanase (Maan *et al*., 2016). Then, Central Composite Design (CCD) is then employed to optimise the parametes which can influence on xylanase production (Xu *et al*., 2008). Based on its reliability, this design is selected in order to identify the seperate and combined effect of various factors through a minimum number of experiments (Salihu *et al*., 2015).

1.3. Objectives

i. To construct the time course profile for the growth and xylanase productivity using *Aspergillus niger.*
ii. To screen the chemical and physical parameters on xylanase production through Plackett-Burman design (PBD).
iii. To optimise the chemical and physical parameters on xylanase production through Central Composite Design (CCD).

1.4. Scope Study

This research is to study the effect of chemical and physical parameters on optimisation of the xylanase production from the filamentous fungi, *A. niger* by using the PBD and CCD statistical methods. Several chemical and physical parameters are selected which are applied in the fermentation growth medium. Growth curves for the carbon sources is plot (xylose concentration against time). The screening of the chemical and physical parameters that can affect the xylanase production is undergone by using the PBD method. After the screening step, several of the chemical and physical parameters will be selected and optimise the production of the xylanase through CCD. The PBD and CCD are designed by using a software, which is Design Expert Version 11. The effect of chemical and physical parameters was determined through the enzymatic activity and xylanase production.

CHAPTER 2

LITERATURE REVIEW

2.1. Xylan

Lignocellulosic biomass is a complex biopolymer that mainly composed hemicellulose, cellulose and lignin. Moreover, it is also containing other components in small quantities, such as acetyl group, minerals and phenolic substituents. At about 19–45% by weight, hemicellulose, a macromolecule made of various sugars, is the second most prevalent substance in plant cell walls. Hemicellulose is comprised of several groups of carbohydrates, such as xylan, galactomannan, glucuronoxylan, arabinoxylan, glucomannan, and xyloglucan. Hemicellulose plays a role in the plant cell wall which provides the structural strength by forming a complex network of bonds with linking cellulose fibres into microfibrils and cross-linking with lignin (Isikgor and Becer, 2015; Lee *et al*., 2014). Figure 2.1 shows the schematic diagram foe the structure of the plant cell wall with three main components including hemicellulose, cellulose and lignin.

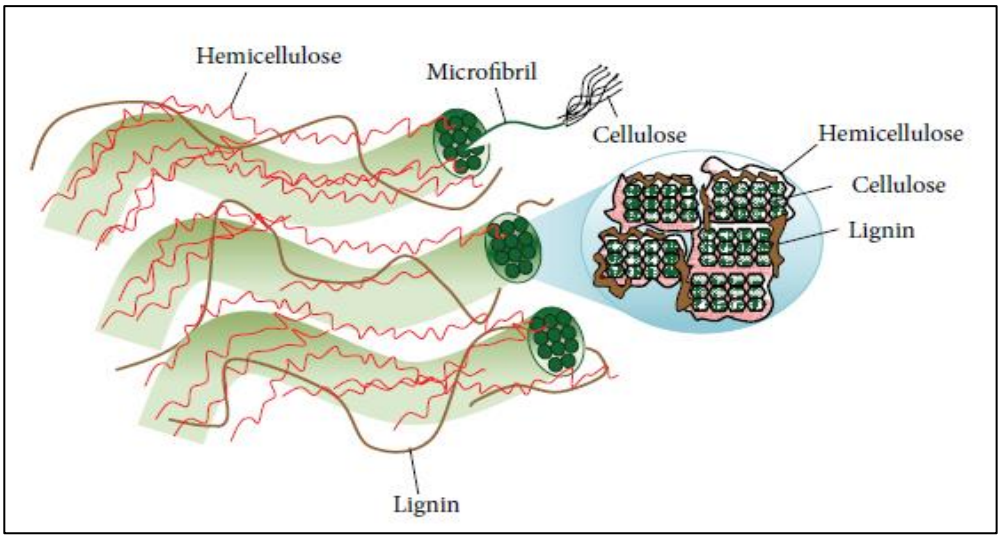

Figure 2.1: Structure of plant cell wall with three main components (hemicellulose, cellulose, lignin) (adapted from Lee *et al*., 2014).

Xylan is a major structural polysaccharide, which is acting as the substrate of the xylanases enzyme that can be found in the plant call walls. Xylan can make up over 30% of the dry weight of plant cell walls. Xylan is composed of an equatorial-bound framework of β-1,4-linked xylopyranosyl residues and a diverse array of substituents, such as arabinose, acetyl groups, glucuronic acids, ferulic acid, and p-coumaric acid. The main chain of xylan resembles that of cellulose, comprising D-xylose instead of D-glucose; however, its structure differs, with variations including linear 1,4-β-linked polyxylose sugars other than D-xylose. Furthermore, lignin and polysaccharides interact with xylan via covalent and non-covalent bonds, respectively.

In the secondary cell wall, xylan and lignin are connected by a variety of covalent bonds. These covalent interactions include glycosidic bonds linking xylopyranosyl and p-coumaric acid, as well as ester bonds connecting arabinofuranosyl residues with either p-coumaric acid or ferulic acid. Feruloyl

residues, which are recognized for their role as linking units between lignin and xylan, are included in arabinoxylans. The distribution pattern of xylan's substituents has an impact on various functional characteristics, including its solubility, interactions with other polymeric cell wall components, enzyme degradability, and behavior in solution. Additionally, the complexity of materials that include xylan is affected by the chemical structure of xylan; these materials might consist of numerous xylan polymers that share structural similarities yet vary in degrees of significance (Basit *et al*., 2021). Figure 2.2 shows a particular xylanolytic enzyme attacks the bonds in the xylan's schematic structure, causing the xylan to completely hydrolyze into its component monomeric units.

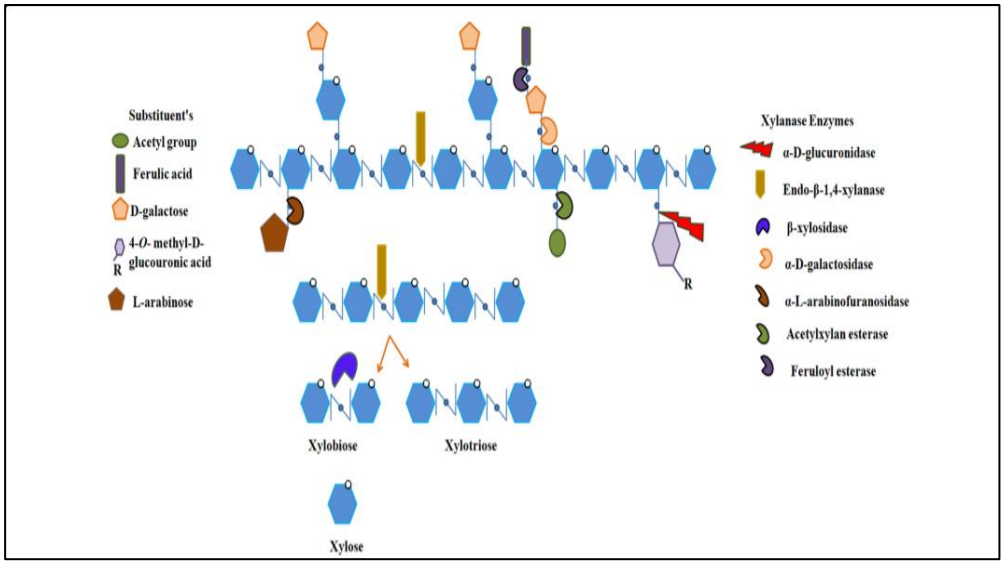

Figure 2.2: Structure of xylan showing bonds which are attacked by specific xylanolytic enzyme for complete hydrolysis of xylan to its constituents (adapted from Bhardwaj *et al*., 2019).

The xylan can be divided into four major families.

i. Arabinoxylans with only single terminal units of α-L-arabinofuranosyl substituents on their side chains. The degree of arabinosyl substitution varies in the specific instance of cereals, both 2-O- and 3-O-mono-substituted xylosyl residues are present.
ii. Glucuronoxylans, where the sole substituent is α-D-glucuronic acid or its 4-O-methyl ether derivative.
iii. Glucuronoarabinoxylan, which contains both α-L-arabinose and α-D-glucuronic (and 4-O-methyl-α-D-glucuronic) acid.
iv. The presence of terminal β-D-galactopyranosyl residues on complex oligosaccharide side chains of xylans distinguishes galactoglucuronoarabinoxylans, which are typically found in perennial plants (Motta *et al*., 2013).

Moreover, cellulose as a major component that is comprised of the repeating unit of glucose up to 12,000 residues in a linear chain. It has been found in the plant cell wall with ~30-50% by weight with the extensive intramolecular and intermolecular hydrogen bonds which are tight binds in between the glucose units. Due to their strong bonding network, the rigidity of cellulose is to strengthen and make the cell wall highly insoluble and highly resistant to most organic solvents. In green technology, cellulose has its important value in the conversion of fuels and valuable chemicals since about half of the organic form is occupied in the cellulose (Anwar *et al*., 2014; Isikgor and Becer, 2015; Lee *et al*., 2014).

Finally, lignin is also one of the important components that found in the plant cell wall with ~15-35% by weight compared with hemicellulose and cellulose. It is a three-dimensional of phenylpropanoid units which commonly bind by ether bonds. As the cellular glue, it can provide the extensive strength to the plant tissue and the individual fibres, stiffness to the cell wall and resistance against insects and pathogens. It is also can be considered as the byproduct or residue in production of bioethanol process since it is present in all of the plant biomass. In the structure of lignin, lignin is consisted of complex and large polymer of phenyl-propane, methoxy groups and non-carbohydrate poly phenolic substance (Lee *et al*., 2014; Anwar *et al*., 2014; Isikgor and Becer, 2015).

2.2. Xylanase

Xylanase is the name given to a classification of extracellular enzyme which also known as endo-1,4-β-xylanases (1,4-β-D-xylan xylohydrolase; EC 3.2.1.8) officially. In year 1955, the xylanase has been first discovered with naming pentossnases and published in a comprehensive database of carbohydrate-active enzymes (CAZy) in 1998. In year 1961, the International Union of Biochemistry and Molecular Biology (IUBMB) is recognized the xylanase to assign the enzyme code EC 3.2.1. (Collins *et al*., 2005; Heinze *et al*., 2017).

Xylanases are the most vital xylan-degrading enzyme. Xylanase is employed in the hydrolysis of xylan into simpler monomeric sugars and xylo-oligosaccharide. The β-1,4-glycosidic link in the xylan backbone is often broken by this enzyme, which lowers the substrate's degree of polymerization. Consequently, the xylanase is breaking down the hemicellulose which is one of the major components of the cell wall of plants. There is a study data showed that the hemicellulose can be degraded into various oligosaccharides and simple monomeric sugars, such as xylose and arabinose (Bajpai, 2014a; Bhardwaj *et al*., 2017; Motta *et al*., 2013; Zhao *et al*., 2016). The Figure 2.3 shows the mode action of xylanase enzyme in the depolymerisation of the xylan when applied to the xylan backbone.

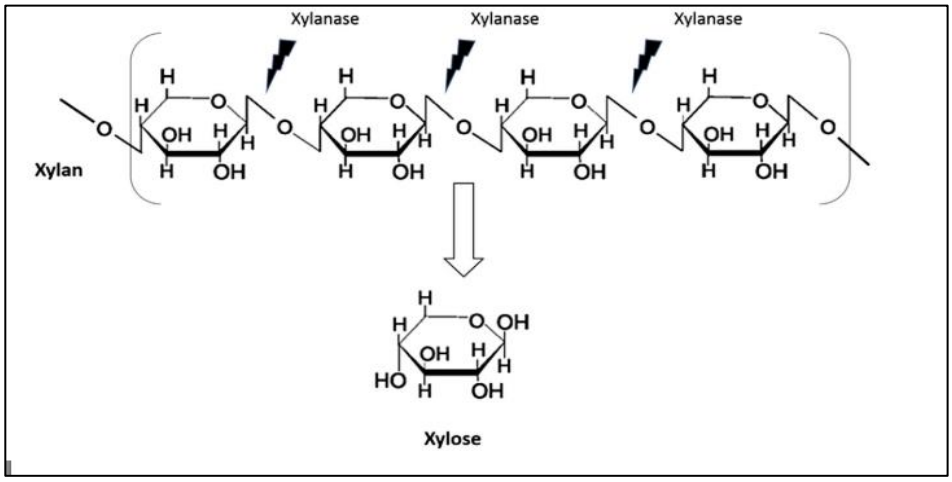

Figure 2.3: Structure of xylan and the mode action of xylanase (adapted from Godoy *et al*., 2018).

From the origin of the 1990s, several industries began to use the xylanase enzyme for commercial purposes, including paper and pulp industry, food and beverage production, food and feed industry, and biofuel production. The commercial xylanase enzyme has been produced by different company in

different countries, for example, India, Australia, Unites State, United Kingdom, Germany, Japan and etc. Normally, *Aspergillus niger (A. niger), Trichoderma sp.,* and *Humicola* were used as the producer to obtain the xylanase enzyme (Bajpai, 2014a; Bhardwaj *et al*., 2019). Figure 2.4 shows the schematic pathway of the bioconversion from lignocellulosic biomass to the production of biofuel.

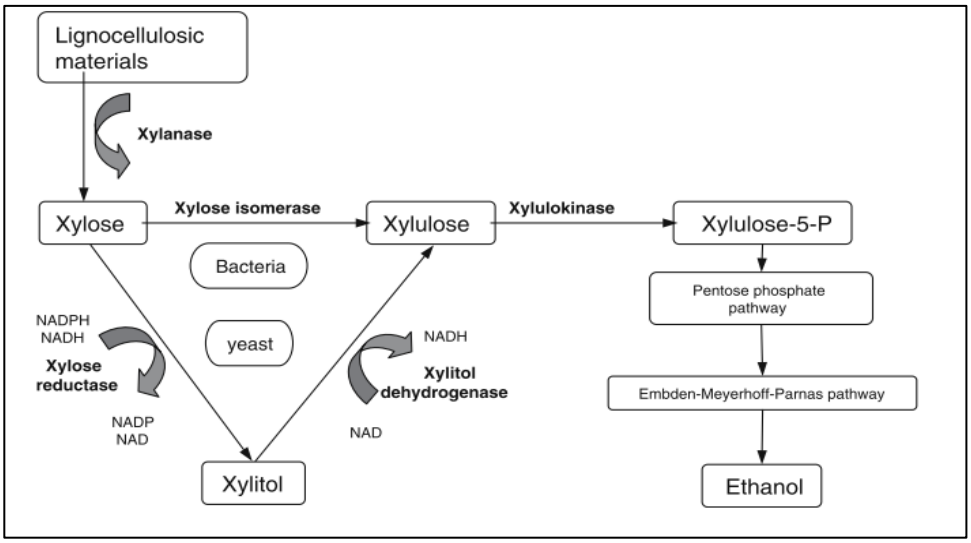

Figure 2.4: Schematic diagram for the biofuel production from lignocellulosic biomass (adapted from Polizeli *et al*., 2005).

2.2.1. Sources of Xylanase

There are various sources have been found to produce the xylanase enzymes, such as bacteria, fungi, actinomycetes, yeast, marine algae, protozoans, crustaceans, insects, snails, and seeds of land plants. However, bacteria and fungus are widely used as the main microorganisms for xylanase production in industrial applications (Beg *et al*., 2001; Bhardwaj *et al*., 2019).

2.2.1.1.Fungi

In economical production point of view, the filamentous fungi are most widely used in the xylanase production compared to the bacteria and other production sources. Studied data shows that the fungi have many benefits compared to bacteria and yeast since it has been widely studied for the alkali-stable xylanases (Amir *et al*., 2013; Pal and Khanum, 2011). First, filamentous fungi are biodiverse, produce high quantities of extracellular enzymes and are more easily cultivate and adapt to the culture medium if the changes in environmental factors occurred. Additionally, they produce the xylan-degrading enzymes into the culture medium which eliminate the needs of the cell disruption prior to the purification. Furthermore, they also can produce the auxiliary enzyme since it is necessary for degradation of the substituted xylan. Moreover, various agro-industrial wastes which are more complex can be utilized efficiently by using the filamentous fungi as the wastes as the substrate for enzyme production (Amir *et al*., 2013; Bajpai, 2014b; Modi *et al*., 2011; Okafor *et al*., 2007).

In the industrial application, various types of filamentous fungi containing *Aspergillus, Disporotrichum, Penicillium, Trichoderma, Neurospora, Neocallimastix, Coniothyrium, T. lanuginosus, Fusarium,* and so on, were used (Kumar *et al*., 2017). The genera *Aspergillus and Trichoderm* are predominant in the xylanase production among the mesophilic fungi. Studied data shows that

various thermophilic fungi have capable to produce the xylanase enzymes, such *as Chaetomium thermophile, Humicola insolens, Humicola lanuginosa, Humicola grisea, Melanocarpus albomyces, Paecylomyces variotii, Talaromyces byssochlamydoides, Talaromyces emersonii, Thermomyces lanuginosus*, and *Thermoascus aurantiacus.* Mostly, these thermophilic fungi can only produce the xylanase enzyme under acidic condition with a range about pH 4.5-6.5 (Bajpai, 2014b; Polizeli *et al*., 2005; Selvarajan and Veena, 2017).

Aspergillus niger (A. niger)

The genus *Aspergillus* is the most abundant fungi that can be found in the globe. It contains a numerous species of fungi, for example, *A. fumigatus, A. flavus, A. terrues, A. oryzae, A. niger,* and so on (Teertstra *et al*., 2017; Visagie and Houbraken, 2020). *A. niger* is a haploid filamentous fungus that can be found in decaying vegetation, soil and/or plants. At year 1917, *A. niger* was first discovered by a food chemist which is named as James Currie. It has been reported by Currie that *A. niger* has capable to produce the high amount of citric acid in the culture medium including growth factor even thought at low pH (2.5-3.5) (Cairns *et al*., 2018; Nadumane *et al*., 2016). This fungus also has the ability to become as the source of various bioactive components and industrial enzymes which is used for waste management and bio-transformations, for example, citric acid production and extracellular enzyme (Nadumane *et al*., 2016). The extracellular enzymes, such as glucose oxidase, pectinase, α-amylase and glucoamylase, organic acids, and recombinant proteins were produced by using

the *A. niger* since it has been safely used in the commercial production (Lopes *et al*., 2011; Van Dijck *et al*., 2003). The production of extracellular enzymes was particularly required the strains of *A. niger* since it is necessary (Shin *et a*l., 2011). *Aspergillus* genus can able to degrade the lignocellulose components, such as lignin, cellulose and hemicellulose. This is because it can produce the xylanase enzymes including endoxylanases (EC 3.2.1.8), β-xylosidases (EC 3.2.1.37), endoglucanases (EC 3.2.1.4), cellobiohydrolases (EC 3.2.1.91), β-Glucosidases (EC 3.2.1.21), exoglucanases, etc. (Andlar *et al*., 2018; Vries and Visser, 2001). Recently, the *Aspergillus* genus has been explored and employed in the xylanase production among the filamentous fungi (Guimaraaes *et al*., 2013). However, there have been few reports of the xylanase production by using *A. niger*. The Figure 2.5 below shows the microbial growth of the *A. niger* on the potato dextrose agar (PDA).

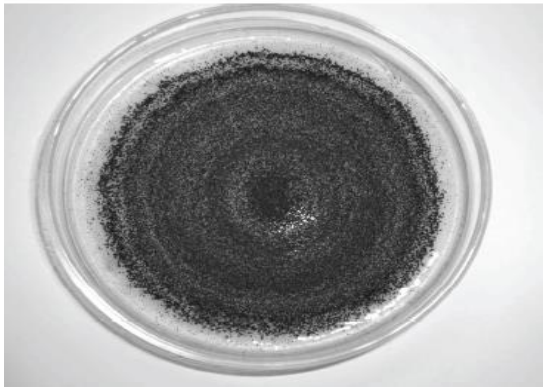

Figure 2.5: Macromophology of the *A. niger* on the PDA (adapted from Lopes *et al*., 2011).

2.2.1.2.Bacteria

Chakdar *et al*. (2016) reported that several bacterial genera, such as *Bacillus, Cellulomonas, Micrococcus, Staphylococcus, Paenibacillus, Arthrobacter, Microbacterium, Pseudoxanthomonas,* and *Rhodothermus* have capable to produce the xylanase production. In these bacterial genera, *Bacillus* was discovered to be a potential source of xylanase compared to other bacterial genera. Several bacterial genera including *Bacillus sp., Stenotrophomonas maltophila, Rhodothermus marinus, Thermotoga sp., Clostridium thermocellum*, and *Streptomyces sp*. have been reported that they can produce thermostable xylanase under high temperature condition (within 60-70 ºC). Many studies chose to use bacteria as the xylanase producer instead of fungi due to the optimum pH for the xylanase production is either in neutral or in alkaline range (Bajpai, 2014b; Abena and Simachew, 2024a).

2.2.1.3.Other Sources of Xylanase

There are several xylan-degrading thermotolerant actimomycetes, such as *Actinomadura, Nonomuraea, Microtetraspora, Streptomyces,* and *Thermomonospora* have been reported that they have capable to produce the alkali stable xylanases (Luo *et al*., 2016; Taibi *et al*., 2012). Some industrial applications also use yeasts to produce the xylanase enzyme due to they have capable to grow in high densities and secrete the protein into the culture medium. Published data shows that the *Saccharomyces cerevisiae* has been officially accepted as an industrial microorganism since it can produce high quantities of xylanase at low production cost at industrial point of view (Motta *et al*., 2013).

However, plenty of fungal and bacterial species have been found to produce the xylanase enzyme, including *Thermomonospora sp., Melanocarpus albomyces, Chaetomium thermophilum, Nonomuraea flexuosa, Streptomyces sp., Dictyoglomus sp., Thermotogales sp., Thermoactinomyces thalophilus, Thermoascus aurantiacus, Fusarium proliferatum, Clostridium abusonum* and others (Bajpai, 2014b). Table 2.1 shows the summary for the various types of microorganisms, including fungi, bacteria, and actinomyces which can produce the xylanase enzyme.

Table 2.1: Various types of microorganisms in producing xylanase enzymes

Major group	Species	Genus	References
Bacteria	*Bacillus*	*Bacillus firmus, Bacillus tequilensis, Bacillus sp.* MCC2212*, Neobacillus sedimentimangrovi, Bacillus amyloliquefaciens, Bacillus halodurans, Bacillus sp.* JB 99	Abena and Simachew, 2024; Mongkorntanyatip *et al.*, 2017; Rashid *et al*., 2024; Siwach *et al*., 2024; Patel and Dudhagara, 2020
	Arthrobacter	*Arthrobacter sp.* MTCC6915	Murugan *et al*., 2011
	Geobacillus	*Geobacillus thermoleovorans, Geobacillus stearothermophilus, Geobacillus thermodenitrificans*	Verma *et al*., 2019; Bibi *et al*., 2022; Verma and Satyanarayana, 2012
	Pediococcus	*Pediococcus acidilactici, Pediococcus pentosaceus*	Kuniyoshi *et al*., 2021; Adiguzel *et al*., 2019
	Clostridium	*Clostridium thermocellum, Clostridium cellulovoran, Clostridium* strain BOH3	Hamann *et al*., 2020; Rajagopalan *et al*., 2017; Balderas Hernández *et al*., 2021
	Dictyoglomus	*Dictyoglomus thermophilum*	Li *et al*., 2015
	Paenibacillus	*Paenibacillus sp., Paenibacillus physcomitrellae, Paenibacillus xylanivorans, Paenibacillus campinasensis, Paenibacillus barengoltzii*	Wang *et al*., 2024; Briganti *et al*., 2021; Thakur *et al*., 2022; Wang *et al*., 2022; Liu *et al*., 2018
	Rhodothermus	*Rhodothermus marinus*	Ramchuran *et al*., 2005

	Staphylococcus	*Staphylococcus aureus, Staphylococcus sp.*	Bhardwaj *et al*., 2019
	Pseudomonas	*Pseudomonas sp., Pseudomonas nitroreducens, Pseudomonas fluorescens, Pseudomonas boreopolis, Pseudomonas mohnii*	Sunder *et al*., 2025; Guo *et al*., 2018; Paul *et al.,* 2020; Dhivahar *et al*., 2020; Van Dorn *et al*., 2018
	Thermoactinomyces	*Thermoactinomyces thalophilus*	Kohli *et al*., 2001
	Thermotoga	*Thermotoga maritima, Thermotoga petrophila, Thermotoga naphthophila*	Haq and Akram, 2019; Shahid *et al*., 2023; Yang *et al*., 2020
Fungi	*Talaromyces*	*Talaromyces thermophilus, Talaromyces cellulolyticus, Talaromyces versatilis, Talaromyces stipitatus, Talaromyces thermophiles*	Teng *et al*., 2017; Bharti *et al*., 2018; Rios *et al*., 2017; Nakamichi *et al.,* 2019; Fan *et al*., 2020
	Thermomyces	*Thermomyces lanuginosus*	Alagöz *et al*., 2022
	Thermoascus	*Thermoascus aurantiacus*	Ping *et al*., 2018
	Melanocarpus	*Melanocarpus albomyces*	Biswas *et al*., 2010
	Chaetomium	*Chaetomium thermophilum, Chaetomium globosum, Chaetomium sp.*	Katapodis *et al*., 2007; Liu *et al*., 2022; Lu *et al.,* 2025

Fusarium	*Fusarium sp., Fusarium solani, Fusarium verticillioides, Fusarium oxysporum, Fusarium heterosporum, Fusarium graminearum*	Liu *et al*., 2024; Huang *et al*., 2024; Rodríguez-Sanz *et al*., 2024; Martínez-Pacheco *et al*., 2020; Wang *et al*., 2025; Paulo *et al*., 2014
Humicola	*Humicola insolens, Humicola grisea* var. *thermoidea, Humicola brevis* var. *thermoidea*	Faria *et al*., 2020; Yang *et al*., 2014; Pereira de Almeida *et al*., 2022
Paecylomyces	*Paecylomyces variotii*	Abdella *et al*., 2021
Scytalidium	*Scytalidium thermophilum, Scytalidium acidophilum*	Joshi and Khare, 2011; Michaux *et al*., 2010
Thielavia	*Thielavia terrestaris*	López-López *et al*., 2023
Corynascus	*Corynascus sepedonium*	Yang and Zhang, 2017
Myceliophthora	*Myceliophthora heterothallica, Myceliophthora thermophilia*	de Amo *et al*., 2024; Lai *et al*., 2025
Sporotrichum	*Sporotrichum thermophile*	Sadaf *et al*., 2016
Rhizomucor	*Rhizomucor miehei*	Fawzi, 2011
Trichoderma	*Trichoderma koningii, Trichoderma pseudokoningii, Trichoderma harzianum,*	Sanguine *et al*., 2022; Nam, 2024; Rezende *et al*., 2002; Askari *et al*., 2024; Dhaver *et al*., 2022; Qi *et al*., 2025; Zheng *et al*., 2024

		Trichoderma longibrachiatum, Trichoderma harzianum, Trichoderma afroharzianum,, Trichoderma gamsii, Trichoderma asperellum	
	Aspergillus	*Aspergillus niger, Aspergillus flavus, Aspergillus niveus, Aspergillus ochraceus, Aspergillus foetidus, Aspergillus fumigates, Aspergillus terreus, Aspergillus tamari*	Guimaraaes et al., 2013; Cunha et al., 2018; Miao *et al*., 2015; Fasiku *et al*., 2023; Bajar *et al*., 2020; Bhardwaj *et al*., 2019
Actinomyces	*Streptomyces*	*Streptomyces costaricanus, Streptomyces sp., Streptomyces geysiriensis, Streptomyces althioticus, Streptomyces thermovulgaris, Streptomyces thermocarboxydus, Streptomyces variabilis*	Sipriyadi *et al*., 2020; Rosmine *et al*., 2017; Poornima *et al*., 2020; Luo *et al*., 2016; Wu *et al*., 2023; Chaiyaso *et al*., 2011; Shrestha *et al*., 2022; Khangkhachit *et al*., 2021; Sanjivkumar *et al.,* 2018
	Kitasatospora	*Kitasatospora sp.*	Rahmani *et al*., 2019
	Nonomuraea	*Nonomuraea flexusa*	Zhang *et al.,* 2011
	Actinomadura	*Actinomadura sp.*	Taibi *et al.,* 2012; Sriyapai *et al*., 2011
	Cellulomonas	*Cellulomonas fimi, Cellulomonas flavigena*	Duedu and French, 2016; González-Bautista *et al*., 2017

Microbacterium	*Microbacterium imperial*	Tang *et al*., 2021
Micrococcus	*Micrococcussp.*	Mmango-Kaseke *et al*., 2016
Thermomonospora	*Thermomonospora fusca*	Sun *et al*., 2007

2.2.2. Application of Xylanase Enzyme

Xylanase enzymes have many potential industrial applications such as pulp and paper, food, textiles, biofuel, animal feed and drinks. Due to its hydrolysis and other properties, the xylanases were mostly produced from the microorganisms for commercial applications. The market for commercial xylanases has been growing for the last few decades (Bajpai, 2014a; Kumar *et al*., 2017). Figure 2.6 shows the xylanase enzyme uses in various industrial applications and there are several applications in major industries are described in this later section.

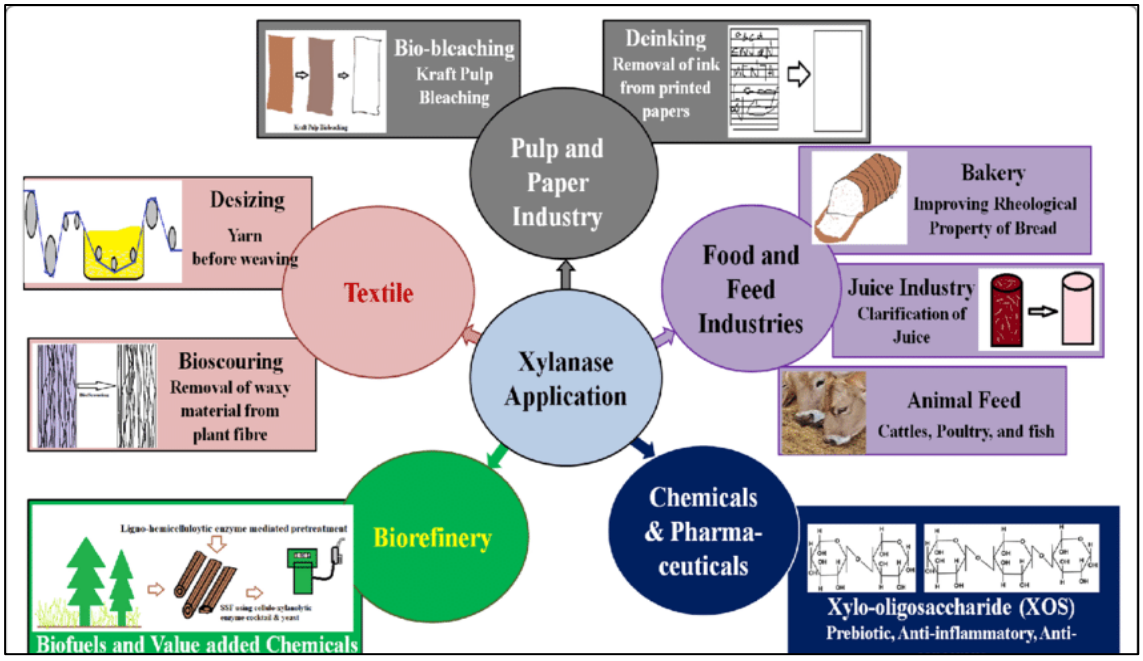

Figure 2.6: The uses of xylanase in various industrial applications (adapted from Bhardwaj *et al*., 2019).

2.2.2.1.Pulp and Paper Industries

In the pulp and paper industries, xylanases enzyme plays an important role in bio-bleaching process. In these industries, bleaching refers to a process that eliminates lignin from wood pulp in order to create bright, thoroughly white finished paper. Conventionally, chlorine and chlorine-based chemicals were used as the chemical bleaching agents for bleaching. Nevertheless, the byproduct formed has been found that they can cause the environment pollution and bring harmful substances influence the biological system. In order to prevent or reduce the negative impacts, the xylanase use was employed in paper industries instead the chlorine and chlorine-based chemicals.

During the treatment of cellulosic pulps with xylanase, it can eliminate residual xylan associated with cellulose and lignin as the pulp dissolves. As a result of the breakdown on the xylan, xylanases are able to decompose the hemicellulose in the pulp. The disruption of xylan will lead to the separation of these compounds, an increase in swelling within the fiber wall, and an enhancement of lignin extraction from the pulp. Eventually, the brightness of pulp will be increased with the combination of the lignin-degrading enzyme. Moreover, enzymatic treatment has been proven to enhance various physical properties of paper, including viscosity, tensile strength, breaking length and tear factor (Bhardwaj *et al*., 2019; Betini *et al*., 2009; Bajpai, 2014a).

2.2.2.2.Biofuel Production

By breaking down the hemicellulose which is a component of plant cell walls, xylanase and other enzymes help break down lignocellulosic biomass for the creation of biofuel. Since they don't interfere with food production and can have positive effects on the environment and the economy, second-generation biofuels made from renewable resources have drawn interest as fossil fuel substitutes. Studies show that xylanase plays an important role in the saccharification of lignocellulosic biomass for the production of biofuel. However, converting lignocellulosic raw materials into ethanol through the enzyme hydrolysis still comes at a high cost.

The initial step in the production of bioethanol fuel is the delignification of lignocellulose, which separates cellulose and hemicellulose from their complex with lignin. The carbohydrate polymers are depolymerized in the second step to yield free sugars, and then a mixture of pentose and hexose sugars is fermented to yield ethanol. Another method is simultaneous saccharification and fermentation, which involves the presence of both fermentative microbes and hydrolytic enzymes in the procedure. Numerous integrated solutions have been developed to enhance the generation of ethanol in the process of producing biofuels from lignocellulosic biomass. These procedures include consolidated bioprocessing (CB), simultaneous saccharification fermentation (SSF), and simultaneous saccharification and co-fermentation (SSCF) (Abena and Simachew, 2024a; Motta *et al*., 2013).

Furthermore, the production of biofuel from lignocellulosic biomass is a major concern for industrial sectors around the world. However, the initial conversion of biomass into sugars requires several enzymes (including xylanases) that have high activity and attractive enzyme characteristics, the manufacture of biofuel remains a bottleneck. As a result, xylanases have recently been used in biotechnological applications for biomass conversion. Furthermore, compared to enzymes of mesophilic or neutrophilic origin, highly stable enzymes that were active at high temperatures and across a broad pH range had a number of advantages. For instance, because of their quick reaction rate, highly active xylanases in harsh environments lower the risk of contamination. Mild pretreatment of biomass is necessary in second-generation ethanol industries in order to maintain high hemicellulose contents while lowering overall costs. The full conversion of hemicellulose still requires a large dosage of additional enzymes, though. Therefore, applying xylanases in biotechnology — especially thermophilic xylanases — and combining them with other enzymes like cellulases, xylosidases, and arabinofuranosidase seems advantageous for the saccharification process (Basit *et al*., 2021). The Figure 2.7 show the process flow from the lignocellulosic biomass to biofuel under the biological conversion.

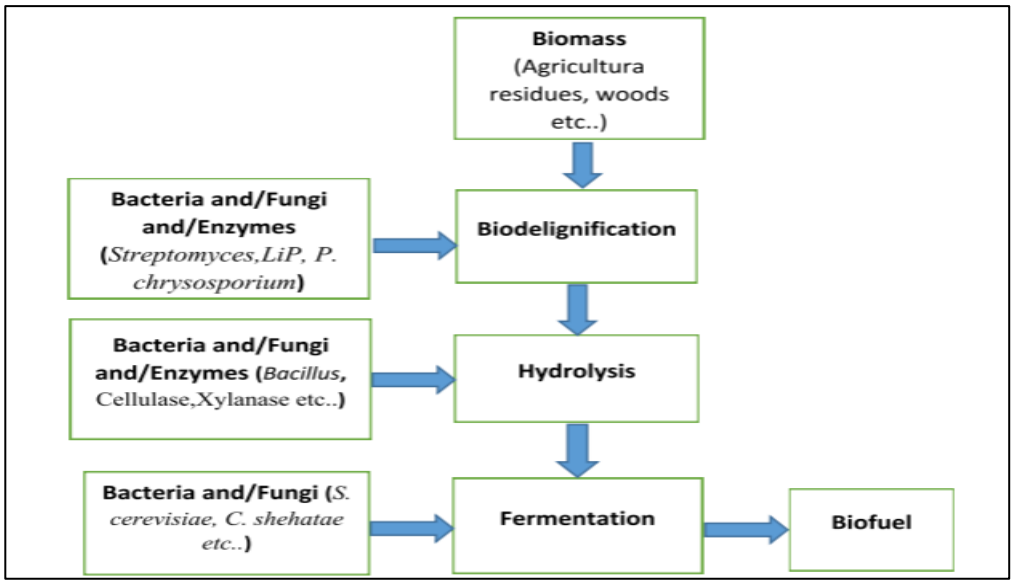

Figure 2.7: Overall process flow for the conversion of biological conversion of lignocellulose biomass to biofuel (adapted from Tsegaye *et al*., 2019)

2.2.2.3.Pharmaceutical, Food and Feed Industry

Fruit juice extraction and clarifying are common uses for the enzymatic process. Raw fruit juices contain polysaccharides like hemicellulose, starch pectin, cellulose, and surface-bound lignin, which reduce the quality of the juice by imparting a hazy appearance and increasing its viscosity. By employing centrifugation and filtration techniques to remove the suspended and undissolved material, enzymes reduce viscosity and prevent cluster formation. This improves the juice's color, clarity, and scent. Additionally, xylanase may enhance the extraction of starch, coffee, and plant oils. Xylitol, a useful sweetener with uses in the food and pharmaceutical industries, can also be produced from the xylose that results from xylan depolymerization.

In the bakery industry, hemicelluloses like arabinoxylan are found in wheat, which is used to make bread. Water-unextractable arabinoxylan can be dissolved by xylanase to become water-extractable arabinoxylan. This promotes better gluten network formation throughout the dough and (uniform water distribution/water distribution uniformly). In addition to bread-specific volume and crumb firmness, the inclusion of xylanase enhances the dough's rheological qualities, including softness, extensibility, and elasticity. The arabino-xylooligosaccharides in bread, which are the breakdown products of arabinoxylan, provide health advantages. In addition to increasing specific volume and shelf life, the addition of xylanase also decreased stiffness and decreased staling with time. Panzea, a novel xylanase sourced from *Bacillus Licheniformis*, can contribute to the improvement of bread properties when used at low enzyme dosages. It aids in obtaining the appropriate crumb structure, volume, texture, and appearance of the loaf. This property (bread's specific volume) was improved when combined with amylases, as was seen when *Aspergillus niger* var. *awamori* was added.

Additionally, xylanase may enhance the nutritional value of grain feed and agricultural silage. Research employing this enzyme in chicken diets has shown that intestinal viscosity is associated with decreased weight gain and feed conversion efficiency in broiler chicks fed rye. By adding xylanase produced from *Trichoderma longibrachiatum* to the broiler chickens' rye-based diet, intestinal viscosity was decreased, increasing the chicks' weight gain and feed conversion efficiency. Because xylanase increases the digestibility of arabinoxylan in monogastric animal diets, it improved weight gain and the feed

conversion ratio. It is possible that xylanase enhances the nutritional value of grain feed and agricultural silage. Research on the application of this enzyme in poultry nutrition indicated that the reduction in weight gain and feed conversion efficiency in rye-fed broiler chicks is related to intestinal viscosity. Including xylanase derived from *Trichoderma longibrachiatum* in the rye-based diet of broiler chickens led to a reduction in intestinal viscosity, which resulted in improved weight gain and feed conversion efficiency for the chicks. The addition of xylanase improved weight gain and enhanced the feed conversion ratio due to improving arabinoxylan digestibility in monogastric animal diets.

Xylanases are used in cereals as a pretreatment for substrates that contain arabinoxylans, due to the fact that arabinoxylans have slight water solubility and yield an aqueous solution of very high viscosity. The high viscosity of the cereal grain water extract might lead to brewing problems by reducing the speed at which filtration or haze development occurs in beer. Furthermore, it adversely affects the cereal grains used for animal feed.

Xylan can also be hydrolyzed by enzymes to produce oligomers called xylooligosaccharides (XOs), which can be utilized in feed, medicine, and agriculture. XOs exhibit prebiotic effects due to the fact that they are not hydrolyzed or absorbed in the upper gastrointestinal tract. They improve health by selectively promoting the growth or activity of one or more bacteria in the colon. Their main physiological benefits include lowering cholesterol, preserving gastrointestinal health, and increasing calcium's biological availability. Additionally, they prevent starch from retrograding, enhancing

food's nutritional value and flavor. Low levels of exoxylanase or β-xylosidase activity are necessary for the enzyme complex to produce XOs since excessive levels of xylose inhibit the formation of XOs (Basit *et al*., 2021; Bajpai, 2014a; Motta *et al*., 2013; Bhardwaj *et al*., 2019).

2.2.2.4.Textile Industry

Desizing (removing the size or sticky component), scouring (removing the inhibiting material from desized fibers), and bleaching (increasing whiteness) are the three primary operations used in the textile industry. The traditional techniques for these procedures are environmentally unfriendly since they require a lot of chemicals, are unspecific, and apply high temperatures in alkaline environments. Several study recommendations support the use of more ecologically friendly enzyme-based remedies for solving these problems. Therefore, desizing and scouring can be carried out effectively by using a xylanolytic enzyme that is extremely thermo-alkali resistant and does not contain cellulase.

Xylanase is one of the enzymes utilized in the textile industry; it helps with desizing, bioscouring, biostoning, fabric softening, releasing excess dye, and biobleaching of denim clothing. In recognition of this, a number of research teams have carried out investigations to identify cellulase-free xylanase enzymes that are highly stable at high temperatures and alkaline pH levels for application in textile industry scouring and desizing procedures. According to certain

findings, xylanase derived from *Bacillus stearothermophilus* SDX *and B. pumilus* has been successfully used for bioscouring and cotton and micropoly fabric desizing (Bhardwaj *et al*., 2019; Bajpai, 2014a; Abena and Simachew, 2024a; Basit *et al*., 2021).

2.3. Fermentation Process

There are two types of fermentation process, which are submerged and solid-state fermentation, were employed in the xylanase production. The published data showed that most of the studies are concerned about the production of xylanase were carried out under the submerged fermentation. Xylanase production involved the use of various microorganisms, with an understanding of their physiology and the different metabolic processes of the microbial system contributing to improvements in the fermentation process. Nonetheless, it still has a constraint when it comes to producing large quantities of xylanase enzymes. Since there are many different parameters can affect the environment conditions of the fermenting medium, subsequently influence the xylanase production, the screening step and optimisation of the fermentation process will be focused and described in a subsequent section (Bhardwaj *et al*., 2019; Motta *et al*., 2013).

2.3.1. Submerged Fermentation (SmF)

Microorganisms and substrates are immersed in a liquid medium during the fermentation process known as submerged fermentation (SmF). Yeast, bacteria, and fungi are among the microorganisms that may use SmF on an industrial scale (Jonathan *et al*., 2021). The desired enzymes are released into solution by the microorganisms when they break down the nutrients. The majority of xylanase producers use SmF procedures to create these enzymes; in fact, SmF as a generating system account for around 90% of global xylanase sales (Güler and Özçelik, 2023). Because SmF offers improved control over environmental factors such moisture content, temperature, aeration, and pH, it has been the subject of most investigations looking into the synthesis of microbial xylanases (Siwach *et al*., 2024).

It is known that a submerged fungal culture is a complicated multiphase, multicomponent process in which a wide range of operating parameters, including temperature, pH, shear stress, initial inoculum, dissolved oxygen, rheology, fungal morphology, and culture broth composition, affect cell growth and formation of product. Enzyme production is known to be influenced by the optimisation of culture conditions and culture medium. It is commonly known that the synthesis of enzymes is influenced by the optimisation of culture conditions and culture medium (Dos Reis *et al*., 2015). Advantages and disadvantages of the SmF was presented in the Table 2.2.

2.3.2. Solid State Fermentation (SSF)

Another technique for producing enzymes is solid-state fermentation (SSF). Growing microorganisms on a solid substrate, like grains, rice, or wheat bran, is known as SSF. This technique is an alternative to SmF, which produces enzymes in liquid. Plenty of interest in producing a broad range of enzymes, including xylanases with fungal origins by employing SSF technique. Certain enzymes and metabolites may be produced more effectively by these fermentation techniques since they have characteristics more similar to the natural environments of microorganisms (Modi *et al*., 2011; Renge *et al*., 2012).

SSF techniques work effectively on complex substrates, including as wastes and residues from forestry, agriculture, and food processing, which are utilized as sources of stimulating carbon to produce xylanases. Since fungus can grow at relatively low water activity, they are particularly well suited for SSF conditions. In contrast, most bacteria and yeast cannot grow under these culture conditions. It is frequently stated that SSF procedures have an advantage over SmF due to their higher enzyme titres. Furthermore, using SSF as the production method can enhance the qualities of the enzyme, such as its pH tolerance and thermostability (Bajpai, 2014b; Jonathan *et al*., 2021; Bhardwaj *et al*., 2019; Siwach *et al*., 2024).

The selection of a suitable substrate and microbe, pre-treatment of the substrate, substrate particle size, water content and water activity (aw) of the substrate, inoculum type and size, relative humidity, pH, controlling the

temperature of fermenting matter and removal of metabolic heat, cultivation duration, maintenance of uniformity in the SSF environment system, and the gaseous atmosphere — that is, the rate at which oxygen is consumed during fermentation and the rate at which carbon dioxide evolves — are the main factors that influence microbial synthesis of enzymes in an SSF system (Uday *et al*., 2016; Walia *et al*., 2017). Advantages and disadvantages of the SSF was presented in the Table 2.2.

2.3.3. Advantages and Disadvantages of SmF and SSF

The advantages and disadvantages of SmF and SSF was displayed in the Table 2.2. The Table 2.2 was referred and adapted from several reviews (Sagar Aryal, 2022; Couto and Sanromán, 2006; David, 2023; Kirimura and Yoshioka, 2019; Bhardwaj *et al*., 2019; Londoño-Hernandez *et al*., 2020).

Table 2.2.: Advantages and disadvantages of SmF and SSF (Sagar Aryal, 2022; Couto and Sanromán, 2006; David, 2023; Kirimura and Yoshioka, 2019; Bhardwaj *et al*., 2019; Londoño-Hernandez *et al*., 2020).

	Advantages	Disadvantages
SmF	– Higher productivity and yields – by controlling the parameters, such as temperature, pH, aeration, etc. – Ease of scale-up – suitable for large scale production and readily adjustable to various bioreactor sizes. – Lower labor costs - manual labor may be less necessary with automated (systems/technologies).	– High equipment costs – using the expensive specialized equipment, for example bioreactors, agitators, and aeration systems. – Exposure to contamination susceptibility: The quality of the product may be impacted by microbial contamination, which is more likely to

	– Lower the contamination risk – Commonly used in production of enzyme	occur in a liquid environment. – Complex process: Needs knowledgeable operators to run and care for the machinery.
SSF	– Lower cost and simpler technology - SSF can use easily accessible, inexpensive substrates and requires less complex equipment. – Simpler downstream processing - solid substrate makes it easy to recover products. – Similar to natural habitat – fungus may can grow natively on solid substrates – Benefits to the environment – Reduce the usage of waste materials and wastewater production can be decreased. – High volumetric productivity – it capable to produce more product in a given volume. – Simpler to manage - SSF is simple to apply on a large industrial scale. – Appropriate for producing enzymes - Good choice for producing enzymes and other bioproducts.	– Challenges with heat removal – Due to the solid substrates have a low thermal conductivity, it is difficult to maintain ideal temperatures. – Difficulties with moisture control – It is difficult to achieve the successful SSF depends on precise moisture control. – Problems with oxygen availability - The solid substrate may restrict the microbes' ability to absorb oxygen. – Limited selection of microorganisms: Only specific species are appropriate for SSF. – Product recovery difficulties: It may be difficult to extract the intended product from the solid substrate.

2.4. Parameters Affecting the Xylanase Production

In order to achieve the optimum xylanase productivity, the condition of the fermenting or culture medium should be optimised. Therefore, the microorganisms can grow in well-suited and optimised culture medium for enzyme production. This is because the optimum culture condition is required for microorganism to metabolize and produce the enzyme efficiently in enzyme production. In addition to the traits of the microbe, environmental factors including, incubation time, pH, temperature, agitation and aeration rate, initial moisture, inoculum sizes, and the growth medium's nutritional components able to affect the synthesis of xylanase and the xylanase activity (Ajijolakewu *et al*., 2017; Tarrsini *et al*., 2020).

2.4.1. Incubation Time Period

The incubation time has a significant impact on the synthesis of an enzyme as we (Devi *et al*., 2022). Different conditions are necessary for fungus to grow optimally. Through biochemical breakdown processes, fungi obtain all of their growth ingredients and energy from their growth medium. However, the growth medium must already include all of the growth-related components. Depending on the species and variety, different time periods of 3–7 days are needed (Ali *et al*., 2017). . Incubation time influences xylanase synthesis by fungi because, generally speaking, xylanase production is directly proportional to the incubation time up to a certain point and then declines (Dhaver *et al*.,

2022). The gradual decline in enzymatic activity may be caused by the medium's nutritional depletion, which strained the fungal physiology and inactivated the enzymes' secretary machinery (El-Nahrawy *et al*., 2017). The enzyme activity dropped as the incubation period increased further; this could be because the extended incubation time caused the enzyme to become denaturated (Devi *et al*., 2022).

Bharti *et al*. (2018) mentioned that the highest xylanase activity (836.97 IU/gds) was found on the 5th day of incubation using *A. niger* NFCCI 4113. It might be because hemicelluloses have a high solubility. There is a study also mentioned that the highest xylanase activity was also found on the 5th day with 1059 ± 90.67 U/gds using the *A. niger* CSCT 2700 (Moran-Aguilar *et al.*, 2021). Pal and Khanum (2010) discovered that *A. niger* DFR-5 produced the highest xylanase activity (2596 IU/gds) when using the wheat bran as a substrate after 6 days of incubation at 40 °C under SSF.

2.4.2. pH

pH is the sole factor that directly influences a molecule's proton concentration, which indicates how acidic or alkaline a solution is (Al-Shaeli *et al*., 2024). pH is another important factor affecting xylanase production. Because microorganisms are sensitive to the concentration of hydrogen ions in the medium, pH is one of the most crucial parameters influencing their growth. It is also essential for enzyme activity since it can change the ionization of amino

acids on the molecule, which means it may can change the shape of the enzyme or denature the enzyme. This usually results in the enzymes losing their catalytic capabilities and cessation of metabolic activity. pH can affects the morphology of the microbes and the mycelial dry cell growth. It can also affect the activity of enzymes by altering the ionic charges on the molecules, which are the surface of substrate and active site of enzymes (Bajar *et al*., 2020; Devi *et al*., 2022; Dhaver *et al*., 2022; Maan *et al*., 2016).

Additionally, it can also transport of various components across the cell membrane by varying the pH value. At the particular pH value, it can influence their ability to transport the substance by altering the membrane transport protein structure and function, which are made of amino acids that are sensitive to pH. By varying the pH value, it can affect the ionization of amino acids, leading to conformational changes in the protein due to the interaction between the amino acids, for example, hydrogen bonding and ionic interactions, can be altered. Moreover, it can potentially disrupt its ability to bind to and transport substances across the membrane at extreme pH value (Ball *et al*., 2012; Enzyme, n.d.).

An optimal pH and stability vary depending on its origin for a specific xylanase. For example, there is a study stated that the endo-1,4-β-xylanase from an acidophilic fungus, which is *Scytalidium acidophilum* shows the optimum enzyme activity at pH 3.2 by decreasing the number of salt bridges and hydrogen bonds in comparison with highly alkaline enzymes (Michaux *et al*., 2010). *Bacillus pumilus* strain BS131 has shown a maximum xylanase production at pH 7.0 (Kalim *et al*., 2023). A recombinant xylanase which is produced using the

Bacillus tequilensis BT21 has an optimum enzyme activity at pH 6.0. It is also found that the *xynBT21* remained highly stability at pH 7.0 and increased its activity at alkaline pH by changing the net charge of the protein (Khandeparker *et al*., 2017). There is a finding found that the *A. niger* generated the highest xylanase activity when the pH between 6.0 (120.0 IU/mL) to 7.0 (123.6 IU/mL) (Pakaweerachat and Chysirichote, 2025). Moreover, there is a previous study stated that *A. niger* shown the highest production of xylanase enzyme at pH 8.0 (Karunakaran *et al*., 2014). On the other hand, the microbe can produce the necessary extracellular enzymes at the certain pH value. Except xylanase enzyme, there are several types of auxiliary or extracellular enzymes, such as β-xylosidases, α-arabinofuranosidases, α-glucuronidases, and etc. can be produced during the xylanase production. The function of β-xylosidases is used to hydrolyze the xylo-oligosaccharide into xylose while the other three extracellular enzymes are side-chain cleaving enzymes which were used to break down the side groups on the xylan polymer. Previous study stated that the *Aspergillus* spp. and *Trichoderma* spp. are regarded as industrially significant producers of xylanase and also the extracellular or auxiliary enzymes.

Thermomyces lanuginosus has been studied that it can produce the β-xylosidases at optimum pH of 5.5 (Corrêa *et al*., 2016). There is a study reported that *Penicillium* as the filamentous fungi are found that can produced the auxiliary enzymes among the microbes. *Penicillium janczewkii* was found that a good producer for producing the β-xylosidase and α-arabinofuranosidase. *Penicillium janczewkii* was generated the optimum production of β-xylosidase at pH 5.0 while the highest β-xylosidase activity at pH 4.0 (Terrasan *et al*., 2013).

According to the Kundu and Ray (2012), an optimum pH value to produce β-xylosidase occurring at pH 6.0 with 27 °C using *Penicillium janthinellum* MTCC 10889. For producing the α-arabinofuranosidase enzyme, the optimal pH from *Penicillium* were found out in between 4.0 to 5.0 which was dependent on the species or its traits. *Penicilium janczewskii* was discovered an optimum enzyme activity is at pH 4.0 (Beatriz *et al*., 2014). Moreover, there is a study also found that the best optimal enzyme activity is at pH 5.0 using the *Penicilium janczewskii* (Terrasan *et al.,* 2010). α-glucuronidase is one of the xylolytic enzyme that can be produced and optimised at different pH values depending on the different microorganisms. There is a research reported that the optimal pH for the α-glucuronidase produced by a strain of *Bacillus* and other bacteria is at pH 7.0, for example, *Geobacillus stearothermophilus* (Rojas-Pérez *et al*., 2022). According to the Tenkanen and Siika-Aho (2000), *Schizophyllum commune* is a fungus can produce the xylolytic enzyme, which is α-glucuronidases that break downs the α-glucuronic acid side chain. The researchers learned that the highest enzyme activity at pH values from 4.5 - 5.5 from the *Schizophyllum commune*.

The optimum pH changes according to the type of fungus. Numerous studies have documented the impact of pH on fungal enzyme production, and efforts have been made to optimise pH in order to promote xylanase production. During fungal fermentation, the pH profile was unstable and fluctuated due to some acidic products would alter the medium's pH value. For example, for producing the optimum α-galactosidase enzyme by *A. foetidus*, the fermentation was started at a pH of 7.0, lower it to 6.0 within 72 hours, maintain that level for 24 hours, and then lower it to 5.0 until the fermentation is finished. To achieve

maximum enzyme synthesis, it needs to be controlled by constant pH adjustment (Zhang *et al.,* 2024). In the process of fermentation, the composition of the enzyme system and the activities of the various enzymes produced by the microbes were also influenced by pH. According to Su *et al*. (2011), *Trichoderma* SG2 generated the maximum levels of cellulase and β-xylosidase activity at an initial pH of 7.0, highest xylanase activity at pH 8.0, and β-glucosidase at pH 6.0.

According to the Abena and Simachew (2024b), optimum xylanase activity was occurring at pH 5 when using the white rot fungus. In contrast, the xylanase activity was declined when the pH values less than 5 and more than 6.5. At pH 5.0, *A. niger* GIO showed its maximum xylanase activity (4.58 U/mL) (Fasiku *et al*., 2023). The pH stability of xylanase has been reported by numerous researchers, although without explanation. The xylanase obtained from *Planococcus sp.* SL4 showed high stability and activity across the neutral and alkaline pH range of 6 to 11, with its peak at pH 7 and greater than 60% activity at pH 11. The xylanase obtained from *Arthrobacter sp.* MTCC 5214 was found to be stable only within the restricted pH range of 7.0–8.0 (Basit *et al*., 2021).

2.4.3. Temperature

One of the most significant variables influencing the xylanase production was temperature. It had an impact on metabolite production, spore formation and germination, and microbial proliferation. Even membrane structure can be upset

by high temperatures, which denatures structural proteins and enzymes. Low temperatures slow down metabolic reactions and decrease plasma membrane permeability, which decreases the exchange of compounds between the extracellular and intracellular spaces and, consequently, nutrient transport. The growth of the organism (mesophilic, psychrophilic, or thermophilic) is primarily linked to the effects of temperature on the creation of enzymes.

Notably, the properties of the enzymes that filamentous fungi produced were affected by different temperatures. As an illustration, xylanase specific activity at 45 °C was 2.5 times more than that at 37 °C using the *Aspergillus* FP-470. For xylanase produced at 37 °C, the ideal pH and temperature were 6.5 and 80 °C, respectively. However, for xylanase produced at 45 °C, the ideal pH and temperature were 4.3 and 50 °C, respectively. Stress caused by temperature caused fungus to release fewer extracellular xylanases, but more different kinds of xylanases (Dhaver *et al*., 2022; Wang *et al*., 2018).

Abena and Simachew (2024b) mentioned that the greater than 77 U/mL xylanase activity at 28 °C when using the white rot fungus. After 30 hours of incubation, the xylanase generated by *A. niger* GIO has the maximum activity (3.67 U/mL) at 40 °C (Fasiku *et al*., 2023). A study examining the impact of *A. niger* DFR-5 xylanase activity at varying temperatures (between 20 and 60°C) was conducted. As the temperature rose, the xylanase activity increased as well, reaching its maximum at 40°C. The enzyme activity rapidly decreased with increasing temperature, reaching 35.5% of its maximal activity at 60°C.

Likewise, the impact of temperature on *A. niger* purified xylanase (xynZF-2) was assessed (Basit *et al*., 2021).

2.4.4. Agitation and Aeration Rate

The mass transport properties are enhanced by aeration. In addition to mixing the nutrients and producing a uniform nutrient availability in the reactor, agitation aids in increasing the mass transfer of air and oxygen from the gaseous phase to the developing cells via the liquid phase. However, the cell may be harmed by the agitation's potential to produce shear forces and unequal mycelium network growth. In optimisation studies, introducing the agitation rates greater than 500 rpm are often avoided to minimize further shear stress. Conversely, a low rate of agitation and aeration may also reduce the formation of xylanase. For mycelium to grow healthily without breaking, agitation rate must be optimised (Iram *et al*., 2022; Rafiee *et al*., 2021; Jonathan *et al*., 2021).

According to Güler and Özçelik (2023), agitation promotes improved aeration, which significantly impacts *Bacillus* species growth and scale-up impacts the production of xylanase. The development of extremely viscous and non-Newtonian broths, which significantly restrict mass transfer and homogeneity of the culture media, is one of the primary difficulties in submerged cultures of filamentous fungus. High agitation rates have been used by a number of writers to get around these restrictions, however excessive mechanical stress can cause hyphal rupture and cell injury (Martínez-Mira *et al*., 2025).

A study was revealed of the xylanase activity in stirred tank bioreactors increased from 3.99 to 52.76 IU/ml with an agitation rate of 310 rpm and aeration of 1.4 vvm. With distillers' dried grains with solubles (DDGS) as the primary feedstock, the results demonstrate the necessity of optimising culture conditions such aeration and agitation for increased production of hydrolytic enzymes by *A. niger* (Iram *et al*., 2022). According to a previous study, utilizing *Bacillus sp*., xylanase activity produced 23.47 U/mL under ideal circumstances of 30 °C, pH 8, and 127.27 rpm (Güler and Özçelik, 2023).

2.4.5. Carbon and Nitrogen Sources

Enzyme synthesis is typically increased when carbon and nitrogen sources are added to the growth medium because this creates a more favourable environment for microbial development. In order to achieved the highest enzyme production and possibly drastically lower xylanase production costs, it is imperative to screen for the important culture conditions and optimise the growing conditions (Dhaver *et al*., 2022). Pure sugars with high enzymatic productivity, such glucose and maltose, were the favoured carbon sources. Agro-industrial byproducts like sugarcane bagasse, rice straw, wheat straw, wheat bran, corn stover, corn cob, corn seed husk, soybean seed husks, and so on have been investigated as alternative fermentation substrates due to the high cost of pure sugar (Zhang *et al*., 2024; Jonathan *et al*., 2021). An essential structural component needed for the microbial system's metabolic functions is nitrogen.

Thus, the selection of a nitrogen source is crucial for the development of microorganisms, which in turn influences the total yield of enzymes. It has been determined that peptone, tryptone, soymeal, yeast extract, etc., are appropriate sources of nitrogen. Since various microorganisms have varying needs for these nitrogen sources, it is crucial to optimise the type of nitrogen source and concentration of nitrogen supply in the media (Bhardwaj *et al*., 2019). Moreover, there have some studies used the different organic and inorganic nitrogen sources as the nutritional parameters on the xylanase production using the microorganism (Bharti, Kumar, Alok, *et al*., 2018; Abena and Simachew, 2024b; Mandal, 2015).

Joshi *et al*. (2020) investigated that how the mycelium *Pleurotus ostreatus* grew on agricultural wastes such sugarcane, sawdust, and wheat bran, as well as their mixes. Because sugarcane and wheat bran contain vital nutrients, the authors found that these substrates had the fastest growth rates. Because *P. ostreatus* finds it difficult to obtain nutrients from sawdust, the sawdust substrate permitted the slowest growth rate. The mycelium cultivations are supported by the millimolar concentrations of macronutrients like carbon and nitrogen. Nitrogen from the supplement aids in the growing process (Rafiee *et al*., 2021). According to Dhaver *et al.* (2022), *Trichoderma harzianum* strain was utilized to produce xylanase, with wheat bran serving as the carbon source and ammonium sulphate [$(NH_4)_2SO_4$] serving as the nitrogen source.

According to the findings, the xylanase activity ranged from 9.8 to 68.7 U/ml. The xylanase activity, on the other hand, was dependent on the substrate

and type of pretreatment. Using an autoclave pretreatment and the microorganism *A. niger* CECT 2700, the maximum xylanolytic activity in surgacane bagasse and brewery spent grain was 1365.58 ± 13.81 and 1400.80 ± 43.91 U/gds, respectively. Moran-Aguilar *et al*. (2021) collected and presented these results. Abena and Simachew (2024b) used the white rot fungus to identify the 0.2% urea, yeast extract, ammonium sulphate, and peptone that function as a nitrogen source on the xylanase activity and the wheat strew that acts as a carbon source. Among the nitrogen sources tested, yeast extract had the highest xylanase production (75.65 ± 1.03 U/mL), followed by ammonium sulfate (59.06 ± 1.89 U/mL) when using the white rot fungus. The impact of several nitrogen sources on *A. niger* NFCCI 4113's xylanase production was also ascertained (Bharti *et al*., 2018).

2.4.6. Phosphate Source

The activity and stability of xylanase can be strongly influenced by the phosphate source utilized in the growth medium. Increasing xylanase activity and improving production efficiency can result from optimising the phosphate source, which may also lower expenses. A certain concentration of phosphate salts can promote the growth of organisms and the creation of extracellular enzymes in the production medium. Phosphate sources are used by microbes to synthesize phospholipids and nucleic acids on the cell wall (Sipriyadi *et al*., 2020). Microbes are necessary for the phosphorus-dependent synthesis of

coenzymes, phospholipids, and nucleic acids. In the cell, potassium functions as an inorganic cation and as an enzyme cofactor (Mardawati *et al*., 2018).

Phosphates would enhance mRNA stability by suppressing RNAase activity, which would boost the production of enzymes. In general, phosphates are needed by microbial cells as an energy source. Once more, a higher phosphate source led to less xylanase being produced. This showed that the organism grew because the available phosphate source increased the cellular energy pool, which, like other operon systems, suppresses the manufacturing of enzymes. The most effective inducer of microbial growth and enzyme synthesis is phosphate (Mandal, 2015).

Mandal (2015) investigated how various inorganic phosphates (0.02% w/v) affected *Bacillus cereus* BSA1's ability to produce xylanase. The presence of Na_2HPO_4 resulted in the highest xylanase production (5.53 ± 0.47 U/ml) among the examined phosphate sources, and 0.10% was the most effective concentration. Furthermore, a study using *Streptomyces costaricanus* 45l-3 demonstrated that the most favored phosphate source is Na_2HPO_4, which also has the highest xylanase activity (2.37 U/mL) among the phosphate sources (Sipriyadi *et al*., 2020). In the meantime, under ideal conditions, xylanase activity of 684.70 U/mL was attained with urea 0.35 g/L, potassium dihydrogen phosphate (phosphate source) 2.0 g/L, and ammonium sulphate (nitrogen source) 1.5 g/L (Mardawati *et al*., 2018).

2.4.7. Salts and Chemical (Metal Ions)

The metal salts and other substances can affect an enzyme's stability and kinetics by interacting with its active sites or by changing the structure of the enzyme. Furthermore, the creation of the enzyme-substrate complex may be interfered with by the development of enzyme-metal complexes, which would ultimately lead to the suppression of enzyme activity. However, metallic ions can function as a cofactor, altering the enzyme's structure to allow for the formation of an enzyme-substrate complex. Enzyme activity increased in the presence of metal ions, which might have been brought on by an alteration in the enzyme's structural conformation (Rashid *et al*., 2024).

The impact of metal salts and chemicals on the xylanase activity generated by *Neobacillus sedimentimangrovi* UE25 has been documented. Numerous metal salts and chemicals, including $FeSO_4$, $MgSO_4$, $CoCl_2$, NaCl, $CaCl_2$, $ZnSO_4$, $MnCl_2$, NH_4Cl, Tween 80, Trion X, SDS, urea and EDTA at concentrations of 1 and 5 mM, were used in this investigation. The study shown that when combined with this enzyme, several metals and compounds increased xylanase activity (Rashid *et al*., 2024). However, utilizing the *Trichoderma harzianum* strain, the impact of metal ions, including Ca^{2+}, Co^{2+}, Fe^{2+}, Mg^{2+}, Mn^{2+}, Zn^{2+}, K^{+}, and Na^{+}, on xylanase activity was also investigated and ascertained (Dhaver *et al*., 2022). In contrast, a variety of metal ions, including manganese, mercury, calcium, sodium, potassium, magnesium, and ferric, were chosen and their effects on *Bacillus cereus* BSA1's ability to produce xylanase were assessed. Since it was discovered that NaCl could produce the highest

xylanase activity, the effects of varying NaCl concentrations on xylanase synthesis were investigated (Mandal, 2015).

Metal ions have the effect of inhibitory or stimulatory which can affect the activity of enzymes since they could be bound with the sulfhydryl or carboxyl groups of the enzyme. Therefore, the enzymes may cause the conformational changes and destabilizing its molecular structure and eventually cause the enzyme activation or inactivation. Ca^{2+} ion as a divalent cation has stimulatory effect which can enhanced the enzyme activity (Dhaver *et al*., 2022; Abena and Simachew, 2024b; Suleman *et al*., 2020). Abena and Simachew (2024b) and Ping *et al*. (2018) mentioned that the effect of Ca^{2+} ion has the stimulatory effect which can enhanced the xylanase activity.

2.5. Design of Experiment (DoE)

Design of experiment (DoE) is a technique that is employed for planning experiments and analyzing the information obtained. It can make peoples to understanding how the process and the effect of product parameters on response variable, for example, processability, product performance or physical properties. DoE is a statistical tool used to understand the importance of specific processing and/or product variables, and how to optimise the system performance while maximizing properties by controlling them. This technique is applied by using a minimum number of experiments by varying several parameters systematically and obtaining sufficient information simultaneously. Then, a mathematical

model of the studied process is created according to the obtained data. Nowadays, there are several custom-designed software can be used to create the experimental designed, such as Design Expert, MINITAB, Chemoface and etc. Currently, DoE approach is used to improve the efficiency in screening for suitable experimental conditions, for example. for cell culture, nutrient complement, factor level, optimisation of a process, or robustness testing (Wagner Jr. *et al*., 2014; Whitford *et al*., 2018).

2.5.1. Plackett-Burman Design (PBD)

Plackett-Burman design (PBD) known as a fractional factorial design which were developed R.L. Plackett and J.P. Burman in 1946. PBD is used to calculate the variables selected with a minimum number of experiments, since this screening method can ignore the correlation between the variables. In general, PBD is an efficient statistical tool used to evaluate the effect of various variables including the physical and chemical parameters, which was applied in biological processes to optimise the production of metabolite (Gomes *et al*., 2025; Vanaja and Rani, 2007).

A type of orthogonal arrays was designed by Plackett and Burman (PB) for screening experiments, where the goal is to identify the most influential factors among a large set of potential variables. PB designs allow for unbiased estimation of main affects with a relatively small number of experiments. which yield unbiased estimates of all main effects in the smallest design possible. PBD

allows screening of various factors (n) in an ‘n+1’ run. A distinctive feature of PBD is the sample size, which is a multiple of four. The sample size is denoted as 4k observations, where k is equal to 1, 2, or any other positive integer. PBD is especially useful for investigating multiple factors, and it is commonly used for experiments with more than seven factors. In particular, PBD is well-suited for 'n x 4' experiment sand especially for n×4 experiments, such as 8, 12, 16, 20 etc. These designs can study up to 7, 11, 15, 19 factors, respectively. - PBD designs are referred to as saturated designs, enabling efficient separation of main effects and interaction effects (Das and Dewanjee, 2018; Lam *et al*., 2010; Vanaja and Rani, 2007). There is an example of PBD is shown in Table 3.6.

From the PBD, first-order polynomial [Eq. (2)] is generally used to depict the various factors effect on it based on the experimental results. Thus, the significant factors can be classify based on the analysis of the ANOVA of the estimated model. The PBD has a complex aliasing pattern, where each main effect is confounded with every two-way interaction not involving that effect. This makes it difficult to assess lack of fit and can lead to confounding of first-order effects with interaction effects (Das and Dewanjee, 2018; Vanaja and Rani, 2007).

2.5.2. Response Surface Methodology (RSM)

Response surface methodology, or RSM, is a statistical and mathematical method. for an empirical model which was developed by Box and Wilson (1951).

It is used for analyzing, improving and optimising the process when two or more quantitative parameters are involved (Bezerra *et al*., 2008; Mahallati, 2020). A functional relationship between interest response, y, and a number of correlated control or input variables, represented by $x_1, x_2, \ldots, x_k$, can be developed using this statistical tool. The relationship can be anticipated using a low-degree polynomial model in the form of equation [Eq. (1)] because it is unknown.

$$y = f'(x)\beta + \in \qquad \text{----- Eq. (1)}$$

where,

$x = x_1, x_2, \ldots, x_k$

$f'(x)$ = vector function of p elements that includes the cross-products of the powers of $x_1, x_2, \ldots, x_k$, and their powers.

β = vector of p parameters, which are unknown constant coefficients.

ε = random experimental error with a zero mean assumed.

There are two models are commonly used in RSM:

i. First degree polynomial model ($d = 1$) [Eq. (2)]

$$y = \beta_0 + \sum_{i=1}^{k} \beta_i x_i + \varepsilon$$

where y is the response function, β_0 is the constant and β_i is the linear coefficient, and x_i is the coded factor levels.

ii. Second degree polynomial model ($d = 2$) [Eq. (3)]

$$y = \beta_0 + \sum_{i=1}^{k} \beta_i x_i + \sum_{i<j} \sum \beta_{ij} x_i x_j + \sum_{i=1}^{k} \beta_{ii} x_i^2 + \epsilon$$

where y is the response, β_0, β_i, β_{ii}, and β_{ij} are the constant, linear, quadratic, and interaction coefficient terms respectively, x_i and x_j are the independent variables (Ahmad and Janahiraman, 2014).

There are various phases of RSM applications that can be used in the optimisation method, including independent variable screening, experimental design development based on the chosen experimental matrix, data treatment using mathematics and statistics, model fitness evaluation, identification and affirmation of the optimal condition, and obtaining the optimal values from each variable under study (Bezerra *et al*., 2008).

2.5.3. Central Composite Design (CCD)

Central composite designs (CCD) are a special type of response surface design that can fit a full quadratic model. They contain an embedded factorial or fractional factorial design with centre points. The centre points in a CCD are augmented with a group of star or axial points. Axial points are used to efficiently determine the coefficients of a second-degree polynomial for the variables. A CCD can be visualized as a cube with corners representing the product of levels. The axial points lie along the axes at or outside the cube, which helps to calculate curvature. Figrue 2.8 shows a graphical representation of CCD as shown as below (Das and Dewanjee, 2018).

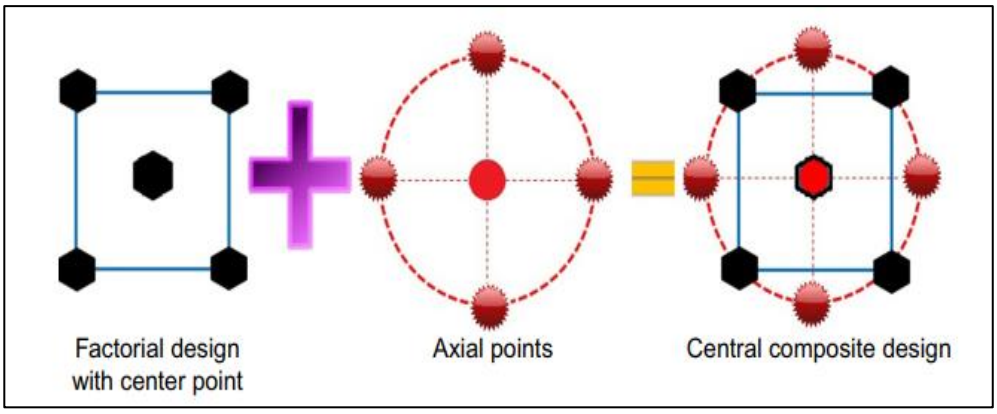

Figure 2.8: A graphical representation of central composite design (adapted from Das and Dewanjee, 2018).

Full uniformly routable central composite designs have specific characteristics. These designs require an experiment number based on the equation Eq. (4):

$$N = k^2 + 2k + c_p \qquad \text{----- Eq. (4)}$$

where N is the actual number of experiments, k is the factor number, c_p is the replicate number of the central point. In order to determine the local axial point, the alpha-values depend on the number of variables in CCD was identified and can be calculated by using the following equation [Eq. (5)]:

$$\alpha = 2^{(k-p)/4} \qquad \text{----- Eq. (5)}$$

For two variables, the alpha-values is the 1.41, while for three and four variables, the alpha-values are 1.68 and 2.00 respectively. All factors in full centrally routable designs are studied in five levels, for example, −α, -1, 0, +1, and +α. These designs provide systematic and comprehensive information. Full uniformly routable central composite designs involve multiple experiments to

gather precise data. All steps in the design are systematic and planned in advance. The design was developed to maximize information collection. It helps to create a detailed model of the response variable. A higher number of replicates provide a more accurate model.

Various steps involved in CCD was illustrated in Figure 2.9 (Bezerra *et al*., 2008). According to the Figure 2.9, the flowchart can be divided into three main phases, such as initial phase, analysis and decision. In the initial phases, it includes selecting process factors and their levels, determining the α-value, choosing the responses to be measured and conducting the experiments. In this phase, it is defining the experiments. After the initial phase, it is entered the next phase which is the analysis. This phase focuses on statistical analysis of the experimental data. It includes the model selection, performing an analysis of variance (ANOVA), and evaluating the model's fitness using tests, such as F-teat, lack of fitness, adjusted and predicted R^2 values, and adequate precision. This phase concludes with obtaining the model equation and comparing predicted values with actual values. Usually, this phase often visualized through the 2D and 3D contour graphs. The final phase, which is the decision, involves evaluating if the objective of the experiment has been achieved. If the objective is met, the process moves to optimisation and confirmation. However, if the experiment is failed to achieve the objective, the reasons are evaluated, and the process can be repeated from an earlier stage until the objective is achieved.

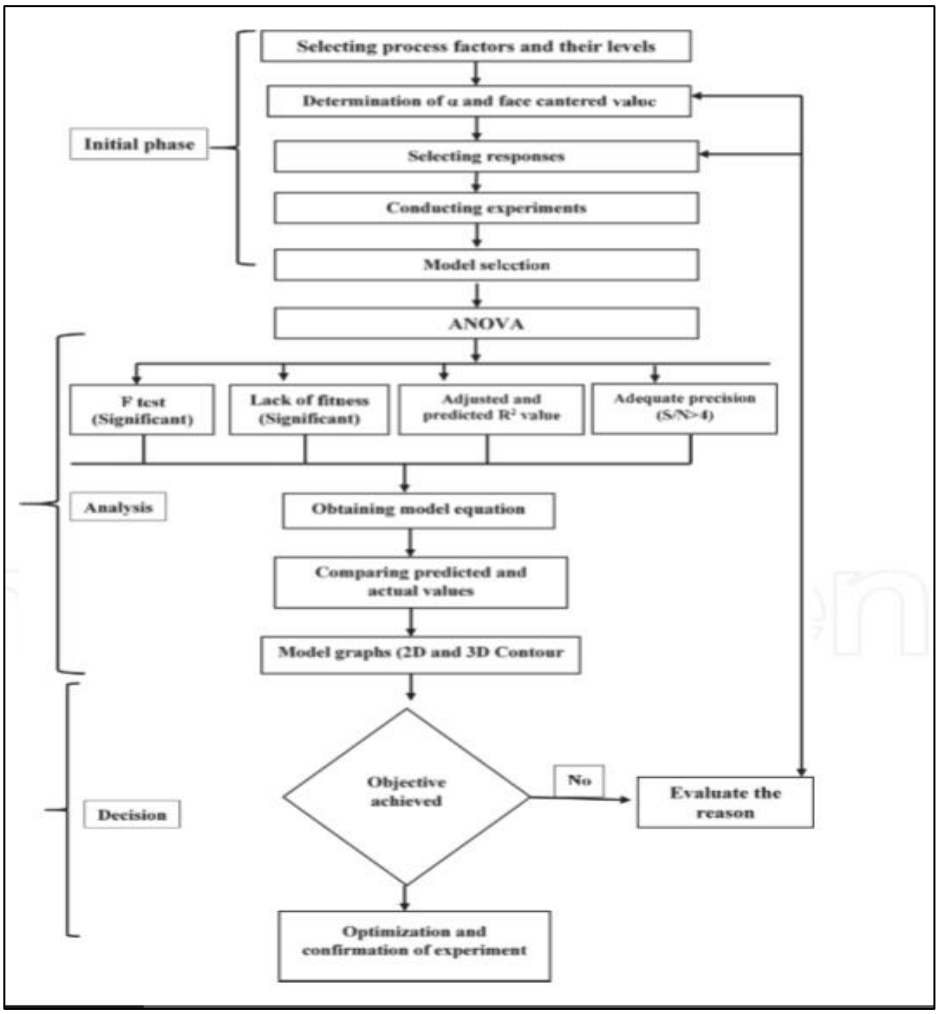

Figure 2.9: Flow schematic diagram for CCD (adapted from the Bhattacharya, 2021)

There are three types of CCD models, such as circumscribed design, inscribed design and face cantered design. The diagrams in Figure 2.10 illustrate the three types of central composite designs for two factors. CCI explores the smallest process space. On the other hand, CCC enjoys the largest process space. CCC models appear as a sphere spinning around the factorial cube. The descriptions for three types of the CCD models are presented and discussed in the Table 2.3 below (Bhattacharya, 2021).

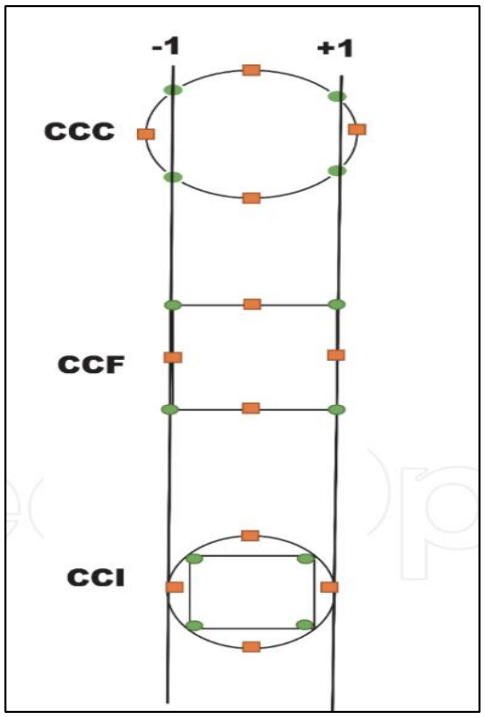

Figure 2.10: Comparison of the Three Types of Central Composite Designs (adapted from Ranade and Thiagarajan, 2017).

Table 2.3: Description for CCC, CCI and CCF

Model	Description
Circumscribed design (CCC)	CCC is the original form of the CCD. In central composite design, the levels of the factors eventually reach extreme points. A star point can establish new limits for the levels of the factors. These designs can be produced by supplementing an existing factor or factorial design with a star point. Each factor in a CCD model would have 5 levels. The design assumes circular, spherical or hyperspherical symmetry.
Inscribed design (CCI)	The CCI design utilizes factor settings as star points to create a factorial design within specified limits. This design is a modified version of the CCC design, where alpha is used to create the CCI model. The CCI and CCC designs are found to be a rotational model of each other.
Face cantered (CCF)	In this model, each face of the factorial space has star points as its center point. Thus, the variable α equals ±1. The design requires 3 levels of each factor. CCFs are a non-rotatable type, as opposed to other designs.

2.5.4. Box-Behnken Design (BBD)

In 1990, George E. P. Box and Donald Behnken have proposed the BBD, which the most distinctive feature of the proposals for a spherical domain. This domain has the specify property where each factor takes only three levels. This makes it possible to estimate the mathematical model's first- and second-order coefficients effectively. The building of balanced incomplete block designs serves as the foundation for this design lesson. Three blocks make up the design for the three variables; two variables are combined in each block using a 22-factorial design, while the third variable is kept at level zero. A number of center points have also been added. Observe that every point on the BBD is situated on a $\sqrt{2}$-radius sphere. Furthermore, there are no points at the vertices of the cubic region formed by the upper and lower bounds for each variable in this design. By comparing to others statistical method, BBD is more efficient and economical then their corresponding 3k designs, mainly for a large number of variables (Ranade and Thiagarajan, 2017; Sarabia *et al*., 2009; Ahmad and Janahiraman, 2014).

The response surface design's complete quadratic model can be accommodated by the box design. Unlike CCD, BBD does not include embedded factorial or fractional factor designs. As seen in Figure 2.11, the treatment combinations in this design are located at the center and halfway between the cube's edges. BBD requires three levels for every factor and is a rotatable design. When doing tests with more than two factors and when it is

expected that the optimum will fall somewhere in the middle of the factor ranges, BBD should be considered (Das and Dewanjee, 2018).

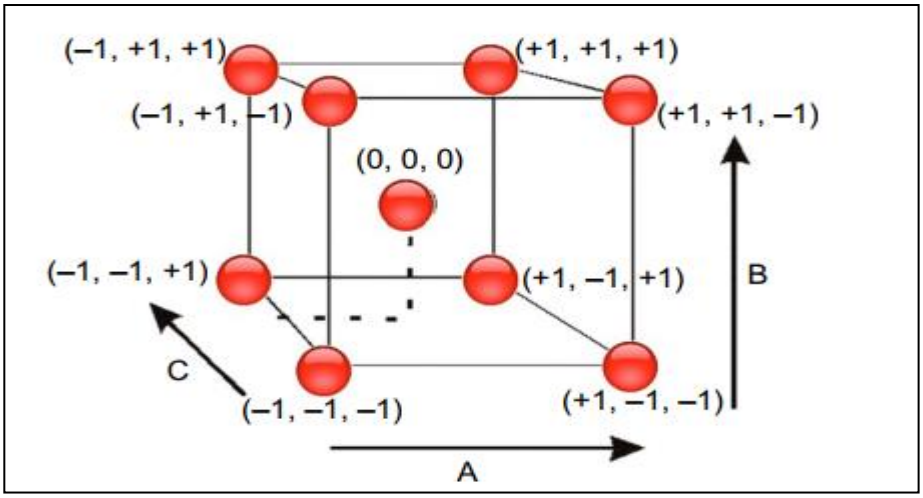

Figure 2.11: A graphical representation of Box-Behnken Design (adapted from Das & Dewanjee, 2018).

In BBD, experimental points are on a hypersphere equidistant from the central point. The design applies to multiple factors and places points at equal distance from the center. Factor levels are adjusted at three levels: +1, 0, and -1. These levels are at equally spaced intervals, providing a range for analysis. The spacing between levels allows for better understanding of the data collected. An experiment number can be determined using the equation [Eq. (6)]

$$N = 2k(k-1) + c_p \qquad \text{----- Eq. (6)}$$

where N is the number of trials, k is the number of factors and c_p is the number of replicates for the centre points. This approach helps in the efficient use of resources in experimentation. It benefits researchers by providing useful insights into the data collected. Optimisation research involving emulsion creation,

enzyme tests, etc. have made use of such designs (Ahmad and Janahiraman, 2014; Ranade and Thiagarajan, 2017; Sarabia *et al*., 2009).

CHAPTER 3

METHODOLOGY

3.1. Material and Equipment

3.1.1. Chemical Reagent

All chemical reagents used throughout the study period were of analytical grade and commercially purchase from local established chemical companies. All the materials related to this study are stated in the Table 3.1.

Table 3.1: List of chemical reagents

Chemical Reagents	Function
70% Ethanol	To kill microbe.
Distilled water	Use for washing, cleaning and mixing ingredients.
Dilute sodium hydroxide, NaOH 0.1M of NaOH	Use for pH adjustment.
2M of NaOH	Ingredient for making DNS reagent solution.
0.1M of hydrochloric acid, HCl	Use for pH adjustment.
Potato Dextrose Agar (PDA)	Use as a medium for growing fungi genera.
Tween-80 0.1% (v/v)	Ingredient for making Mendel's and Sternburg medium.
1.0% (v/v)	Use to make spore suspension.

Xylan	Ingredient for making Mendel's and Sternburg medium.
Ammonium nitrate, NH_4NO_3	Ingredient for making Mendel's and Sternburg medium.
Dipotassium hydrogen phosphate, K_2HPO_4	Ingredient for making Mendel's and Sternburg medium.
Magnesium sulfate heptahydrate, $MgSO_4 \cdot 7H_2O$	Ingredient for making Mendel's and Sternburg medium.
Calcium chloride, $CaCl_2$	Ingredient for making Mendel's and Sternburg medium.
Ferrous sulfate heptahydrate, FeSO4•7H2O	Ingredient for making Mendel's and Sternburg medium.
Manganese (II) sulfate tetrahydrate, MnSO4•4H2O	Ingredient for making Mendel's and Sternburg medium.
Zinc sulfate heptahydrate, ZnSO4•7H2O	Ingredient for making Mendel's and Sternburg medium.
Cobalt chloride hexahydrate, $CoCl_2 \bullet 6H_2O$	Ingredient for making Mendel's and Sternburg medium.
0.05M citrate buffer	Use for collection of enzyme.
3,5-dinitrosalicylic acid (DNS)	Ingredient for making DNS reagent solution.
Potassium tartrate tetrahydrate, $KNaC_4H_4O_6 \cdot 4H_2O$	Ingredient for making DNS reagent solution.

3.1.2. Apparatus

Apparatus includes all kinds of small unit functional tools that aid in conducting experiment. Table 3.2 shows list of the apparatus that were used in the experiments of this study.

Table 3.2: List of apparatus

Materials	Function
Erlenmeyer flask	To contain and inoculate the sample for microbial cultures
Aluminium foil	To seal the mouth of Erlenmeyer flask and media before autoclaving
Cotton plunger	To plug the Erlenmeyer flask for prevention of contaminant
Weighing boat	To contain the material that has been weighed
Inoculating loop	– Use for cultivation of microbes on plates by transferring inoculum. – Use to take and transfer a small sample of the *A. niger* to new culture medium gently.
Spatula	– To transfer the material or sample – To stir liquid substance –
Petri dish	Used for agar solidification and culture the microbes
Petri dish with cover	Used as a container for biomass analysis of sample.
Filter paper	For filtration purpose
Micropipette and tips	To transfer the specific volume of the material or sample
Glove and mask	To prevent the contamination of the sample and perform under aseptic condition
Cuvettes	To hold samples for measuring the absorbance of the sample.
Dropper	Used to measure and transfer small quantity of reagent or solution.
Parafilm	To seal the media
Haemocytometer	To place the culture under the light microscope for observing
Cover slip	To cover the culture und the light microscope for observing
Magnetic stirrer	To employ a rotating magnetic field for string and mixing the agar solution in flask
Bunsen burner	Used for flame sterilization for inoculation loop.

Beaker	To hold the liquid in large amount.
Measuring cylinder	To measure the volume of liquid sample
Test tube	To hold and transfer chemical reagent or sample waste.
Test tube stand	To keep and stand for a few numbers of test tubes.
Conical flask	- - To hold the chemical reagent. - Used as a container for pre-culture of *A. niger*. - Used as a container for incubation process.
Microfuge tube	Used as a container to store sample for centrifuge.

3.1.3. Equipment

Table 3.3 shows the list of equipment that were used in the experiments of this study.

Table 3.3: List of equipment

Equipment	Brand/Model	Function
Laminar flow	Edamas	Provide an aseptic environment for inoculation, transfer media and microbial cell.
Chiller (4°C)	REMI	To store PDA plates
UV-Vis spectrophotometer		To determine the absorbance of the sample for evaluate the microbial growth.
Water bath	Memmert	Use for heating sample in constant temperature.
Autocalve	HIRAMAYA	To sterilize the agar medium
Incubator shaker	LabTech	To provide agitation or shaking to introduce oxygen transfer uniformly during incubation

Oven	Memmert	To dry the sample biomass or apparatus
Analytical balance	Kern ABJ	To measure small quantity in the sub-milligram ranges samples.
Hotplate stirrer	IKA	To heat and mix well the agar solution with magnetic stirrer
Light microscope		To observe and count the spore suspension in haemocytometer.
pH meter	Mettler Toledo	To measure the pH of solution.

3.2. Research Flow Chart

Figure 3.1 shows the flow chart of xylanase production using *Aspergillus niger.*

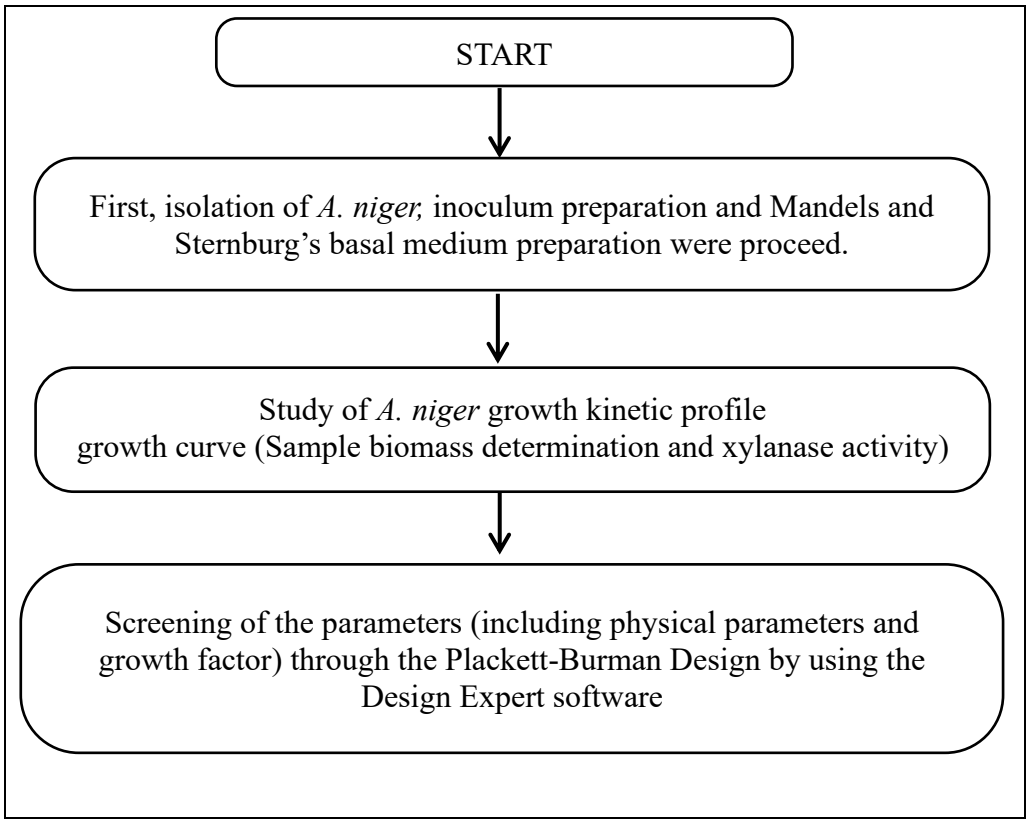

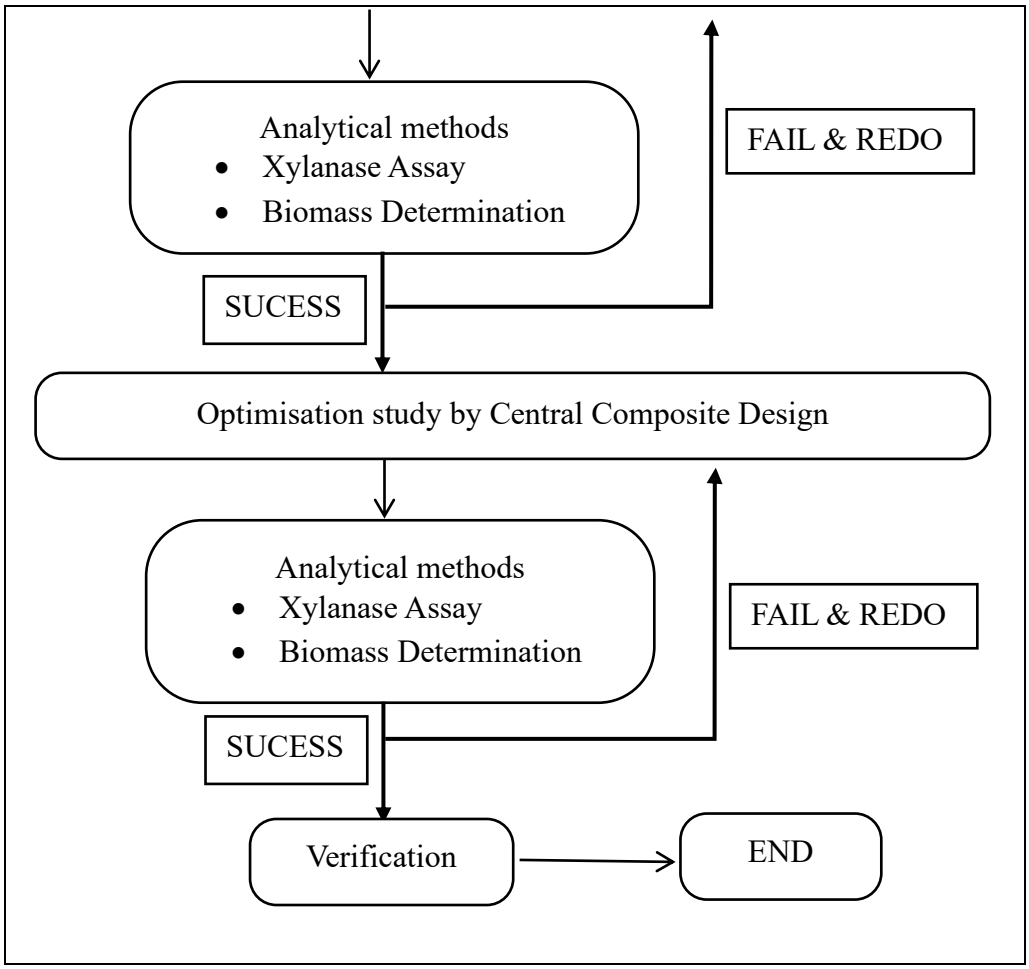

Figure 3.1: Flowchart for the xylanase production by *A. niger*.

3.3. Microorganism Maintenance

The fungal strain identified as *Aspergillus niger (A. niger)* was obtained from Universiti Tunku Abdul Rahman (UTAR). The strain was maintained on Potato Dextrose Agar (PDA) slants by monthly transfer and was stored at 4°C for storage.

3.4. Inoculum Development

A mother culture of *A. niger* on an agar plate that was 4–6 days old was mixed with 10 mL of 1% (v/v) Tween-80 sterile distilled water to create spore suspension. In order to prepare the inoculum, the agar surface was gently scraped using the sterilized inoculating loop. Mycelia were then eliminated from the suspension by sieving it through Whatman no. 1 paper. To obtain the proper concentration for spore counting in a hemocytmeter, the dilutions were carried out correctly. The inoculum sizes (2 x 10^6 spores/mL) were assessed by direct microscopic examination using a hemocytometer following the proper dilution (Ajijolakewu *et al*., 2017; Rodriguez-Tudela *et al*., 2003).

3.5. Construction of Fungal Growth Profile

A 1 mL aliquot of fungal isolate spores suspension with an inoculum size of 2 x 10^6 spores/mL was added to 100 mL of Mandels and Sternburg's basal medium and 5.0 g/L xylan in 250 mL of Erlenmeyer flasks and incubated at 32ºC at 150 rpm for 7 days. Composition of the growth medium includes: 2.0 g/L NH_4NO_3, 2.0 g/L K_2HPO_4, 1.0 g/L $MgSO_4 \cdot 7H_2O$, 0.3 g/L $CaCl_2$, and 0.012 g/L trace elements: 5.0 mg/L $FeSO_4 \cdot 7H_2O$, 1.6 mg/L $MnSO_4 \cdot 4H_2O$, 3.45 mg/L $ZnSO_4 \cdot 7H_2O$, and 2.0 mg/L $CoCl_2 \cdot 6H_2O$, and 0.1% (v/v) Tween 80 (Ajijolakewu *et al*., 2017).

Twenty-two flasks in total, including the control, were employed, and one flask was taken out of the rotary shaker each day for sampling. Following a 24-hour oven-drying period at 60ºC, the cells were filtered through Whatman filter paper No. 1, and their mycelial dry weight was measured. The dry cell weights (g/L) and the xylanase activity (U/mL) plotted against the incubation period (days) were used to create the *A. niger* growth curve.

3.6. Submerged Fermentation (SmF)

Xylanase biosynthesis was performed in a 250 mL Erlenmeyer flask using SmF in a production medium containing 100 mL of Mandels and Sternburg's basal medium and 5.0 g/L of xylan as carbon source. Composition of the growth medium has been stated in the earlier section. Prior to sterilization, the medium's pH was brought down to 5.0 at 121°C for 15 minutes. After aseptically inoculating the medium with an aliquot of 1 mL of standardized inoculum (2 x 10^6 spores/mL), fermentation proceeded to agitate at 150 rpm and continue for five days at 32°C. 50 mL of 0.05 M sodium acetate buffer (pH 4.8) was used to extract the crude enzyme. The entire flask will be in a rotary incubator set at 150 rpm (32°C) for 15 minutes after the buffer has been added. The filtrate, which was extracted from the cell using Whatman no. 1 filter paper, was centrifuged for 15 minutes at 4°C at 10,000 rpm. The crude enzyme will be extracted from the supernatant.

3.7. Design of Experiment for Screening and Optimisation

3.7.1. Screening of the Parameters Affecting Xylanase production with Plackett-Burman Design (PBD)

Screening of parameters that can affect xylanase production was conducted using a Plackett-Burman Design (PBD). To investigate the effects of various culture conditions, the PBD was employed as a preliminary step in the optimisation process. There are 11 parameters of culture conditions (growth factors and physical factors) were used as a fractional factorial design with certain combination in this design. Software used in this study is Design Expert version 11.1.2.0.

The 10 parameters that manipulated were temperature of incubation, pH, incubation time, agitation rate, xylan, NH_4NO_3, K_2HPO_4, $CaCl_2$, $MgSO_4{\cdot}7H_2O$, and $FeSO_4{\cdot}7H_2O$. Each parameter was varied into few sets of experiments. The range for each parameter was stated in the Table 3.4 and Table 3.5 as shown as below. Based on previous studies, these 10 parameters were selected as possible factors affecting xylanase production, with responses based on dry cell weight and xylanase activity. Then, these parameters were tested at two distinct levels, for example, high and low, represented by "+" and "-" respectively. Since this design would not describe the interaction, the highest p-value of variables and over 95% of confidence level was considered as highly significant (Bajpai, 2014a; Maan *et al*., 2016). One dummy variable (X11) was studied in 11 experiments to calculate the standard error (Wang *et al*., 2018). Levels of factor chosen and factor coded for PBD are given in Table 3.6.

Table 3.4: Ranges for different 4 physical parameters

Physical Parameters	Ranges
Temperature (ºC)	30-40
pH	6.0-8.0
Incubation time (days)	1-7
Agitation rate (rpm)	100 – 200

Table 3.5: Ranges for different 6 chemical parameters

Chemical Parameters	Ranges
Xylan (g/L)	1.0 - 3.0
NH_4NO_3 (g/L)	1.0 - 3.0
K_2HPO_4 (g/L)	1.0 - 3.0
$CaCl_2$ (g/L)	0.5 -1.0
$MgSO_4 \cdot 7H_2O$ (g/L)	0.3 – 0.7
$FeSO_4 \cdot 7H_2O$ (mg/L)	0.01 – 0.05

Table 3.6: Plackett-Burman experimental design matrix for screening the media composition and culture condition for xylanase production

Trial	Variables										
	X1	X2	X3	X4	X5	X6	X7	X8	X9	X10	X11
T1	1 (5)	-1 (6)	1 (40)	-1 (100)	-1 (1)	-1 (1)	1 (3)	1 (0.7)	1 (1.0)	-1 (0.01)	1
T2	-1 (3)	-1 (6)	1 (40)	1 (200)	1 (3)	-1 (1)	1 (3)	1 (0.7)	-1 (0.5)	1 (0.05)	-1
T3	-1 (3)	-1 (6)	-1 (30)	-1 (100)	-1 (1)	-1 (1)	-1 (1)	-1 (0.3)	-1 (0.5)	-1 (0.01)	-1
T4	1 (5)	1 (8)	-1 (30)	1 (200)	1 (3)	-1 (1)	1 (3)	-1 (0.3)	-1 (0.5)	-1 (0.01)	1
T5	-1 (3)	1 (8)	1 (40)	-1 (100)	1 (3)	-1 (1)	-1 (1)	-1 (0.3)	1 (1.0)	1 (0.05)	1

T6	1 (5)	1 (8)	-1 (30)	1 (200)	-1 (1)	-1 (1)	-1 (1)	1 (0.7)	1 (1.0)	1 (0.05)	-1
T7	-1 (3)	-1 (6)	-1 (30)	1 (200)	1 (3)	1 (3)	-1 (1)	1 (0.7)	1 (1.0)	-1 (0.01)	1
T8	1 (5)	1 (8)	1 (40)	-1 (100)	1 (3)	1 (3)	-1 (1)	1 (0.7)	-1 (0.5)	-1 (0.01)	-1
T9	1 (5)	-1 (6)	1 (40)	1 (200)	-1 (1)	1 (3)	-1 (1)	-1 (0.3)	-1 (0.5)	1 (0.05)	1
T10	-1 (3)	1 (8)	1 (40)	1 (200)	-1 (1)	1 (3)	1 (3)	-1 (0.3)	1 (1.0)	-1 (0.01)	-1
T11	-1 (3)	1 (8)	-1 (30)	-1 (100)	-1 (1)	1 (3)	1 (3)	1 (0.7)	-1 (0.5)	1 (0.05)	1
T12	1 (5)	-1 (6)	-1 (30)	-1 (100)	1 (3)	1 (3)	1 (3)	-1 (0.3)	1 (1.0)	1 (0.05)	-1

*The variables represent as X1 – pH, X2 – temperature (ºC), X3 – Incubation time (day), X4 – agitation rate (rpm)., X5: xylan (g/L), X6 – NH_4NO_3, X7 – K_2HPO_4, X8 – $CaCl_2$, X9:$MgSO_4 \cdot 7H_2O$, X10 – $FeSO_4 \cdot 7H_2O$, and X11- dummy.

3.7.2. Optimisation of Parameters that Affecting Xylanase Production

Central Composite Design (CCD) of the Design expert version 11.1.2.0 was utilized to optimise the environment for *A. niger*'s synthesis of xylanase employing response surface methods. Based on preliminary data before optimisation, xylanase production was optimised for five days. To confirm the impacts of factors on xylanase production, 13 runs total — including 4 factorial points, 4 axial points, and 3 center points in triplicate — were conducted independently. Table 3.7 displays the statistical combination of the independent variables' real and coded values.

$CaCl_2$ (X2) and the incubation pH (X1) were the variables examined in this model. Three levels were assigned to each parameter: low (-1), medium (0), and high (+1). To create a model for enzyme activity (U/mL), the ideal pH and CaCl values obtained during CCD optimisation were utilized as functions. Regression and ANOVA analysis were used to analyze the model.

Table 3.7: Experimental design using Central Composite Design (CCD) with three center points.

Run	Coded Level		Real Values	
	X_1 (°C)	X_2 (pH)	X_1 (pH)	X_2 (g/L)
1	0	0	7.0	0.75
2	+1	+1	8.0	1.00
3	+1	0	8.0	0.75
4	-1	0	6.0	0.75
5	0	0	7.0	0.75
6	-1	-1	6.0	0.50
7	0	+1	7.0	1.00
8	+1	-1	8.0	0.50
9	0	0	7.0	0.75
10	0	-1	7.0	0.50
11	0	0	7.0	0.75
12	0	0	7.0	0.75
13	-1	+1	6.0	1.00

3.8. Analytical Method

In this study, two analytical methods were used to measure mycelial dry cell weight and xylanase activity: biomass determination and the 3,5-dinitrosalicylic acid (DNS) method, respectively. These two analytical methods were used in the *A. niger* growth kinetic profile to find the optimum period. Moreover, the DNS method was used for screening and optimisation to identify the optimal conditions for the highest xylanase activity.

3.8.1. Biomass Determination

This method was used to measure the dry cell weight before plotting a graph of dry cell weight (g/L) versus incubation time. Sampling was done by collecting one flask from the rotary shaker every day. First, the tray was weighed and recorded on the analytical balance before sampling. Then, the cells were filtered using Whatman filter paper no. 1, and their mycelial dry weight will be determined after drying at 60 °C for 24 hours in the oven. A triplicate set of fungi was incubated simultaneously to enhance data accuracy. Then the growth curve of *A. niger* was determined by plotting mycelial dry cell weight versus incubation time.

3.8.2. Xylanase Assay

Using 1% xylan in 0.05 M citrate buffer (pH 5.0), xylanase activity was measured. The 3,5-dinitrosalicylic acid (DNS) technique with a xylose standard curve was used to measure the release of reducing sugars. The quantity of enzyme needed to release one μmol of reducing sugars per minute is known as one unit (U) of enzyme activity. 50 mg of xylan was used as the substrate in the reaction mixture, which also contained 1.0 mL of sodium acetate buffer. 1.0 mL of the crude enzyme from the culture-filtered supernatant was added to this solution. After that, the mixture was incubated for 30 minutes at 50°C in a water bath. 3,5-dinitrosalicylic acid and xylose were used as indicators to measure the amount of released reducing sugar. After five minutes of boiling in a water bath at 95°C to develop the color, absorbance was measured at 540 nm using a UV/vis spectrophotometer (Bhardwaj *et al*., 2017).

The main problem that can alter xylanase activity in the DNS test is the impact of inorganic salts. During the incubation period, the present of the inorganic salts can directly increase or decrease the rate at which the formation of the xylose from the xylan. Higher reducing sugar levels and increased absorbance in the DNS assay indicate enhanced xylanase activity, which may be promoted by activating salts. Conversely, lower reducing sugar levels and lower absorbance readings suggest reduced xylanase activity due to inhibitory salts (El-Gendi *et al*., 2023; Sokač *et al*., 2023).

CHAPTER 4

RESULT AND DISCUSSION

4.1. Constructing the Time Course Profile for the Growth and Xylanase Productivity Using *Aspergillus niger* (*A. niger*)

In this study, a growth curve was constructed to determine the time course profile for the growth and xylanase productivity of *Aspergillus niger* (*A. niger*). The growth curve, which reflects the growth profile of *A. niger*, is shown in Figure 4.1**.** The fungal growth curve is significant due to it can provide a framework to understand how the fungi grow and produce valuable products. It was used to visually represent and analyse the stages of fungal population increase over time. By analysing the fungal growth curve, we can determine the optimal conditions, for example, the optimum incubation time for cultivating fungi to maximize the xylanase production in this study (Sagal Aryal, 2022; Pasrija and Kumari, 2025).

In this study, there are two primary responses were selected for analysis: mycelial dry cell weight (g/L) and xylanase activity (U/mL). These parameters were measured to monitor the growth and enzyme production during the experiment. The detailed data corresponding to the construction of the growth curve for *A. niger* are provided in Appendix C (Tables C.1 and C.2).

4.1.1. Growth Curve Phases and Interpretation

The growth curve in Figure 4.1 can be divided into four distinct phases: the lag phase, log (exponential) phase, stationary phase, and death phase. Each phase represents specific metabolic and growth dynamics of *A. niger*.

As shown in Figure 4.1, the lag phase occurs between Day 0 and Day 1, where the organism adapts to its new environment. During this period, the fungal cells undergo physiological adjustments, including the synthesis of enzymes necessary for metabolizing available nutrients in the basal medium. There is minimal or no cell division during the lag phase, as the organism focuses on internal preparations before growth and reproduction commence (Ughy *et al*., 2023; Yates and Smotzer, 2007; Willey *et al*., 2020).

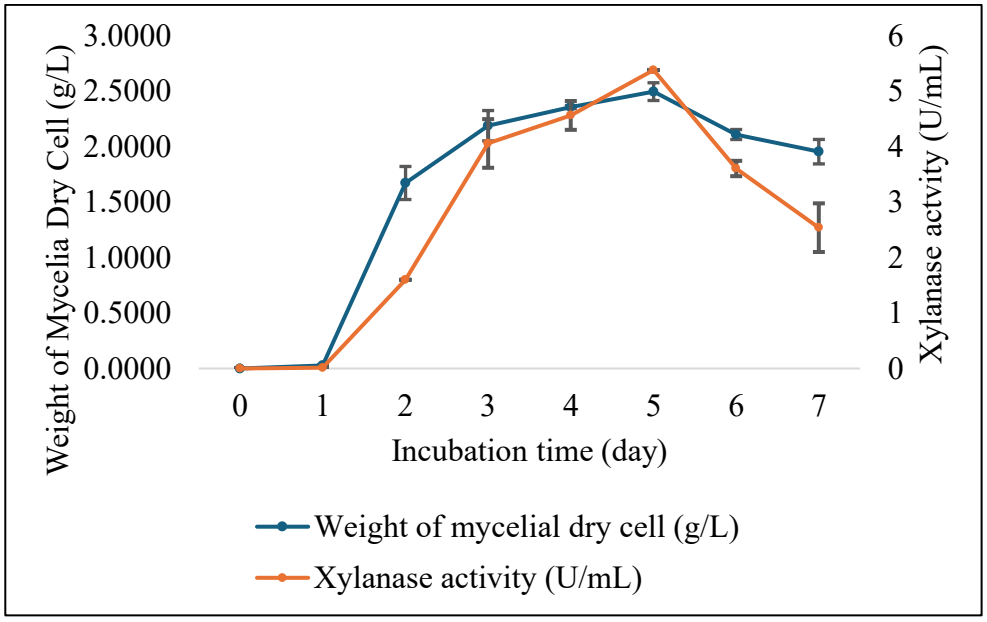

Figure 4.1: Growth profile of *A. niger*

Following the lag phase, *A. niger* enters the exponential phase between Day 1 and Day 3, as depicted in Figure 4.1. During this phase, both mycelial dry cell weight and xylanase activity increase dramatically. The cells are dividing at their maximum rate, leading to exponential growth. This phase is characterized by rapid mycelium development, which forms clumps or microcolonies under optimal growth conditions (Krijgsheld *et al*., 2013). The rapid increase in both mycelial dry cell weight and xylanase activity reflects the high metabolic activity during this stage. According to Ughy *et al*. (2023) and Willey *et al*. (2020), microbial growth rate is strongly influenced by the nutrient composition of the culture medium, with enriched nutrient conditions supporting faster growth.

After Day 3, *A. niger* enters the stationary phase, during which growth slows and eventually stabilizes between Day 3 and Day 5 (as shown in Figure 4.1). In this phase, the rate of cell division is balanced by the rate of cell death, leading to a plateau in both mycelial dry cell weight and xylanase activity. This can be attributed to nutrient depletion, accumulation of toxic metabolic byproducts, and possible space constraints within the closed culture system (Ughy *et al*., 2023; Willey *et al*., 2020). Although cell division may slow or cease, the fungal cells remain metabolically active, and the mycelium continues to grow, albeit at a reduced rate.

After Day 5, both mycelial dry cell weight and xylanase activity begin to decline sharply, marking the entry into the death phase (as shown in Figure 4.1). This decline is attributed to environmental factors such as nutrient exhaustion and accumulation of toxic waste products, which can impair cellular function

and lead to cell death. In this phase, the population of viable *A. niger* cells decreases as a result of these detrimental conditions (Willey *et al*., 2020; Ughy *et al*., 2023).

The growth curve phases observed in Figure 4.1 correlate with typical microbial growth patterns under nutrient-limited conditions. The early exponential phase represents the rapid increase in mycelial biomass and enzyme production, whereas the stationary and death phases highlight the effects of nutrient limitations and waste accumulation on both growth and productivity. The relationship between mycelial dry cell weight and xylanase activity provides valuable insight into the microbial production of industrial enzymes. A well-coordinated balance between fungal biomass accumulation and enzyme production is essential for maximizing xylanase yield in industrial applications.

4.1.2. Optimised Growth Conditions and Productivity

Based on the data presented in Figure 4.1 and the corresponding tables in Appendix C (Tables C.1 and C.2), the optimal growth time for *A. niger* was determined to be Day 5. During this period, the highest mycelial dry cell weight of 2.4975 g/L and the highest xylanase activity of 5.3842 U/mL were observed. These findings suggest that Day 5 represents the point at which both growth and enzyme production are maximized. Therefore, Day 5 was chosen as the optimum time for further optimisation steps in this study.

Meanwhile, the observed peak in xylanase activity during Day 5 aligns with the conclusion drawn from the growth curve, where the stationary phase's metabolic stability coincides with optimal enzyme production. This time point was selected for subsequent screening and optimisation processes aimed at maximizing xylanase yield.

4.2. Screening of Physical and Chemical Parameters for the Production of Xylanase from *A. niger* in SmF by Using the Plackett-Burman Design (PBD)

In this study, a total of 10 variables and 1 dummy variable were analysed with regard to their effects on xylanase production using a Plackett-Burman Design (PBD). These variables were examined for their physical and chemical impacts on the enzyme production process, with subsequent discussions and results presented in the later sections. The PBD was designed and executed using Design Expert Software (Version 11). The xylanase production was measured by transferring an aliquot of 1 mL of spore suspension containing *A. niger* at 2 x 10^6 spores/mL into Mandels and Sterrnburg's basal medium.

4.2.1. Effect of Physical and Chemical Parameters for the Production of Xylanase from *A. niger* through PBD

In this study, a statistical method, named PBD was used to filter and determine the effect of various parameters that can affecting the production of xylanase from *A. niger.* The efficiency of PBD as a statistical method makes it ideal for this screening phase (Siwach *et al*., 2024). A total of 10 parameters, including four physical parameters were selected, including 4 physical parameters (e.g., incubation time, pH, temperature, and agitation speed) and 6 chemical parameters (concentration of xylan, ammonium nitrate (NH_4NO_3), dipotassium hydrogen phosphate (K_2HPO_4), magnesium sulphate ($MgSO_4$), calcium chloride ($CaCl_2$), and iron sulfate heptahydrate ($FeSO_4 \bullet 7H_2O$))

Incubation time is critical physical parameter influencing enzyme production by fungi. Usually, the optimum incubation period is indicated that the greatest production of xylanase enzyme in SmF. The physical and nutritional factors, such as the nature of substrate, organism, addition of nutrient, and many others fermentable conditions that can affect the xylanase productivity using the fungi (Mostafa *et al*., 2014). Typically, the optimal incubation period for xylanase production is between 3 to 7 days, although the optimal range may vary depending on the fungal species and environmental conditions (Ali *et al*., 2017). In this study, the incubation time was adjusted between 3 to 5 days, based on the growth and xylanase production curves observed in Figure 4.1.

Agitation plays an important role in transporting the dissolved oxygen from the gaseous phase through the liquid phase to the microbial cell. Moreover, agitation also can provide a homogenous nutrient availability by mixing the nutrient, at the same time, it can remove the waste products in the basal medium. An additional advantage of the agitation effect is to reduce the size of mycelial aggregates which can making the oxygen more easily to access to the microbial cell. However, high agitation can cause the cell damage through the strong shear stress which can physically damage the fungal mycelial and rupture cellular structures, leading to lower the enzyme activity. There is a study reported that the higher xylanase activity of *A. niger* SS7 was shown at 200 rpm while lower xylanase activity was shown at 100 rpm and 300 rpm (Abdella *et al*., 2020; Rafiee *et al*., 2021; Bakri *et al*., 2011; Najafpour, 2015). The agitation rate for the study was varied between 100 rpm to 200 rpm, based on previous research.

Temperature affects the growth and metabolism of *A. niger*, with higher temperatures increasing the rate of enzymatic reactions. However, beyond an optimal temperature, enzyme denaturation and microbial damage can occur (Ali *et al*., 2017; Tsegaye *et al*., 2019; Maan *et al*., 2016; Agustí-Brisach and Armengol, 2012). For most *Aspergillus* species, an optimal range for xylanase production typically between 28 °C and 37 °C. It can be said that the exact optimum temperature depends on the specific species and strain, which can be vary between different *Aspergillus* species. For example, the optimum temperature for *A. niger* at 20 – 40 °C. There is a study stated that the increases xylanase production by *A. niger* GIO when increasing the temperature from 30 °C to 40 °C. Also, it found that the highest xylanase activity at 40 °C with 3.67

U/mL after 30 minutes incubation time. While the xylanase activity starts to decrease when the temperature above 40 °C (Fasiku *et al*., 2023; d'Halewyn and Chevalier, 2025). Therefore, the temperature range for this screening was chosen between 30°C to 40°C.

The effect of the pH to xylanase activity and xylanase production has been discussed in the section 2.4.2. pH influences enzyme stability and microbial metabolism. By increasing or controlling the medium pH, it can cause the changing in the enzyme stability and denaturing by deactivating the enzyme activities. In this study, *A. niger* was chosen as the producer to produce the xylanase enzyme. Except the xylanase enzyme, there are several types of extracellular enzymes can be produced, such as cellulases (endoglucanse, exoglucanase and β-glucosidase) From the previous studies, the optimal pH value for producing the extracellular enzyme from the *Aspergillus* species in the range of 4.0 to 5.0. For example, pH 5.0 for producing cellulase from the *A. niger, A. foetidus,* and *A. oryzae* was frequently cites as the optimum for both cellulase and xylanase production. An optimum cellulase production appeared at pH 7.0 with temperature of 35 °C from *Aspergillus* sp. IN5 (Akula and Golla, 2018; Li *et al*., 2018; Boondaeng *et al*., 2024; Bhardwaj *et al*., 2017). . The pH range used in this study was between 6.0 to 8.0, which is ideal for *A. niger* growth and enzyme activity.

Xylan, a polysaccharide in plant cell walls, serves as the carbon source for *A. niger* growth and stimulates xylanase production (Bajpai, 2014c). When the xylanase enzyme is produced, the simpler monosaccharide and xylo-

saccharide are produced by breaking down the xylan through the hydrolysis process (Bueno and Brienzo, 2025; Bhardwaj *et al*., 2019). In this study, the range of 1.0 g/L to 3.0 g/L was selected based on literature values. Ammonium nitrate (NH_4NO_3) as an inorganic nitrogen source, is critical for xylanase productivity. Previous studies have shown its role in enhancing xylanase activity (Modi *et al*., 2011; Mandal, 2015). In this study, 1.0 g/L to 3.0 g/L of NH_4NO_3 was selected based on literature values.

Phosphates are essential for microbial growth and enzyme synthesis, influencing energy metabolism. Phosphate is used to inhibit the activity of RNAase which it might can increase the mRNA stability. Therefore, it can increase the production of enzyme. Although the phosphate can increase the enzyme productivity, it also can cause the decrease the xylanase production by increasing the amount of phosphate. On the other view, it can be explained that the suitable phosphate source induced the organism growth by strengthening the cellular energy pool, which repress the enzyme biosynthesis like other operon systems (Mandal, 2015; Maan *et al*., 2016). In this study, dipotassium hydrogen phosphate (K_2HPO_4) was chosen as one of the chemical parameters in this study. K_2HPO_4 can acts as an inorganic cation and a cofactor to increase the enzyme productivity at certain optimal level for maximum production. Previous studies have shown that K_2HPO_4 can be a significant factor that can influences the xylanase production. Therefore, optimisation step was necessary for optimal xylanase productivity depending on the microorganism and other growth conditions since the low or high concentration of K_2HPO_4 can inhibit the enzyme's output (Ali *et al*., 2025; Mardawati *et al*., 2018; Budhathoki *et al*.,

2011). Therefore, the range of 1.0 g/L to 3.0 g/L for the K_2HPO_4 was selected in the PBD.

Metal ions, such as magnesium sulphate ($MgSO_4$), calcium chloride ($CaCl_2$), and iron sulfate heptahydrate ($FeSO_4 \bullet 7H_2O$) play significant roles in various metabolic pathways and enzyme activity (Maan *et al*., 2016; Bhardwaj *et al*., 2017; Singh *et al*., 2013). In this study, the concentration of $MgSO_4$, $CaCl_2$, and $FeSO_4 \bullet 7H_2O$ were adjusted within literature-based ranges to optimise xylanase production, as recorded in Table 3.5.

4.2.2. Analysis of ANOVA through the PBD

PBD is a powerful statistical tool that provides valuable insights into the significance of individual variables in the xylanase production process. For this study, Design Expert Software (Version 11) was utilized to construct the design matrix and analyze the experimental data. A total of 10 physical and chemical parameters, along with 1 dummy variable, were selected for this fractional factorial design. These parameters included incubation time, pH, temperature, agitation rate, xylan, NH_4NO_3, K_2HPO_4, $MgSO_4$, $CaCl_2$, and $FeSO_4 \bullet 7H_2O$. Each variable was assessed at two levels, denoted as -1 (low) and +1 (high). The effectiveness of these parameters was evaluated based on the response variable, xylanase activity (U/mL). The chosen parameter levels and their corresponding factor coding for PBD are summarized in Table 4.1.

Based on the data presented in Table 4.1, a total of twelve distinct experimental runs were conducted to measure the observed xylanase activity. The results from the PBD experiments reveal that xylanase activity varied across the runs, with values ranging from 0.10 U/mL to 9.10 U/mL. The highest xylanase activities were recorded in runs 2, 8, and 10, with respective values of 9.0810 U/mL, 8.9878 U/mL, and 8.9878 U/mL. These findings suggest that *A. niger*, the fungal species used in the study, effectively produces the xylanase enzyme, which hydrolyzes xylan into simpler monosaccharides (sugars) in an environmentally friendly culture medium. By analyzing the three highest-performing experimental runs, it can be inferred that *A. niger* exhibits optimal growth and xylanase production in an alkaline fermenting medium at high temperatures in run 8 and 10. On the other hand, the highest microbial growth and xylanase production in an acidic fermenting medium at high temperature in run 2. This highlights the critical role of specific growth conditions in maximizing enzyme activity and provides insights into the conditions that favor enhanced xylanase production by the fungus.

Table 4.1: Plackett-Burman experimental design matrix for screening the media composition and culture condition for xylanase production

Run	Variables											Xylanase activity (U/mL)	
	X1	X2	X3	X4	X5	X6	X7	X8	X9	X10	X11	Experimental	Predicted
1	1 (5)	-1 (6)	1 (40)	-1 (100)	-1 (1)	-1 (1)	1 (3)	1 (0.7)	1 (1.0)	-1 (0.01)	1	0.3203 ± 0.0463	0.2440
2	-1 (3)	-1 (6)	1 (40)	1 (200)	1 (3)	-1 (1)	1 (3)	1 (0.7)	-1 (0.5)	1 (0.05)	-1	9.0810 ± 0.1050	8.0181
3	-1 (3)	-1 (6)	-1 (30)	-1 (100)	-1 (1)	-1 (1)	-1 (1)	-1 (0.3)	-1 (0.5)	-1 (0.01)	-1	0.6888 ± 0.1059	0.6547
4	1 (5)	1 (8)	-1 (30)	1 (200)	1 (3)	-1 (1)	1 (3)	-1 (0.3)	-1 (0.5)	-1 (0.01)	1	6.6137 ± 0.8792	6.8343
5	-1 (3)	1 (8)	1 (40)	-1 (100)	1 (3)	-1 (1)	-1 (1)	-1 (0.3)	1 (1.0)	1 (0.05)	1	4.3675 ± 0.5104	6.3831
6	1 (5)	1 (8)	-1 (30)	1 (200)	-1 (1)	-1 (1)	-1 (1)	1 (0.7)	1 (1.0)	1 (0.05)	-1	0.1027 ± 0.0318	-0.9602
7	-1 (3)	-1 (6)	-1 (30)	1 (200)	1 (3)	1 (3)	-1 (1)	1 (0.7)	1 (1.0)	-1 (0.01)	1	2.8433 ± 0.2609	1.9246
8	1 (5)	1 (8)	1 (40)	-1 (100)	1 (3)	1 (3)	-1 (1)	1 (0.7)	-1 (0.5)	-1 (0.01)	-1	8.9878 ± 0.0702	7.8145

9	1 (5)	-1 (6)	1 (40)	1 (200)	-1 (1)	1 (3)	-1 (1)	-1 (0.3)	-1 (0.5)	1 (0.05)	1	0.4818 ± 0.2549	1.6551
10	-1 (3)	1 (8)	1 (40)	1 (200)	-1 (1)	1 (3)	1 (3)	-1 (0.3)	1 (1.0)	-1 (0.01)	-1	8.4545 ± 0.3095	7.5781
11	-1 (3)	1 (8)	-1 (30)	-1 (100)	-1 (1)	1 (3)	1 (3)	1 (0.7)	-1 (0.5)	1 (0.05)	1	7.1327 ± 0.2313	8.0090
12	1 (5)	-1 (6)	-1 (30)	-1 (100)	1 (3)	1 (3)	1 (3)	-1 (0.3)	1 (1.0)	1 (0.05)	-1	1.0262 ± 0.2114	1.9448

* The variables represent as X1 – Incubation time (day), X2 – pH, X3 - Temperature (ºC), X4 – Agitation rate (rpm), X5: Xylan (g/L), X6 – NH_4NO_3 (g/L), X7 – K_2HPO_4 (g/L), X8:$MgSO_4 \cdot 7H_2O$ (g/L), X9 – $CaCl_2$, (g/L) , X10 – $FeSO_4 \cdot 7H_2O$ (mg/L), X11- dummy, and R - Xylanase activity.
* Mean values with standard deviation (±SD) from three replicates.

As presented in Table 4.2, the results demonstrate that the media composition and culture conditions significantly influenced xylanase production ($p < 0.05$). The analysis of variance (ANOVA) conducted through the F-test further affirmed the adequacy of the model, with an F-value of 6.3296, suggesting statistical significance. The probability of obtaining an F-value this large due to random chance is only 4.69%, indicating a strong model. With a p-value of less than 0.05, the F-value suggests that the model provides a meaningful representation of the experimental data and that the variables included in the model are significantly influencing xylanase production. In statistical terms, a low p-value indicates strong evidence against the null hypothesis, supporting the conclusion that the observed data is not due to random chance.

PBD can be more simplified by excluding the insignificant variables, thus, making it easier to interpret and use for optimisation or prediction. PBD method is not only used for identifying significant variables, it is also can assuming that higher-order interactions are negligible. There are three variables, such as agitation rate (X4), $MgSO_4 \cdot 7H_2O$ (X8) and $FeSO_4 \cdot 7H_2O$ (X10), were excluded or screened out due to having little to no statistically significant effect on the response, which allows for the reduction of the experimental model to the key factors. This is because the p-values for these three insignificant variables, were greater than 0.1 based on the ANOVA analysis. Therefore, the high or low level of the insignificant variables does not have a significant impact on the selected factorial model (Vanaja and Rani, 2007).

The variation demonstrated that the effect of the media composition and culture condition on the xylanase production was significant ($p < 0.05$). The coefficient determination, R^2, is used to determine the fitting quality of the model in the PBD. If the value of R^2 approximate to 1, the design model was indicated better fitting of the predicted value from the equation to the values of experimental. The analysis of variance (F-test) showed that the model was well adjusted to the experimental data. The model F-value of 6.3296 implies that the model is significant. There was only a 4.69% chance that an F-value this large could occur due to noise. Values of Prob > F less than 0.05 indicated that the model terms were significant while values greater than 0.10 indicated the non-significance of the model term.

Table 4.2: ANOVA analysis using the selected factorial model for xylanase production.

Source	Coefficient Estimate	Sum of Squares	df	Mean Square	F-value	p-value	
Model	Intercept: 4.1750	136.85	7	19.556	6.3294	0.0469	Significant
X1	-1.2529	18.8379	1	18.838	6.0990	0.0690	
X2	1.7681	37.5149	1	37.515	12.1462	0.0252	
X3	1.1071	14.7089	1	14.709	4.7621	0.0945	
X5	1.3116	20.6423	1	20.642	6.6831	0.0610	
X6	0.6460	5.0082	1	5.0082	1.6214	0.2719	
X7	1.2630	19.1433	1	19.143	6.1978	0.0675	
X9	-1.3226	20.9917	1	20.992	6.7963	0.0596	
Residual		12.3548	4	3.0887			
Cor Total		149.20	11				

* The variables represent as X1 – Incubation time, X2 – pH, X3 - Temperature, X5: Xylan, X6 – NH_4NO_3, X7 – K_2HPO_4, X9 – $CaCl_2$; df: degree of freedom

To assess the robustness of the model, the coefficient of determination (R^2) was utilized. An R^2 value close to 1 signifies that the model fits well, with the predicted values aligning closely with the experimental data. According to Dhaver *et al*. (2022), an R^2 value of at least 90% is recommended to ensure a strong model fit. As presented in Table 4.3, the model achieved an R^2 value of 0.9172, which is a critical indicator of its explanatory power. This implies that 91.72% of the variation in xylanase production can be explained by the factors and interactions incorporated in the model, confirming the model's effectiveness in predicting enzyme production. The remaining 8.28% of the variation can be attributed to unaccounted variables or random experimental error, emphasizing the model's precision and its ability to capture the primary determinants of xylanase production.

Furthermore, the p-value ($p < 0.05$) for each variable, as shown in Table 4.2, supports the statistical significance of the selected factors. With a 95% confidence level, this confirms that the variables included in the design model have a significant impact on xylanase production (Dhaver *et al.,* 2022; Wang *et al*., 2018). The predicted R^2 value of 0.2548 did not closely align with the adjusted R^2 value of 0.7723, with a deviation exceeding 0.2, suggesting the presence of a large block effect. This discrepancy warrants attention to factors such as model reduction, response transformation, or outliers (additional references needed). It is also recommended to conduct confirmation runs to validate the empirical models.

In addition to the R^2 analysis, the coefficient of variation (CV) was calculated to evaluate the reproducibility of the experiments. With a CV value of 42.10%, the experiments demonstrated good repeatability and reliability. A CV greater than 4 is considered indicative of adequate precision in the experimental setup (Maan *et al*., 2016). The Adequate Precision ratio of 6.257 further supports the reliability of the model, confirming that it provides a strong signal and is suitable for predictive applications. A ratio above 4 is generally desirable, and the current study's ratio of 6.257 signifies that the model offers a dependable and precise signal for future predictions.

Table 4.3: Statistical variables obtained from ANOVA analysis of xylanase production by *A. niger.*

Variable	Response	Variable	Response
Standard deviation	1.7575	R^2	0.9172
Mean	4.1750	Adjusted R^2	0.7723
Coefficient of variation (%)	42.10	Predicted R^2	0.2547
		Adequate precision	6.2568

The corresponding response of the xylanase production was expressed in terms of the following regression equation [Eq. (7)]:

$$R = 4.1750 - 1.2529 * X1 + 1.7681 * X2 + 1.1071 * X3 + 1.3116 * X5 + 0.6460 * X6 + 1.2630 * X7 - 1.3226 * X9 \quad \text{-----Eq. (7)}$$

where R is defined as the xylanase activity, X1 is refers to incubation time, X2 is the pH, X3 is the temperature, X5 is the xylan, X6 is the NH_4NO_3, X7 is the K_2HPO_4, and X9 is the $CaCl_2$,

In the context of PBD, the main effects for each variable were evaluated. These effects were classified into positive and negative categories. When the variable shows the positive effects, it means that the influence of the corresponding variable is greater at high level. On the other hand, when the variable shows the negative effect, it means that the influence of the corresponding variable is greater at low level (Maan *et al*., 2016; Dhaver *et al*., 2022). As shown in Table 4.2, incubation time (X_1) and $CaCl_2$ (X_9) showed negative effects on xylanase production, meaning that increasing their levels decreased enzyme activity. In contrast, the other variables exhibited positive effects, implying that higher concentrations or conditions of these variables enhanced xylanase production.

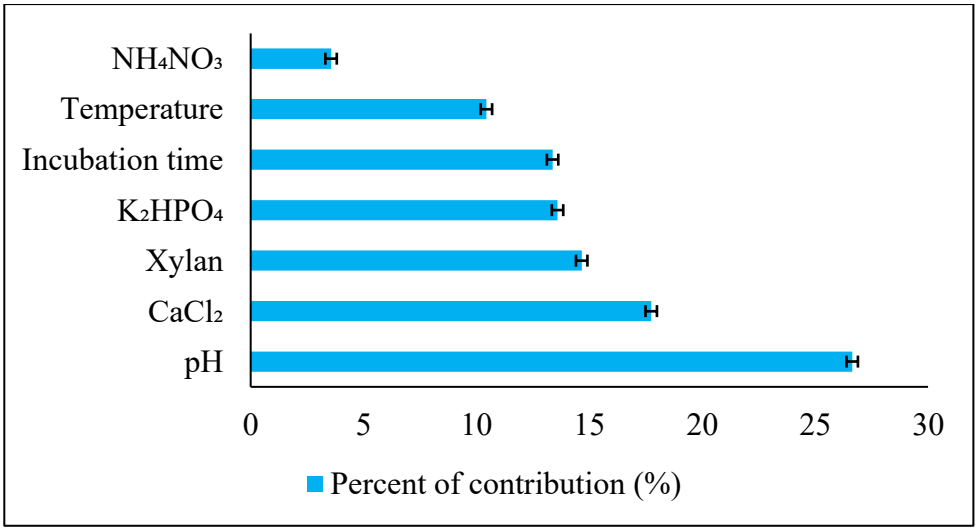

Figure 4.2: Pareto chart of standardized effects of different physical and chemical parameters showing the significance at p <0.05 on xylanase activity (U/mL).

Pareto chart is an effective tool for assessing the significance of each variable, particularly when interpreting the results of the PBD (Maan *et al*., 2016; Rosmine *et al*., 2017). As shown in Figure 4.2, the Pareto chart of standardized effects highlights the relative importance of various physical and chemical parameters on xylanase production, with statistical significance set at $p < 0.05$. The chart clearly reveals that pH and $CaCl_2$ have the greatest impact on xylanase production by *A. niger*, as indicated by the longest bars extending beyond the critical value line.

The effect of the pH on the xylanase production has been explained in detailed in the Section 2.4.2. pH acts as a crucial role in xylanase production because it can influence microbial growth and the activity of enzymes involved in xylanase synthesis. While, $CaCl_2$ concentration affects xylanase production and activity, with optimal production achieved at specific concentrations and activity potentially enhanced by the presence of calcium ions (Ca^{2+}), which act as a cofactor for some xylanases, though high concentrations can be inhibitory. Ca^{2+} significantly influences xylanase by enhancing its thermal and proteolytic stability, and this is primarily achieved through the binding of Ca^{2+} to a specific calcium-binding domain on the enzyme. This binding doesn't change the fundamental catalytic mechanism but stabilizes the enzyme's structure, making it more robust against harsh conditions. Therefore, the mechanism involves Ca^{2+} stabilizing the enzyme's structure for activity and promoting growth, but excessive concentrations can hinder cell growth and enzyme synthesis (Santos *et al*., 2014; Corrêa Junior *et al*., 2022; Shahriarinour *et al*., 2011).

Given their significant impact on enzyme production, pH and $CaCl_2$ were selected for further optimisation in the next phase of the study, using Central Composite Design (CCD). This will allow for precise adjustments to these variables, refining the fermentation process to maximize xylanase production.

4.3. Optimisation of Significant Variables on Xylanase Productivity through Central Composite Design (CCD)

In Section 4.2, two key variables, pH and $CaCl_2$, were identified for optimisation with respect to their effects on xylanase production. To enhance the accuracy of this optimisation, CCD was employed. CCD is a robust experimental design approach that enables the determination of the optimal levels of these variables. The experimental procedure was conducted using Design Expert Software (Version 11), which facilitated the design of the CCD matrix and analysis of the data. The optimisation process began with the inoculation of 1 mL aliquots of spore suspension of *A. niger*, containing 2 x 10^6 spores/mL, into the Mandels and Sterrnburg's basal medium. The cultures were incubated for five days. Other variables, including the composition of the medium and incubation conditions, were held constant at their central values, with only pH and $CaCl_2$ concentration varying according to the experimental design. It is suggested the central value of the medium composition and incubation conditions other than pH and $CaCl_2$ concentration be provided in the text or in the note of Table 4.4.

4.3.1. Experimental Design and Model Selection

The pH value and $CaCl_2$ concentration were further optimised through Response Surface Methodology (RSM) using the CCD after the initial screening. The pH and CaCl2 were assigned three levels: +1 (high), -1 (low), and 0 (central point). A total of 13 experimental runs were designed, and the corresponding experimental and predicted xylanase activities are presented in Table 4.4. The highest xylanase activities were observed in Run 2 and Run 7, with values of 6.4910 U/mL and 6.1335 U/mL, respectively. These results suggest that a higher concentration of $CaCl_2$ can significantly enhance xylanase production by *A. niger* in an alkaline fermenting medium.

Table 4.4: CCD matrix with coded value and its corresponding experimental and predicted xylanase production by *A. niger*.

Run	A	B	Xylanase activity (U/mL)	
			Experimental (±SD)	Predicted
1	0 (7)	0 (0.75)	0.4930 ± 0.0196	1.2222
2	+1 (8)	+1 (1.00)	6.4910 ± 0.0404	6.6078
3	+1 (8)	0 (0.75)	1.5820 ± 0.0092	1.7319
4	-1 (6)	0 (0.75)	0.2930 ± 0.0019	-0.3855
5	0 (7)	0 (0.75)	0.8989 ± 0.0040	1.2222
6	-1 (6)	-1 (0.50)	0.1355 ± 0.0259	0.2830
7	0 (7)	+1 (1.00)	6.1335 ± 0.0142	5.4858

8	+1 (8)	-1 (0.50)	1.4423 ± 0.1042	1.1756
9	0 (7)	0 (0.75)	1.0951 ± 0.0125	1.2222
10	0 (7)	-1 (0.50)	1.1590 ± 0.0045	1.2783
11	0 (7)	0 (0.75)	1.9365 ± 0.0085	1.2222
12	0 (7)	0 (0.75)	1.1591 ± 0.0012	1.2222
13	-1 (6)	+1 (1.00)	2.7347 ± 0.0422	3.2657

*The variables represent as A – pH, and B - $CaCl_2$.
* Mean values with standard deviation (±SD) from three replicates

Among the tested regression models, the quadratic model demonstrated the best fit for describing the relationship between the variables and xylanase production by *A. niger*. As shown in Table 4.5 it was the only model with a statistically significant p-value ($p < 0.05$), while the linear, two-factor interaction, and cubic models showed p-values greater than 0.05, indicating lower relevance. This confirms that the quadratic polynomial model was the most appropriate for accurately predicting xylanase activity.

Table 4.5: ANOVA of regression model for xylanase production by *A. niger*.

Source	Sequential *p*- value	Lack of fit *p*-value	Adjusted R^2	Predicted R^2	
Linear	0.0045	0.0232	0.5928	0.3715	
2Fl	0.3765	0.0206	0.5872	0.1842	
Quadratic	0.0016	0.3160	0.9159	0.7198	Suggested
Cubic	0.2945	0.2937	0.9278	0.0334	Aliased

4.3.2. Statistical Analysis of the Quadratic Model

Table 4.6 presents the analysis of variance (ANOVA) for the quadratic regression model used to predict xylanase production. The model F-value of 27.44 with a very low p-value (0.0002) implied that the model is statistically significant. This means there is only a 0.02% probability that such a high F-value could be due to random variation (noise), confirming the robustness of the model.

In addition, a "Prob > F" value, or p-value, less than 0.0500 indicates that the model terms are significant. In this study, term A shows a significant linear effect (p = 0.0033), term B was the most influential variable with a highly significant effect (p < 0.0001), and term B^2 also had a strong impact on the response with p = 0.0005. On the other hand, the interaction term AB had a p-value of 0.0782, which, although not less than 0.05, suggests a moderately influential interaction. Meanwhile, the quadratic term of A^2 was not significant (p = 0.1631), indicating that non-linear changes in pH had minimal additional influence beyond its linear contribution.

As reported by Bhardwaj *et al*. (2017), the model's performance was rigorously evaluated using several statistical parameters, including R^2, adjusted R^2, predicted R^2, adequate precision, and lack of fit. As shown in Table 4.6, the coefficient of determination (R^2) was 0.9515, indicating that the model could explain 95.15% of the variability in xylanase production. This high value confirms the model's strong explanatory power. The adjusted R^2 value of 0.9168 further supports the model's reliability by accounting for the number of

predictors involved. Moreover, the predicted R^2 of 0.7258 aligns well with the adjusted R^2, with a difference of less than 0.2—signifying good agreement between observed and predicted values and confirming the model's strong predictive ability.

Table 4.6: Analysis of variance (ANOVA) for quadratic model

Source	Sum of squares	df	Mean square	F-value	p-value	
Model	47.9048	5	9.5810	27.1344	0.0002	Significant
A - pH	6.7250	1	6.7250	19.0459	0.0033	
B- $CaCl_2$	26.5542	1	26.5542	75.2045	< 0.0001	
AB	1.4999	1	1.4999	4.2480	0.0782	
A^2	0.8324	1	0.8324	2.3574	0.1686	
B^2	12.8835	1	12.8835	36.4875	0.0005	
Residual	2.4717	7	0.3531			
Lack of Fit	1.3609	3	0.4536	1.6336	0.3160	Not significant
Pure Error	1.1108	4	0.2777			
Cor Total	50.3765	12				
Std. Dev.	0.5942			R^2		0.9510
Mean	1.9657			Adjusted R^2		0.9159
C.V. %	30.2297			Predicted R^2		0.7198
				Adeq Precision		17.3234

*df, degrees of freedom; Significant level = 95%

A ratio of more than 4 is desirable and indicates an adequate precision. In this study, the ratio of 17.4035 was an adequate signal. This suggests that the

model provides a sufficiently strong signal and is suitable for navigating the design space. Furthermore, the lack of fit test yielded a *p*-value of 0.3216, indicating that the lack of fit is not statistically significant. This suggests the model fits the experimental data well, and that any variation between predicted and actual values is due to pure error rather than model inadequacy (Singh *et al*., 2013; Cunha *et al*., 2018).

The regression equation was derived following the ANOVA analysis, which quantified how the independent variables, pH (A) and $CaCl_2$ concentration (B), influence the xylanase production. This polynomial model (Eq. 8) captures both the individual and interactive effects of the variables, allowing for accurate prediction of enzyme activity under different experimental conditions.

$$R = 1.2222 + 1.0587 * X2 + 2.1037 * X9 + 0.6124 * X2\ X9 - 0.5490 * X2^2 + 2.1598 * X9^2 \quad \text{--Eq. 8}$$

where R is the xylanase activity, X2 is the pH and X9 is the $CaCl_2$ (g/L)

The coefficients indicate the direction and strength of each factor's influence. In this study, the positive coefficients for A, B, and B^2 suggest that increasing pH and $CaCl_2$ generally enhances xylanase activity, while the negative coefficient for A^2 indicates that very high or low pH may reduce activity due to a non-linear response.

In the PBD, $CaCl_2$ (X9) shows a negative effect on xylanase production as shown in Table 4.2. Yet, the CCD shows that there is a positive linear effect of the calcium ion concentration on the xylanase production. It can be explained that a parameter with a negative effect in a PBD might have a positive effect due to the PBD is a screening tool that can obscure interaction effects. PBD acts as a preliminary step to identify the most significant factors from many variables with a minimal number of experiments. But it is not designed to determine for interactions between variables. Moreover, the situation occurred in this study can be explained the "negative" effect showing for a specific parameter might be due to the way it's interacting with other parameters in the experimental setup. For example, increasing a factor might be negative at a certain high level, while it could be positive at lower levels or in combination with other factors. The effect direction (positive or negative) might not be the true one if the variable is confounded with other factors that have a stronger effect. Therefore, the parameter that shows a negative effect in PBD should not be discarded outright, on the contrary, it should be further investigated in the next optimisation step, such as Response Surface Methodology (RSM) using the CCD method. By using the CCD, it can easily to understand its true relationship with the response variable, especially in combination with other parameters (Ekpenyong *et al*., 2017; Six Sigma, 2024; Tafazzoli *et al*., 2024).

4.3.3. The Diagnostics of Residuals

The final result may not be as fit as it may be due to the residual content in the tested sample. By creating the data with the normal percentage probability axis against the externally standardized residuals axis, Fig. 4.3 displayed the normal plot of residuals. The dots in the illustration generally create a pattern of ascending linear lines. This demonstrated that noteworthy outcomes were attained. The color difference appropriately supported the plot of the color spots by enzyme activity value. The highest enzyme activity was shown by the color red, while the lowest enzyme activity was indicated by the color blue. The likelihood of a deviation from normalcy increased with the distance of the locations from the linear line. Given that the residuals roughly follow a straight line, the normality requirement is fulfilled.

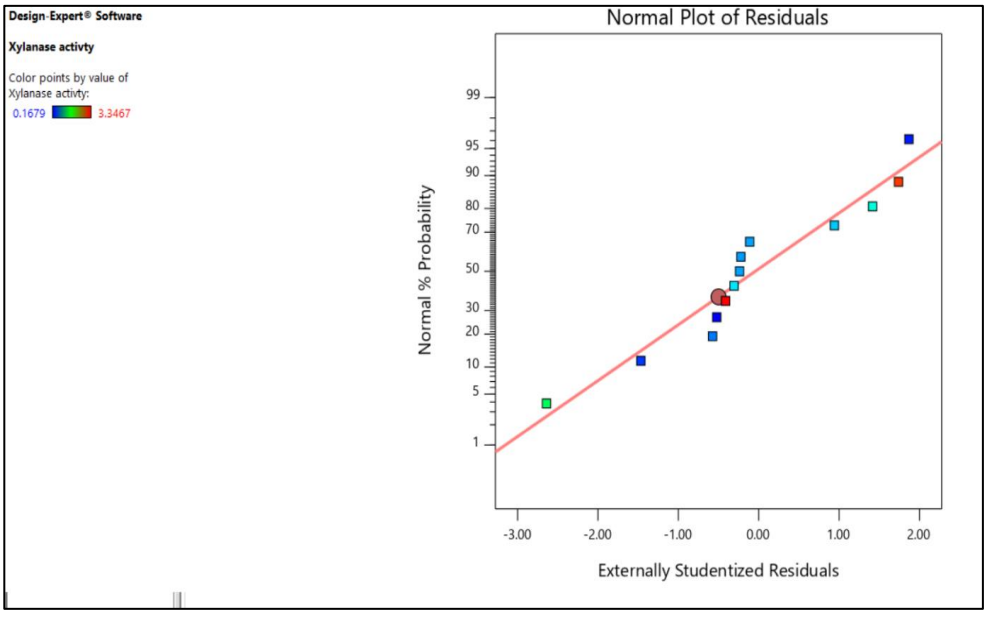

Figure 4.3: Normal plot of residuals for xylanase activity.

The residuals against expected plot was displayed in Figure 4.4. With estimated responses on the x-axis and residuals on the y-axis, it was a dispersed plot. Non-linearity, uneven error variances, and outliers were all detectable by the figure. The data points are uniformly distributed around the line in the figure, indicating that the model produced an accurate prediction. This implied that there were no outliers and that the relationship's assumption was linear and appropriate with equal error variances.

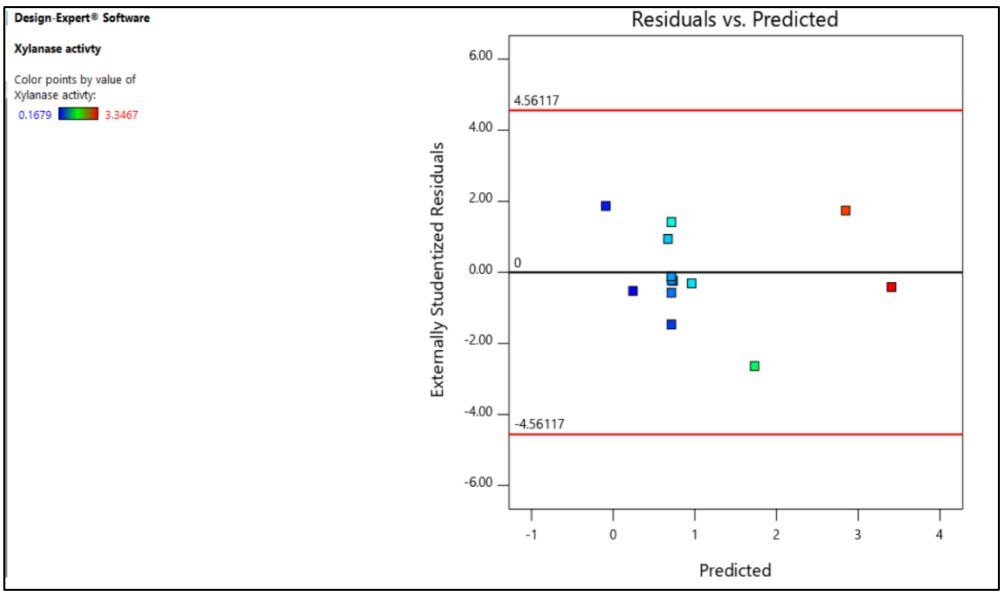

Figure 4.4: Residuals against predicted value for the xylanase activity

4.4. Model Analysis of Key Variables

Analysis of Variance (ANOVA) using Design of Experiment (DoE) software was used to determine the model analysis in the present study. DoE software was able to offer optimisation solutions and detailed analysis that included one factor or a 3D surface view model graph. The model's anticipated

values and the actual output of the parameters assessed by these experiments matched well.

4.4.1. One Factor Plot for pH

The effect of pH on xylanase activity is depicted in the one-factor plot shown in Figure 4.5. The highest enzyme activity was recorded at pH 7.0, yielding 1.9365 U/mL, while lower activities were observed at pH 6.0 (0.2930 U/mL) when comparing with to pH 8.0 (1.5820 U/mL). Statistical analysis revealed that the linear effect of pH on xylanase production was significant (p = 0.0033), indicating a meaningful influence on enzyme yield. However, the quadratic effect (A^2) was not statistically significant (p = 0.1686), suggesting that while pH impacts production, it does not exhibit a pronounced curvilinear trend within the tested range. Güler and Özçelik (2023) and Amir *et al*. (2013) reported that optimal xylanase production by alkaliphilic strains such as *A. fumigatus* MA28 occurs around pH 8. Furthermore, Ali *et al*. (2017) noted that most *Aspergillus* species demonstrate robust growth and enzyme production in alkaline conditions. Thus, the results of this study are consistent with the broader understanding that xylanase activity typically peaks between neutral and slightly alkaline pH levels.

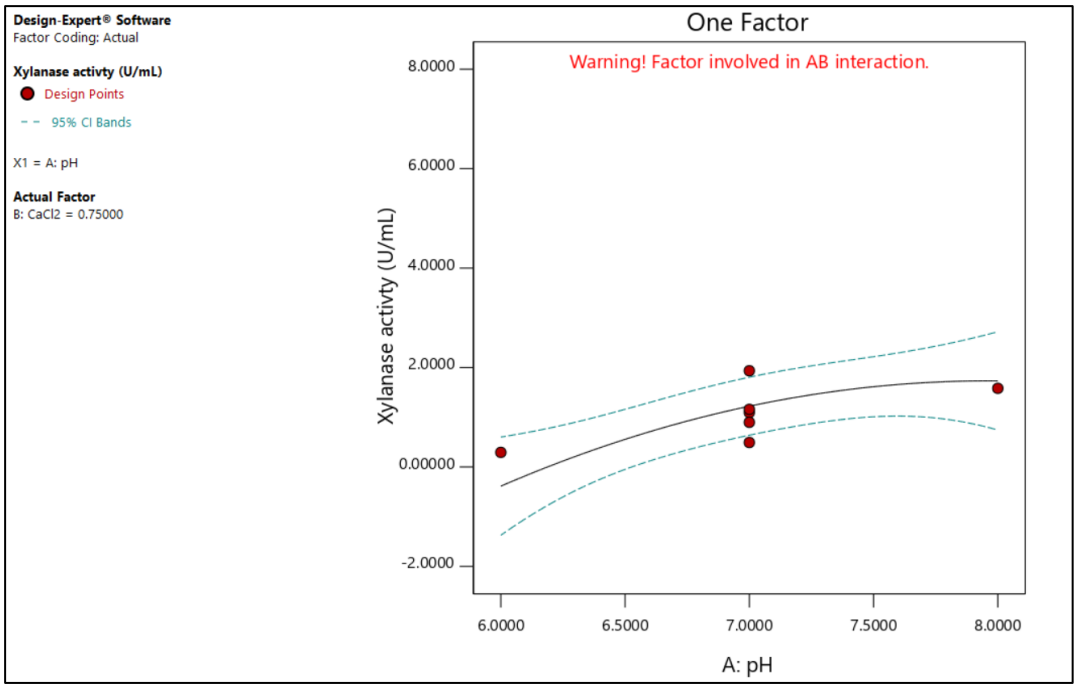

Figure 4.5: One factor plot of enzyme activity against medium pH. (X1 = B: Medium pH; actual factor B: $CaCl_2$ = 0.75 g/L

4.4.2. One Factor Plot for $CaCl_2$

Figure 4.6 presents the one-factor plot illustrating the effect of $CaCl_2$ concentration on xylanase activity. The highest xylanase activity (6.1335 U/mL) was achieved at a $CaCl_2$ concentration of 1.0 g/L, compared to 1.9365 U/mL at 0.75 g/L and 1.1590 U/mL at 0.50 g/L. According to Table 4.5, the linear effect of $CaCl_2$ (factor B) was highly significant, with a *p*-value of < 0.0001, indicating a strong influence on xylanase production by *A. niger*. Additionally, the quadratic effect of $CaCl_2$ (B^2) was also statistically significant (p = 0.0005), suggesting a nonlinear relationship. The concave curvature of the plot supports this, implying a strong interaction between $CaCl_2$ concentration and xylanase yield.

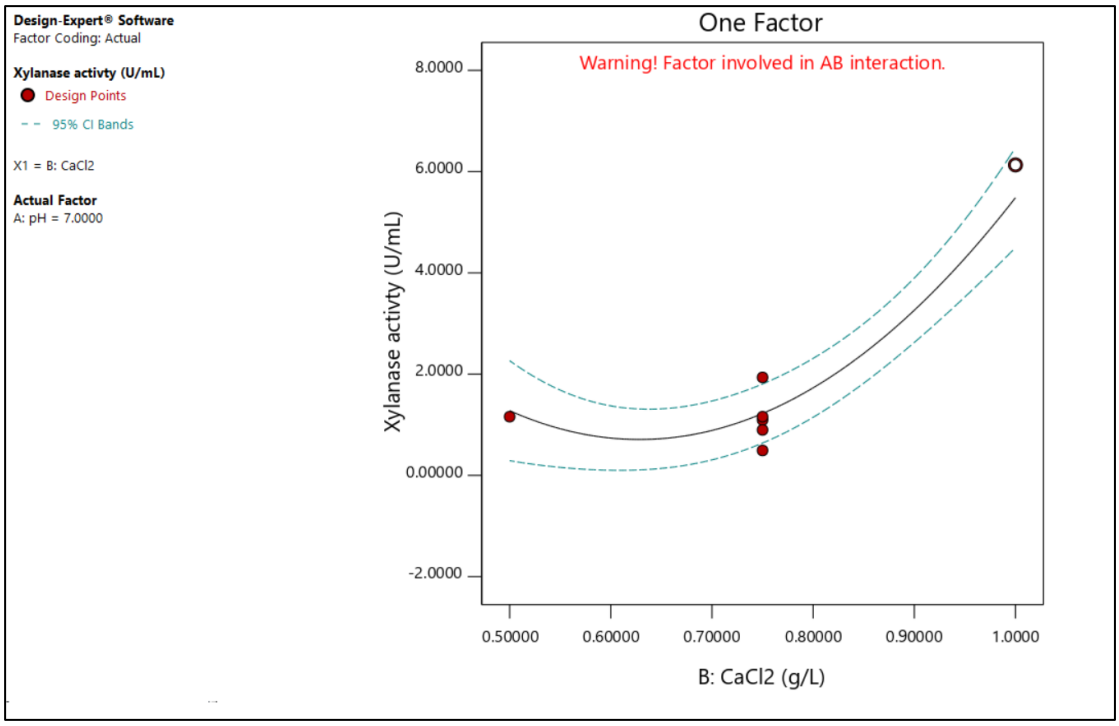

Figure 4.6: One factor plot of enzyme activity against $CaCl_2$ (g/L). (X2 = B: $CaCl_2$; actual factor A: pH = 7)

4.4.3. Interaction Effect between the pH and $CaCl_2$

The relationship between the coded variables, A (pH) and B ($CaCl_2$), and the xylanase activity response was further explored through a three-dimensional (3D) response surface plot, as illustrated in Figure 4.7. These plots were generated by holding all other medium components and culture conditions at their central levels. According to Table 4.5, the interaction between pH and $CaCl_2$ (term AB) yielded a *p*-value of 0.0782, which, while not below the conventional 0.05 threshold, is still below 0.1. This suggests that the interaction has a moderate yet notable effect on xylanase production.

The response surface plot provided a three-dimensional visualization that clearly identified the maximum and minimum xylanase activity values, not only

through surface contours but also via color gradients. As illustrated in Figure 4.7, the plot rises toward a red-colored peak, indicating the optimal conditions for enzyme production. This upward trend reflects increased xylanase activity as both pH and $CaCl_2$ concentration approach their higher levels. Based on software analysis, the optimum point was determined at a pH of 8.0 and a $CaCl_2$ concentration of 1.0 g/L, confirming the most favorable conditions for xylanase production in this study.

Furthermore, Figure 4.7 also reveals that pH exhibited a relatively minor effect on xylanase production when $CaCl_2$ was kept constant at 0.5 g/L or 1.0 g/L. However, xylanase activity significantly increased improved when the concentration of $CaCl_2$ increased from 0.75 g/L to 1.0 g/L, especially at pH values of 6.0 and 8.0. These findings are consistent with the hypothesis that Ca^{2+} ions play a crucial role in enhancing xylanase activity. In addition, this demonstrates that $CaCl_2$ concentration had a stronger influence than pH within the tested range.

The response surface plot provided a three-dimensional display that made it simple to identify the maximum and minimum values without the need for distinct color indications. It is evident from Figure 4.7 that the ideal incubation conditions for optimal xylanase production for both parameters, such as pH and $CaCl_2$. It was seen that the 3D response surface plot projected upward to a red region. This indicated that the analysis had succeeded in achieving the optimal state. According to the study interpreted from the software, the optimal condition was assigned at that point where the pH was at 8 and the $CaCl_2$

concentration was 1.0 g/L since the xylanase activity was highest (6.4910 U/mL) compared to other conditions. Contrarily, the lowest xylanase activity is 0.1350 U/mL.

By changing the ionic charges on the molecule (the substrate surface and the enzyme's active site), the pH can have an impact on the activity of enzymes. The basicity of the fermenting medium reduced as a result of a lower propensity to generate hydrogen bonds. Eventually, it made the enzyme easily to bind the substrate by resulting in conformational changes. The situation was happening that might can be explained that the Ca^{2+} ion has the stimulatory effect to enhanced the xylanase activity by changing the structure of the enzyme. It acts as a cofactor to help the active site of the enzyme to bind with the substrate by changing the its molecular structure (Siwach *et al*., 2024; Suleman *et al*., 2020).

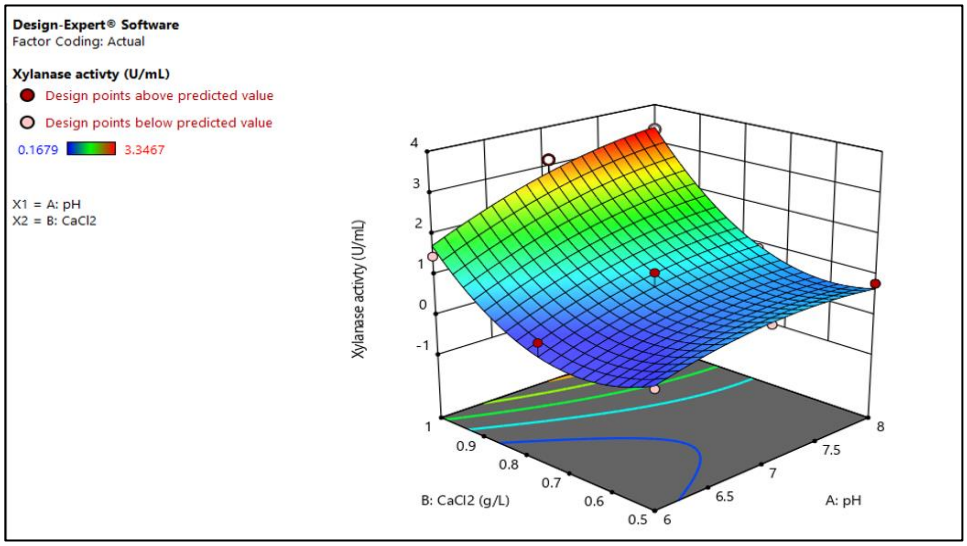

Figure 4.7: 3D surface response for xylanase activity as function of the variable A: pH and variable B: $CaCl_2$
(Design point above predicted value ●; design point below predicted value ○)
(0.13550 ▬ 6.4910 color points by value of enzyme activity)

4.5. Validation Test

A validation experiment was carried out to confirm the accuracy of the model-predicted optimal conditions. By using CCD in RSM, the pH and $CaCl_2$ concentration parameters were adjusted to be "within range," and the xylanase activity response was set to "maximize". To ensure the reliability of the results, the validation was conducted in triplicate under the optimised conditions. After that, any variation or experimental error was evaluated by comparing the actual xylanase activity that was achieved with the expected values. The optimal conditions identified (pH 6.5; $CaCl_2$ concentration of 0.931 g/L) were selected on a desirability value of 100% desirability, as summarized in Table 4.7.

Table 4.7: Suggested optimum conditions by Design Expert

No.	pH	CaCl2 (g/L)	Mycelial dry cell weight (g/L)	Xylanase activity (U/mL)	Desirability	
1	6.5	0.931	1.109	1.768	1	Selected
2	8	0.75	0.879	1.732	1	
3	6	0.5	0.257	0.283	1	

According to the objectives, the software developed the ideal conditions that, based on the incubation result, should yield 1.768 U/mL of enzyme activity with a desirability of 1.0. To determine the error, the predicted and real enzyme activities were compared. Under the specified ideal environment, 1.7569 U/mL was obtained in the experiment.

The percentage error between the actual and anticipated enzyme activity was 0.63 percent, which was regarded as low and near the expected value of 1.553 U/mL. As a result, the outcome of real enzyme activity under ideal xylanase production conditions was consistent with the production that was anticipated. our demonstrated the validity of the optimisation our study was able to achieve (Mardawati *et al*., 2018).

CHAPTER 5

CONCLUSION AND RECOMMENDATION

5.1. Conclusion

This study demonstrated the potential of *Aspergillus niger* as a robust filamentous fungus for the production of xylanase, an important enzyme for lignocellulosic biomass degradation. The research successfully achieved its objective of optimising xylanase production using *A. niger* which was cultured in Mandels and Sternburg's basal medium under submerged fermentation.

The time course profile of *A. niger* growth and xylanase production revealed a typical microbial growth pattern with four distinct phases: lag, exponential, stationary, and death phases. Maximum mycelial biomass and xylanase activity were observed between Day 3 to Day 5, indicating this period as optimal for enzyme productivity. The study also demonstrated a strong correlation between fungal biomass accumulation and enzyme output, emphasizing the importance of monitoring growth dynamics for optimising xylanase production in submerged fermentation systems. These findings serve as a foundational reference for selecting the appropriate cultivation period for enhanced industrial enzyme yield.

Initially, ten physical and chemical variables were evaluated for their influence on xylanase production. These included incubation time, pH, temperature, agitation rate, and concentrations of the growth factors (including xylan, NH_4NO_3, K_2HPO_4, $MgSO_4$, $CaCl_2$, and $FeSO_4 \cdot 7H_2O$). The variables were screened using the Plackett-Burman Design (PBD) via Design Expert software (Version 11). Among the ten variables tested, incubation time and $CaCl_2$ showed negative effects on enzyme production, while pH, temperature, xylan, NH_4NO_3, K_2HPO_4, and others showed positive effects. The statistical analysis, including ANOVA, revealed that the model was significant (F-value = 6.3294, $p < 0.05$) with a high coefficient of determination ($R^2 = 0.9172$), indicating good model predictability. The Pareto chart further confirmed that pH and $CaCl_2$ were the most influential factors.

Subsequently, optimisation using Central Composite Design (CCD) under Response Surface Methodology (RSM) further refined these conditions. Based on the analysis of variance (ANOVA), the quadratic model was selected as the most appropriate, with a sequential p-value of 0.0016, an adjusted R^2 of 0.9186, and a predicted R^2 of 0.7258, all indicating excellent model fit and predictive capability. The lack-of-fit p-value of 0.3216 further confirmed that the model was statistically valid. The model's significance was then further validated by ANOVA, with a model F-value of 27.44 and a p-value of 0.0002, indicating that the model was highly significant. Among the tested terms, the linear effects of pH (A) and $CaCl_2$ concentration (B) were both significant ($p = 0.0033$ and $p < 0.0001$, respectively). Additionally, the quadratic term for $CaCl_2$ (B^2) was also significant ($p = 0.0005$), indicating a strong curvature in its effect on xylanase

production. Although the interaction term AB had a p-value of 0.0728, slightly above the conventional 0.05 threshold, it still suggested a meaningful interactive effect within the experimental context.

The validation experiments for the optimal conditions for xylanase production were determined to be pH 6.5 and $CaCl_2$ concentration of 0.931 g/L. The experiments conducted in triplicate under these optimised conditions yielded a xylanase activity of 1.7569 U/mL, closely aligning with the model's prediction. These results confirmed the reliability and predictive power of the RSM-CCD approach for optimising enzyme production parameters in *A. niger*.

Overall, the study confirmed that pH and $CaCl_2$ significantly influence xylanase production by *A. niger*, and the optimised conditions can serve as a baseline for scaling up in industrial enzyme production. This research contributes valuable insights into fungal fermentation and enzyme optimisation for biotechnological applications.

5.2. Recommendation for Future Research

1. Recommendation for Future Research

Certain laboratory experiments proposed in this study could not be carried out due to practical constraints. However, these limitations open avenues for future research that may yield more comprehensive and reliable results. The following recommendations are suggested for further investigation:

i. Further research should explore a broader range of incubation parameters affecting xylanase production by *A. niger*. This includes optimising inoculum size, substrate particle size, moisture content, and evaluating the effects of various nitrogen sources, carbon sources, phosphate sources, and metal ions.

ii. A detailed analysis of *A. niger* mycelial morphology is recommended to understand its correlation with xylanase production and how it is influenced by different environmental and incubation conditions.

iii. The purified xylanase should be further characterized in terms of its enzymatic activity and stability under varying pH levels, temperatures, and metal ion concentrations. This would provide insight into its potential industrial applications.

iv. Future studies may consider exploring other microbial sources, such as protozoa and archaea, as potential producers of xylanase to broaden the spectrum of high-yielding enzyme-producing organisms

v. Investigating the use of low-cost, renewable agro-industrial residues—such as corn cobs, oil palm empty fruit bunches, and other lignocellulosic materials—as substrates could offer a sustainable and economically viable approach to xylanase production.

2. Commercialization Potential

Agro-wastes like bagassessae, rice husk, rice straw, and wheat bran, as well as other lignocellulosic materials such sawdust and vegetable waste, can be

bioconverted into fermentative products by producing xylanases. In Malaysia, oil palm is the second-largest producer and exporter of palm oil globally. Lignocellulosic biomass which is produced from the oil palm industries include oil palm trunks (OPT), oil palm fronds (OPF), empty fruit bunches (EFB) and palm pressed fibres (PPF), palm shells and palm oil mill effluent palm (POME). However, the presence of these oil palm wastes has created a major disposal problem which can cause the environmental problem. Therefore, the lignocellulosic biomass can be recycled into useful bioenergy, such as bioethanol. As a result, it is indirectly lowering the quantity of industrial waste. Enzymatic hydrolysis is still a significant expense in the process of turning lignocellulosic raw materials into ethanol, though. Enhancing the production and activity of enzymes requires optimisation research. This process can occur under simultaneous saccharification and fermentation to produce the xylanase using the microbial producer.

The bleaching of pulp is one of the most interesting biotechnological uses of xylanase. Chlorine gas can be replaced by using xylanase, as a biobleaching agent which can reduce the usage of chlorine during the process. This is due to the fact that chlorine-based chemicals are poisonous, dangerous, and exhibit a high resistance to biodegradation. It can lead to detrimental disruptions in biological systems and constitutes one of the primary contributors to environmental pollution. In addition to raising the brightness ceiling, this practice may lower the cost of bleaching chemicals.

REFERENCES

Abdella, A. et al., 2021. Paecilomyces variotii xylanase production, purification and characterization with antioxidant xylo-oligosaccharides production. *Scientific Reports*, 11(1), p.16468.

Abdella, A., Segato, F. and Wilkins, M.R., 2020. Optimization of process parameters and fermentation strategy for xylanase production in a stirred tank reactor using a mutant Aspergillus nidulans strain. *Biotechnology Reports*, 26, p.e00457.

Abena, T. and Simachew, A., 2024a. A review on xylanase sources, classification, mode of action, fermentation processes, and applications as a promising biocatalyst. *Journal of Biotechnology, Computational Biology and Bionanotechnology*, 105(3), pp.273–285.

Abena, T. and Simachew, A., 2024b. Production and characterization of acidophilic xylanase from wood degrading white rot fungus by solid-state fermentation of wheat straw. *Heliyon*, 10(15), p.e35496.

Adiguzel, G. et al., 2019. A novel endo-β-1,4-xylanase from Pediococcus acidilactici GC25; purification, characterization and application in clarification of fruit juices. *International Journal of Biological Macromolecules*, 129, pp.571–578.

Agustí-Brisach, C. and Armengol, J., 2012. Effects of temperature, pH and water potential on mycelial growth, sporulation and chlamydospore production in culture of Cylindrocarpon spp. associated with black foot of grapevines. *Phytopathologia Mediterranea*, 51(1), pp.37–50. Available at: www.fupress.com/pm.

Ahmad, N. and Janahiraman, T. V, 2014. A Study on Regression Model Using Response Surface Methodology. *Applied Mechanics and Materials*, 666, pp.235–239. Available at: https://www.researchgate.net/publication/265414527.

Ajijolakewu, A.K., Leh, C.P., Wan Abdullah, W.N. and Lee, C. keong, 2017. Optimization of production conditions for xylanase production by newly isolated strain Aspergillus niger through solid state fermentation of oil palm empty fruit bunches. *Biocatalysis and Agricultural Biotechnology*, 11, pp.239–247.

Akula, S. and Golla, N., 2018. Optimization of Cellulase Production by Aspergillus niger Isolated from Forest Soil. *The Open Biotechnology Journal*, 12(1), pp.256–269.

Alagöz, D., Varan, N.E., Yildirim, D. and Fernandéz-Lafuente, R., 2022. Optimization of the immobilization of xylanase from Thermomyces lanuginosus to produce xylooligosaccharides in a batch type reactor. *Molecular Catalysis*, 531, p.112647.

Ali, N.L. et al., 2025. Efficient Assessment and Optimisation of Medium Components Influencing Extracellular Xylanase Production by Pediococcus pentosaceus G4 Using Statistical Approaches. *International Journal of Molecular Sciences*, 26(15), p.7219.

Ali, S.R.M., Fradi, A.J. and Al-Aaraji, A.M., 2017. Effect of some physical factors on growth of five fungal species. *European Academic Research*, V(2), pp.1069–1078. Available at: www.euacademic.org.

Al-Shaeli, M. et al., 2024. pH-responsive membranes: Mechanisms, fabrications, and applications. *Science of the Total Environment*, 946, p.173865.

Amir, A., Arif, M. and Pande, V., 2013. Purification and characterization of xylanase from Aspergillus fumigatus isolated from soil. *Afr. J. Biotechnol.*, 12(20), pp.3049–3057. Available at: http://www.academicjournals.org/AJB.

de Amo, G.S. et al., 2024. Heterologous expression of GH11 xylanase from Myceliophthora heterothallica F.2.1.4 in Pichia pastoris. *Biocatalysis and Agricultural Biotechnology*, 61, p.103343.

Andlar, M. et al., 2018. Lignocellulose degradation: An overview of fungi and fungal enzymes involved in lignocellulose degradation. *Engineering in Life Sciences*, 18(11), pp.768–778.

Anwar, Z., Gulfraz, M. and Irshad, M., 2014. Agro-industrial lignocellulosic biomass a key to unlock the future bio-energy: A brief review. *Journal of Radiation Research and Applied Sciences*, 7(2), pp.163–173.

Aryal, Sagal, 2022, *Bacterial growth curve and its significance* [Online]. Available at: https://microbenotes.com/bacterial-growth-curve-and-its-significance/ [Accessed: 25 October 2025].

Aryal, Sagar, 2022, *Submerged Fermentation* [Online]. Available at: https://microbenotes.com/submerged-fermentation/#advantages-of-submerged-fermentation [Accessed: 24 May 2025].

Askari, H., Soleimanian-Zad, S., Kadivar, M. and Shahbazi, S., 2024. Creating a novel genetic diversity of Trichoderma afroharzianum by γ-radiation for xylanase-cellulase production. *Heliyon*, 10(7), p.e28349.

Bajar, S., Singh, A. and Bishnoi, N.R., 2020. Exploration of low-cost agro-industrial waste substrate for cellulase and xylanase production using Aspergillus heteromorphus. *Applied Water Science*, 10(6), p.153.

Bajpai, P., 2014a. Introduction. In: Bajpai, P., (ed.) *Xylanolytic Enzymes*. Elsevier, pp. 1–7.

Bajpai, P., 2014b. Sources, Production, and Classification of Xylanases. In: *Xylanolytic Enzymes*. Elsevier, pp. 43–52.

Bajpai, P., 2014c. Xylan. In: *Xylanolytic Enzymes*. Elsevier, pp. 9–18.

Bakri, Y., Mekaeel, A. and Koreih, A., 2011. Influence of Agitation Speeds and Aeration Rates on the Xylanase Activity of Aspergillus niger SS7. *Brazilian Archives of Biology and Technology*, 54(4), pp.659–664.

Balderas Hernández, V.E., Salas-Montantes, C.J., Barba-De la Rosa, A.P. and De Leon-Rodriguez, A., 2021. Autodisplay of an endo-1,4-β-xylanase from Clostridium cellulovorans in Escherichia coli for xylans degradation. *Enzyme and Microbial Technology*, 149, p.109834.

Ball, D.W., Hill, J.W. and Scott, R.J., 2011. Amino Acids, Proteins, and Enzymrs. In: *The Basics of General, Organic, and Biological Chemistry*. Saylor Foundation, pp. 1009–1082.

Basit, A., Jiang, W. and Rahim, K., 2021. Xylanase and Its Industrial Applications. In: Peixoto Basso, T., Olitta Basso, T.O. and Carlos Basso, L., (eds.) *Biotechnological Application of Biomass*. IntechOpen, pp. 1–22.

Beatriz, T., Csar, R.F.T. and Eleonora, C.C., 2014. α-L-Arabinofuranosidase from Penicillium janczewskii: Production with brewers spent grain and orange waste. *African Journal of Biotechnology*, 13(17), pp.1796–1806.

Beg, Q.K., Kapoor, M., Mahajan, L. and Hoondal, G.S., 2001. Microbial xylanases and their industrial applications: A review. *Applied Microbiology and Biotechnology*, 56(3–4), pp.326–338.

Betini, J.H.A. et al., 2009. Xylanases from Aspergillus niger, Aspergillus niveus and Aspergillus ochraceus produced under solid-state fermentation and their application in cellulose pulp bleaching. *Bioprocess and Biosystems Engineering*, 32(6), pp.819–824.

Bezerra, M.A. et al., 2008. Response surface methodology (RSM) as a tool for optimization in analytical chemistry. *Talanta*, 76(5), pp.965–977.

Bhardwaj, N. et al., 2017. Statistical Optimization of Nutritional and Physical Parameters for Xylanase Production from Newly Isolated Aspergillus oryzae LC1 and Its Application in the Hydrolysis of Lignocellulosic Agro-Residues. *BioResources*, 12(4), pp.8519–8538. Available at: www.ncbi.nlm.nih.gov.

Bhardwaj, N., Kumar, B. and Verma, P., 2019. A detailed overview of xylanases: an emerging biomolecule for current and future prospective. *Bioresources and Bioprocessing*, 6(1), p.40.

Bharti, A.K., Kumar, A., Alok, K. and Dharm, D., 2018. Wheat bran fermentation for the production of cellulase and xylanase by Aspergillus Niger NFCCI 4113. *Res. J. Biotech*, 13(5), pp.11–18. Available at: https://www.researchgate.net/publication/324604233.

Bharti, A.K., Kumar, Amit, Kumar, Alok and Dutt, D., 2018. Exploitation of Parthenium hysterophorous biomass as low-cost substrate for cellulase and xylanase production under solid-state fermentation using Talaromyces stipitatus MTCC 12687. *Journal of Radiation Research and Applied Sciences*, 11(4), pp.271–280.

Bhattacharya, S., 2021. Central Composite Design for Response Surface Methodology and Its Application in Pharmacy. In: Kayaroganam, P., (ed.) *Response Surface Methodology in Engineering Science*. IntechOpen, pp. 1–19.

Bibi, Z. et al., 2022. Polyacrylamide hydrogel carrier (matrix-type macrogel beads): Improvement in the catalytic behavior, stability, and reusability of industrially valuable xylanase from a thermophile Geobacillus stearothermophilus. *Current Research in Biotechnology*, 4, pp.229–237.

Biswas, R., Sahai, V., Mishra, S. and Bisaria, V.S., 2010. Bioprocess strategies for enhanced production of xylanase by Melanocarpus albomyces IITD3A on agro-residual extract. *Journal of Bioscience and Bioengineering*, 110(6), pp.702–708.

Boondaeng, A. et al., 2024. Cellulase production under solid-state fermentation by Aspergillus sp. IN5: Parameter optimization and application. *Heliyon*, 10(5), p.e26601.

Briganti, L. et al., 2021. Structural and molecular dynamics investigations of ligand stabilization via secondary binding site interactions in Paenibacillus xylanivorans GH11 xylanase. *Computational and Structural Biotechnology Journal*, 19, pp.1557–1566.

Budhathoki, U., Thapa, P. and Poluri, E., 2011. Medium optimization of production of xylanase by solid state fermentation from Brevibacillus borstelensis - MTCC 9874 isolated from soil sample of eastern Nepal. *Malaysian Journal of Microbiology*, 7(2), pp.83–91.

Bueno, D. and Brienzo, M., 2025. Production of bioplastics with chemical and enzymatic modificated xylan (lignin- and arabinose-free) from sugarcane bagasse. *Biotechnology for Sustainable Materials*, 2(1), p.2. Available at: https://biotechsustainablematerials.biomedcentral.com/articles/10.1186/s44316-024-00024-9.

Cairns, T.C., Nai, C. and Meyer, V., 2018. How a fungus shapes biotechnology: 100 years of aspergillus niger research. *Fungal Biology and Biotechnology*, 5, p.13.

Cao, Y., Meng, D.-J., Lu, J. and Long, J., 2008. Statistical optimization of xylanase production by Aspergillus niger AN-13 under submerged fermentation using response surface methodology. *African Journal of Biotechnology*, 7(5), pp.631–638. Available at: http://www.academicjournals.org/AJB.

Chaiyaso, T. et al., 2011. Optimization of cellulase-free xylanase production by thermophilic streptomyces thermovulgaris TISTR1948 through Plackett-Burman and response surface methodological approaches. *Bioscience, Biotechnology and Biochemistry*, 75(3), pp.531–537.

Chakdar, H. et al., 2016. Bacterial xylanases: biology to biotechnology. *3 Biotech*, 6(2), p.150.

Collins, T., Gerday, C. and Feller, G., 2005. Xylanases, xylanase families and extremophilic xylanases. *FEMS Microbiology Reviews*, 29(1), pp.3–23.

Corrêa, J.M. et al., 2016. High levels of β-xylosidase in Thermomyces lanuginosus: potential use for saccharification. *Brazilian Journal of Microbiology*, 47(3), pp.680–690.

Corrêa Junior, L.C.S., Gautério, G.V., de Medeiros Burkert, J.F. and Kalil, S.J., 2022. Purification of xylanases from Aureobasidium pullulans CCT 1261 and its application in the production of xylooligosaccharides. *World Journal of Microbiology and Biotechnology*, 38(3), p.52.

Couto, S.R. and Sanromán, M.Á., 2006. Application of solid-state fermentation to food industry-A review. *Journal of Food Engineering*, 76(3), pp.291–302.

Cunha, L. et al., 2018. Optimization of Xylanase Production from Aspergillus foetidus in Soybean Residue. *Enzyme Research*, 2018, p.6597017.

Das, A.K. and Dewanjee, S., 2018. Optimization of Extraction Using Mathematical Models and Computation. In: Sarker, S.D. and Nahar, L., (eds.) *Computational Phytochemistry*. Elsevier, pp. 75–106.

David, A., 2023. Submerged Fermentation: The Versatile Process for Industrial Biotechnology. *Fermentation Technology*, 12, p.165.

Devi, S., Dwivedi, D. and Bhatt, A.K., 2022. Utilization of Agroresidues for the Production of Xylanase by Bacillus safensis XPS7 and Optimization of Production Parameters. *Fermentation*, 8(5), p.221.

d'Halewyn, M.-A. and Chevalier, P., 2025, *Aspergillus niger: INSPQ* [Online]. Available at: https://www.inspq.qc.ca/en/moulds/fact-sheets/aspergillus-niger [Accessed: 30 October 2025].

Dhaver, P., Pletschke, B., Sithole, B. and Govinden, R., 2022. Optimization, purification, and characterization of xylanase production by a newly isolated Trichoderma harzianum strain by a two-step statistical experimental design strategy. *Scientific Reports*, 12, p.17791.

Dhivahar, J. et al., 2020. Production and partial purification of extracellular xylanase from Pseudomonas nitroreducens using frugivorous bat (Pteropus giganteus) faeces as ideal substrate and its role in poultry feed digestion. *Journal of King Saud University - Science*, 32(4), pp.2474–2479.

Van Dijck, P.W.M., Selten, G.C.M. and Hempenius, R.A., 2003. On the safety of a new generation of DSM Aspergillus niger enzyme production strains. *Regulatory Toxicology and Pharmacology*, 38(1), pp.27–35.

Van Dorn, R., Shanahan, D. and Ciofalo, V., 2018. Safety evaluation of xylanase 50316 enzyme preparation (also known as VR007), expressed in Pseudomonas fluorescens, intended for use in animal feed. *Regulatory Toxicology and Pharmacology*, 97, pp.48–56.

Duedu, K.O. and French, C.E., 2016. Characterization of a Cellulomonas fimi exoglucanase/xylanase-endoglucanase gene fusion which improves microbial degradation of cellulosic biomass. *Enzyme and Microbial Technology*, 93–94, pp.113–121.

Ekpenyong, M.G., Antai, S.P., Asitok, A.D. and Ekpo, B.O., 2017. Plackett-Burman Design and Response Surface Optimization of Medium Trace Nutrients for Glycolipopeptide Biosurfactant Production. *Iranian Biomedical Journal*, 21(4), pp.249–260.

El-Gendi, H. et al., 2023. Valorization of lignocellulosic wastes for sustainable xylanase production from locally isolated Bacillus subtilis exploited for xylooligosaccharides' production with potential antimicrobial activity. *Archives of Microbiology*, 205(9), p.315.

El-Nahrawy, S. et al., 2017. Optimization of Culture Conditions for Production of Cellulase by Aspergillus tubingensis KY615746. *Environment, Biodiversity and Soil Security*, 1(2017), pp.177–189.

Enzyme, C., *Effect of pH on Enzymatic Reaction* [Online]. Available at: https://www.creative-enzymes.com/resource/effect-of-ph-on-enzymatic-reaction_51.html [Accessed: 4 November 2025].

Fan, G. et al., 2020. Impact of the disulfide bond on hydrolytic characteristics of a xylanase from Talaromyces thermophiles F1208. *International Journal of Biological Macromolecules*, 164, pp.1748–1757.

Faria, S.P. et al., 2020. Production of cellulases and xylanases by Humicola grisea var. thermoidea and application in sugarcane bagasse arabinoxylan hydrolysis. *Industrial Crops and Products*, 158, p.112968.

Fasiku, S.A., Bello, M.A. and Odeniyi, O.A., 2023. Production of xylanase by Aspergillus niger GIO and Bacillus megaterium through solid-state fermentation. *Access Microbiology*, 5(6), p.000506.

Fawzi, E., 2011. Highly thermostable xylanase purified from Rhizomucor miehei NRL 3169. *Acta Biologica Hungarica*, 62(1), pp.85–94.

Godoy, M.G., Amorim, G.M., Barreto, M.S. and Freire, D.M.G., 2018. Agricultural Residues as Animal Feed. In: Pandey, A., Larroche, C. and Ricardo Soccol, C., (eds.) *Current Developments in Biotechnology and Bioengineering*. Elsevier, pp. 235–256.

Gomes, M.M., Sakamoto, I.K. and Varesche, M.B.A., 2025. Operational and physiological strategies for co-fermentation of solid and liquid brewery waste to produce hydrogen and organic acids using Plackett-Burman design. *International Journal of Hydrogen Energy*, 103, pp.911–925.

González-Bautista, E. et al., 2017. Phenolic compounds inhibit cellulase and xylanase activities of Cellulomonas flavigena PR-22 during saccharification of sugarcane bagasse. *Fuel*, 196, pp.32–35.

Guimaraaes, N.C. de A. et al., 2013. Bioprocess and biotecnology: effect of xylanase from Aspergillus niger and Aspergillus flavus on pulp biobleaching and enzyme production using agroindustrial residues as substract. *SpringerPlus*, 2, p.380. Available at: http://www.springerplus.com/content/2/1/380.

Güler, F. and Özçelik, F., 2023. Screening of xylanase producing Bacillus species and optimization of xylanase process parameters in submerged fermentation. *Biocatalysis and Agricultural Biotechnology*, 51, p.102801.

Guo, H. et al., 2018. Bioflocculants' production from a cellulase-free xylanase-producing Pseudomonas boreopolis G22 by degrading biomass and its application in cost-effective harvest of microalgae. *Bioresource Technology*, 255, pp.171–179.

Hamann, P.R.V., Gomes, T.C., de M.B.Silva, L. and Noronha, E.F., 2020. Influence of lignin-derived phenolic compounds on the Clostridium thermocellum endo-β-1,4-xylanase XynA. *Process Biochemistry*, 92, pp.1–9.

Haq, I. ul and Akram, F., 2019. Insight into kinetics and thermodynamics of a novel hyperstable GH family 10 endo-1,4-β-xylanase (TnXynB) with broad substrates specificity cloned from Thermotoga naphthophilaRKU-10T. *Enzyme and Microbial Technology*, 127, pp.32–42.

Heinze, S. et al., 2017. Identification of endoxylanase XynE from Clostridium thermocellum as the first xylanase of glycoside hydrolase family GH141. *Scientific Reports*, 7(1), p.11178.

Huang, J. et al., 2024. Improving the inhibitory resistance of xylanase FgXyn11C from Fusarium graminearum to SyXIP-I by site-directed mutagenesis. *International Journal of Biological Macromolecules*, 271(1), p.132434.

Iram, A., Cekmecelioglu, D. and Demirci, A., 2022. Optimization of the fermentation parameters to maximize the production of cellulases and xylanases using DDGS as the main feedstock in stirred tank bioreactors. *Biocatalysis and Agricultural Biotechnology*, 45, p.102514.

Isikgor, F.H. and Becer, C.R., 2015. Lignocellulosic biomass: a sustainable platform for the production of bio-based chemicals and polymers. *Polymer Chemistry*, 6(25), pp.4497–4559.

Jonathan, Tania, V., Tanjaya, J.C. and Katherine, 2021. Recent Advancements of Fungal Xylanase Upstream Production and Downstream Processing. *Indonesian Journal of Life Sciences | ISSN: 2656-0682 (online)*, 3(1), pp.37–58.

Joshi, C. and Khare, S.K., 2011. Utilization of deoiled Jatropha curcas seed cake for production of xylanase from thermophilic Scytalidium thermophilum. *Bioresource Technology*, 102(2), pp.1722–1726.

Joshi, K., Meher, M.K. and Poluri, K.M., 2020. Fabrication and Characterization of Bioblocks from Agricultural Waste Using Fungal Mycelium for Renewable and Sustainable Applications. *ACS Applied Bio Materials*, 3(4), pp.1884–1892.

Kalim, B. et al., 2023. Modulating the production of xylanase by Bacillus pumilus BS131 through optimization using waste fiber sludge. *Brazilian Journal of Biology*, 83, p.e243874.

Kalpana, V.N. and Devi Rajeswari, V., 2015. Production of xylanase from various lignocellulosic waste materials by Streptomyces sp. and its potential role in deinking of newsprint. *Asian Journal of Biochemistry*, 10(5), pp.222–229.

Karunakaran, S. et al., 2014. Xylanase Production from Aspergillus niger. *International Journal of ChemTech Research*, 6(9), pp.4207–4211.

Katapodis, P., Christakopoulou, V., Kekos, D. and Christakopoulos, P., 2007. Optimization of xylanase production by Chaetomium thermophilum in wheat straw using response surface methodology. *Biochemical Engineering Journal*, 35(2), pp.136–141.

Khandeparker, R., Parab, P. and Amberkar, U., 2017. Recombinant Xylanase from Bacillus tequilensis BT21: Biochemical Characterization and Its Application in Production of Xylobiose from Agricultural Residues. *Food Technology and Biotechnology*, 55(2), pp.164–172. Available at: http://www.ftb.com.hr/images/pdfarticles/2017/April_June/ftb-55-164.pdf.

Khangkhachit, W., Suyotha, W., Leamdum, C. and Prasertsan, P., 2021. Production of thermostable xylanase using Streptomyces thermocarboxydus ME742 and application in enzymatic conversion of xylan from oil palm empty fruit bunch to xylooligosaccharides. *Biocatalysis and Agricultural Biotechnology*, 37(1), p.102180.

Kirimura, K. and Yoshioka, I., 2019. Citric acid. In: Moo-Young, M., (ed.) *Comprehensive Biotechnology*. Elsevier, pp. 158–165.

Kohli, U., Nigam, P., Singh, D. and Chaudhary, K., 2001. Thermostable, alkalophilic and cellulase free xylanase production by Thermoactinomyces thalophilus subgroup C. *Enzyme and Microbial Technolog*, 28, pp.606–610. Available at: www.elsevier.com/locate/enzmictec.

Krijgsheld, P. et al., 2013. Development in aspergillus. *Studies in Mycology*, 74, pp.1–29.

Kumar, D. et al., 2017. XYLANASES AND THEIR INDUSTRIAL APPLICATIONS : A REVIEW. *Biochem. Cell. Arch.*, 17(1), pp.353–360. Available at: www.connectjournals.com/bca.

Kundu, A. and Ray, R.R., 2012. Production of intracellular β-xylosidase from the submerged fermentation of citrus wastes by Penicillium janthinellum MTCC 10889. *3 Biotech*, 3(3), pp.241–246.

Kuniyoshi, T.M. et al., 2021. Pediocin PA-1 production by Pediococcus pentosaceus ET34 using non-detoxified hemicellulose hydrolysate obtained from hydrothermal pretreatment of sugarcane bagasse. *Bioresource Technology*, 338, p.125565.

Lai, Y. et al., 2025. Identification of a novel forkhead transcription factor MtFKH1 for cellulase and xylanase gene expression in Myceliophthora thermophila (ATCC 42464). *Microbiological Research*, 294, p.128097.

Lam, L.T. et al., 2010. Influence of residual elements in lead on oxygen- and hydrogen-gassing rates of lead-acid batteries. *Journal of Power Sources*, 195(14), pp.4494–4512.

Lee, H. V., Hamid, S.B.A. and Zain, S.K., 2014. Conversion of Lignocellulosic Biomass to Nanocellulose: Structure and Chemical Process. *The Scientific World Journal*, 2014, p.631013.

Li, H., Voutilainen, S., Ojamo, H. and Turunen, O., 2015. Stability and activity of Dictyoglomus thermophilum GH11 xylanase and its disulphide mutant at high pressure and temperature. *Enzyme and Microbial Technology*, 70, pp.66–71.

Li, Q. et al., 2018. Leveraging pH profiles to direct enzyme production (cellulase, xylanase, polygalacturonase, pectinase, A-galactosidase, and invertase) by Aspergillus foetidus. *Biochemical Engineering Journal*, 137, pp.247–254.

Liu, C. et al., 2024. Combined strategies for improving the heterologous expression of a novel xylanase from Fusarium oxysporum Fo47 in Pichia pastoris. *Synthetic and Systems Biotechnology*, 9(3), pp.426–435.

Liu, X. et al., 2022. Biochemical characterization of a novel glycoside hydrolase family 11 xylanase from Chaetomium sp. suitable for bread making. *Process Biochemistry*, 117, pp.1–9.

Liu, X. et al., 2018. Biochemical characterization of a novel xylanase from Paenibacillus barengoltzii and its application in xylooligosaccharides production from corncobs. *Food Chemistry*, 264, pp.310–318.

Londoño-Hernandez, L. et al., 2020. Advantages and Progress Innovations of Solid-State Fermentation to Produce Industrial Enzymes. In: Arora, N.K., Mishra, J. and Mishra, V., (eds.) *Microbial Enzymes: Roles and Applications in Industries*. Springer, pp. 87–113.

Lopes, F.C. et al., 2011. Production of proteolytic enzymes by a keratin-degrading aspergillus niger. *Enzyme Research*, 2011, p.487093.

López-López, A. et al., 2023. TtCel7A: A Native Thermophilic Bifunctional Cellulose/Xylanase Exogluclanase from the Thermophilic Biomass-Degrading Fungus Thielavia terrestris Co3Bag1, and Its Application in Enzymatic Hydrolysis of Agroindustrial Derivatives. *Journal of Fungi*, 9(2), p.152.

Lu, Y. et al., 2025. Characterization of a rare trifunctional xylanase from endophytic fungus Chaetomium globosum and its synergistic effect with cellulase cocktail. *International Journal of Biological Macromolecules*, 309, p.143065.

Luo, L. et al., 2016. Purification and characterization of an alkaliphilic endo-xylanase from Streptomyces althioticus LMZM and utilization in the pulp paper industry. *Journal of Chemical Technology and Biotechnology*, 91(4), pp.1093–1098.

Maan, P., Bharti, A.K., Gautam, S. and Dutt, D., 2016. Screening of Important Factors for Xylanase and Cellulase Production from the Fungus C. cinerea RM-1 NFCCI-3086 through Plackett-Burman Experimental Design. *BioResources*, 11(4), pp.8269–8276.

Mahallati, M.N., 2020. Advances in modeling saffron growth and development at different scales. In: Koocheki, A. and Khajeh-hosseini, M., (eds.) *Saffron: Science, Technology and Health*. Elsevier, pp. 139–167.

Mandal, A., 2015. EFFECT OF NITROGEN SOURCES, PHOSPHATE SOURCES AND METAL IONS ON THE PRODUCTION OF XYLANASE BY BACILLUS CEREUS BSA1. *International Journal of Current Research*, 7(8), pp.19391–19394. Available at: http://www.journalcra.com.

Mardawati, E., Parlan, Rialita, T. and Nurhadi, B., 2018. Optimization of moistening solution concentration on xylanase activity in solid state fermentation from oil palm empty fruit bunches. *IOP Conference Series: Earth and Environmental Science*, 141, p.012018.

Martínez-Mira, A. et al., 2025. Culture media design and scaling-up of submerged fermentation for the nematophagous fungus Duddingtonia flagrans. *Experimental Parasitology*, 269, p.108901.

Martínez-Pacheco, M.M. et al., 2020. Optimization of production of xylanases with low cellulases in Fusarium solani by means of a solid state fermentation using statistical experimental design. *Revista Argentina de Microbiologia*, 52(4), pp.328–337.

Miao, Y. et al., 2015. Characterization and identification of the xylanolytic enzymes from Aspergillus fumigatus Z5. *BMC Microbiology*, 15, p.126.

Michaux, C. et al., 2010. Structural insights into the acidophilic pH adaptation of a novel endo-1,4-β-xylanase from Scytalidium acidophilum. *Biochimie*, 92(10), pp.1407–1415.

Mmango-Kaseke, Z. et al., 2016. Optimization of cellulase and xylanase production by Micrococcus species under submerged fermentation. *Sustainability (Switzerland)*, 8(11), p.1168.

Modi, H.A. et al., 2011. PROCESS OPTIMIZATION FOR XYLANASE PRODUCTION BY ASPERGILLUS NIGER IN SOLID STATE FERMENTATION. *Int. J. Biotech Biosci*, 1(4), pp.423–430. Available at: https://www.researchgate.net/publication/318338709.

Mongkorntanyatip, K., Limsakul, P., Ratanakhanokchai, K. and Khunrae, P., 2017. Overexpression and characterization of alkaliphilic Bacillus firmus strain K-1 xylanase. *Agriculture and Natural Resources*, 51(6), pp.437–444.

Moran-Aguilar, M.G. et al., 2021. Production of cellulases and xylanases in solid-state fermentation by different strains of Aspergillus niger using sugarcane bagasse and brewery spent grain. *Biochemical Engineering Journal*, 172, p.108060.

Mostafa, F.A., Abas Abd El Aty, A. and Refaat Wehaidy, H., 2014. Improved Xylanase production by mixing low cost wastes and novel co-culture of three marine-derived fungi in solid state fermentation. *Int.J.Curr.Microbiol.App.Sci*, 3(7), pp.336–349. Available at: http://www.ijcmas.com.

Motta, F.L., Andrade, C.C.P. and Santana, M.H.A., 2013. A Review of Xylanase Production by the Fermentation of Xylan: Classification, Characterization and Applications. In: Chandel, A.K. and Silverio da Silva, S., (eds.) *Sustainable Degradation of Lignocellulosic Biomass - Techniques, Applications and Commercialization*. InTech, pp. 251–275.

Mujtaba, M. et al., 2023. Lignocellulosic biomass from agricultural waste to the circular economy: a review with focus on biofuels, biocomposites and bioplastics. *Journal of Cleaner Production*, 402, p.136815.

Murugan, S., Arnold, D., Pongiya, U.D. and Narayanan, P.M., 2011. Production of xylanase from arthrobacter sp. MTCC 6915 using saw dust as substrate under solid state fermentation. *Enzyme Research*, 2011(1), p.696942.

Nadumane, V.K., Venkatachalam, P. and Gajaraj, B., 2016. Aspergillus Applications in Cancer Research. In: Kumar Gupta, V., (ed.) *New and Future Developments in Microbial Biotechnology and Bioengineering: Aspergillus System Properties and Applications*. Elsevier Inc., pp. 243–255.

Najafpour, G.D.., 2015. Gas and Liquid System (Aeration and Agitation). In: *Biochemical engineering and biotechnology*. Elsevier, pp. 51–102.

Nakamichi, Y. et al., 2019. Structural and functional characterization of a bifunctional GH30-7 xylanase B from the filamentous fungus Talaromyces cellulolyticus. *Journal of Biological Chemistry*, 294(11), pp.4065–4078.

Nam, K.H., 2024. Temperature-dependent structural changes in xylanase II from Trichoderma longibrachiatum. *Carbohydrate Research*, 541, p.109173.

Okafor, U.A., Okochi, V.I., Onyegeme-Okerenta and Nwodo-Chinedu, 2007. Xylanase production by Aspergillus niger ANL 301 using agro-wastes. *African Journal of Biotechnology*, 6(14), pp.1710–1714. Available at: http://www.academicjournals.org/AJB.

Pakaweerachat, P. and Chysirichote, T., 2025. Comparative Evaluation of Culture Media and pH Conditions for Xylanase Production in Aspergillus niger. *Journal of Pure and Applied Microbiology*, 19(3), pp.2260–2270.

Pal, A. and Khanum, F., 2010. Production and extraction optimization of xylanase from Aspergillus niger DFR-5 through solid-state-fermentation. *Bioresource Technology*, 101(19), pp.7563–7569.

Pal, A. and Khanum, F., 2011. Purification of xylanase from Aspergillus niger DFR-5: Individual and interactive effect of temperature and pH on its stability. *Process Biochemistry*, 46(4), pp.879–887.

Pasrija, R. and Kumari, D., 2025. Growth Curve Preparation for the Calculation of Fungal Cell Count Over Time. In: *Protocols for Studying Pathogenic Fungi*. Springer Singapore, pp. 63–71.

Patel, K. and Amaresan, N., 2022. Mass Multiplication, Production Cost Analysis and Marketing of Xylanase. In: Amaresan, N., Dharumadurai, D. and Cundell, D.R., (eds.) *Industrial Microbiology Based Entrepreneurship: Making Money from Microbes*. Springer Singapore, pp. 25–35.

Patel, K. and Dudhagara, P., 2020. Optimization of xylanase production by Bacillus tequilensis strain UD-3 using economical agricultural substrate and its application in rice straw pulp bleaching. *Biocatalysis and Agricultural Biotechnology*, 30, p.101846.

Paul, M., Nayak, D.P. and Thatoi, H., 2020. Optimization of xylanase from Pseudomonas mohnii isolated from Simlipal Biosphere Reserve, Odisha, using response surface methodology. *Journal of Genetic Engineering and Biotechnology*, 18, p.81.

Paulo, R.H. et al., 2014. Xylanase from Fusarium heterosporum: Properties and influence of thiol compounds on xylanase activity. *African Journal of Biotechnology*, 13(9), pp.1047–1055.

Pereira de Almeida, A. et al., 2022. Investigation of biochemical and biotechnological potential of a thermo-halo-alkali-tolerant endo-xylanase (GH11) from Humicola brevis var. thermoidea for lignocellulosic valorization of sugarcane biomass. *Biocatalysis and Agricultural Biotechnology*, 44, p.102424.

Ping, L. et al., 2018. Production and characterization of a novel acidophilic and thermostable xylanase from Thermoascus aurantiacu. *International Journal of Biological Macromolecules*, 109, pp.1270–1279.

Polizeli, M.L.T.M. et al., 2005. Xylanases from fungi: Properties and industrial applications. *Applied Microbiology and Biotechnology*, 67(5), pp.577–591.

Poornima, S. et al., 2020. Aqueous two-phase partitioning and characterization of xylanase produced by Streptomyces geysiriensis from low cost lignocellulosic substrates. *Journal of Bioscience and Bioengineering*, 130(6), pp.571–576.

Qi, X. et al., 2025. A novel wheat arabino-xylanase from Trichoderma gamsii: Study on biochemical characterization, substrate recognition mechanism and its application in wheat flour dough and Chinese bread. *LWT - Food Science and Technology*, 219, p.117550.

Rafiee, K., Kaur, G. and Brar, S.K., 2021. Fungal biocomposites: How process engineering affects composition and properties? *Bioresource Technology Reports*, 14, p.100692.

Rahmani, N. et al., 2019. GH-10 and GH-11 Endo-1,4-B-xylanase enzymes from Kitasatospora sp. produce xylose and xylooligosaccharides from sugarcane bagasse with no xylose inhibition. *Bioresource Technology*, 272, pp.315–325.

Rajagopalan, G., Shanmugavelu, K. and Yang, K.L., 2017. Production of prebiotic-xylooligosaccharides from alkali pretreated mahogany and mango wood sawdust by using purified xylanase of Clostridium strain BOH3. *Carbohydrate Polymers*, 167, pp.158–166.

Ramchuran, S.O., Mateus, B., Holst, O. and Karlsson, E.N., 2005. The methylotrophic yeast Pichia pastoris as a host for the expression and production of thermostable xylanase from the bacterium Rhodothermus marinus. *FEMS Yeast Research*, 5(9), pp.839–850.

Ranade, S.S. and Thiagarajan, P., 2017. Selection of a design for response surface. *IOP Conference Series: Materials Science and Engineering*, 263(2), p.022043.

Rashid, R., Ejaz, U., Moin, S.F. and Sohail, M., 2024. Xylanase from Neobacillus sedimentimangrovi UE25: Characterization, purification and applications. *Biocatalysis and Agricultural Biotechnology*, 60, p.103331.

Dos Reis, L. et al., 2015. Statistical optimization of mineral salt and urea concentration for cellulase and xylanase production by Penicillium echinulatum in submerged fermentation. *Brazilian Journal of Chemical Engineering*, 32(1), pp.13–22.

Renge, V.C., Khedkar, S. V. and Nandurkar, N.R., 2012. ENZYME SYNTHESIS BY FERMENTATION METHOD : A REVIEW. *Scientific Review & Chemical Communications*, 2(4), pp.585–590. Available at: www.sadgurupublications.com.

Rezende, M.I., Barbosa, A.D.M., Vasconcelos, A.F.D. and Endo, A.S., 2002. Xylanase production by Trichoderma harzianum Rifai by solid state fermentation on sugarcane bagasse. *Brazilian Journal of Microbiology*, 33(1), pp.67–72.

Rios, H. V. et al., 2017. Energy and nutrient utilisation of maize-soy diet supplemented with a xylanase-β-glucanase complex from Talaromyces versatilis. *Animal Feed Science and Technology*, 232, pp.80–90.

Rodríguez-Sanz, A. et al., 2024. A comprehensive method for the sequential separation of extracellular xylanases and β-xylosidases/arabinofuranosidases from a new Fusarium species. *International Journal of Biological Macromolecules*, 272, p.132722.

Rodriguez-Tudela, J.L. et al., 2003. Interlaboratory Evaluation of Hematocytometer Method of Inoculum Preparation for Testing Antifungal Susceptibilities of Filamentous Fungi. *Journal of Clinical Microbiology*, 41(11), pp.5236–5237.

Rojas-Pérez, L.C. et al., 2022. Production of xylose through enzymatic hydrolysis of glucuronoarabinoxylan from brewers' spent grain. *Bioresources and Bioprocessing*, 9(1), p.105.

Rosmine, E. et al., 2017. Statistical optimisation of xylanase production by estuarine Streptomyces sp. and its application in clarification of fruit juice. *Journal of Genetic Engineering and Biotechnology*, 15(2), pp.393–401.

Sadaf, A., Morya, V.K. and Khare, S.K., 2016. Applicability of Sporotrichum thermophile xylanase in the in situ saccharification of wheat straw pre-treated with ionic liquids. *Process Biochemistry*, 51(12), pp.2090–2096.

Salihu, A., Bala, S.M. and Olagunju, A., 2015. A Statistical Design Approach for Xylanase Production by Aspergillus niger Using Soybean Hulls: Optimization and Determining the Synergistic Effects of Medium Components on the Enzyme Production. *Jordan Journal of Biological Sciences*, 8(4), pp.319–323.

Sanguine, I.S. et al., 2022. Xylanases of Trichoderma koningii and Trichoderma pseudokoningii: Production, characterization and application as additives in the digestibility of forage for cattle. *Biocatalysis and Agricultural Biotechnology*, 44, p.102482.

Sanjivkumar, M., Silambarasan, T., Balagurunathan, R. and Immanuel, G., 2018. Biosynthesis, molecular modeling and statistical optimization of xylanase from a mangrove associated actinobacterium Streptomyces variabilis (MAB3) using Box-Behnken design with its bioconversion efficacy. *International Journal of Biological Macromolecules*, 118, pp.195–208.

Santos, C.R. et al., 2014. Molecular Mechanisms Associated with Xylan Degradation by Xanthomonas Plant Pathogens. *The Journal of Biological Chemistry*, 289(46), pp.32186–32200.

Sarabia, L.A., Ortiz, M.C. and Sánchez, M.S., 2009. 1.12 - Response Surface Methodology. In: Brown, S.D., Tauler, R. and Walczak, B., (eds.) *Comprehensive Chemometrics: Chemical and Biochemical Data Analysis*. Elsevier, pp. 345–390.

Selvarajan, E. and Veena, R., 2017. Recent advances and future perspectives of thermostable xylanase. *Biomedical and Pharmacology Journal*, 10(1), pp.261–279.

Shahid, S. et al., 2023. Improved catalytic efficiency of chimeric xylanase 10B from Thermotoga petrophila RKU1 and its synergy with cellulases. *Enzyme and Microbial Technology*, 166, p.110213.

Shahriarinour, M. et al., 2011. CYANOBACTERIAL BIOMASS AS N-SUPPLEMENT TO OIL PALM EMPTY FRUIT BUNCH (OPEFB) FIBRE FOR IMPROVEMENT OF CELLULASE PRODUCTION BY ASPERGILLUS TERREUS IN SUBMERGED FERMENTATION. *BioResources*, 6(2), pp.1696–1706.

Shin, H.D., Vo, T. and Chen, R., 2011. Novel Aspergillus hemicellulases enhance performance of commercial cellulases in lignocellulose hydrolysis. *Biotechnology Progress*, 27(2), pp.581–586.

Shrestha, S. et al., 2022. Formulation of the agro-waste mixture for multi-enzyme (pectinase, xylanase, and cellulase) production by mixture design method exploiting Streptomyces sp. *Bioresource Technology Reports*, 19, p.101142.

Singh, A., Manju, Yadav, A. and Bishnoi, N.R., 2013. Statistical screening and optimization of process variables for xylanase production utilizing alkali-pretreated rice husk. *Annals of Microbiology*, 63(1), pp.353–361.

Sipriyadi, Wahydi, A.T., Suhartono, M.T. and Meryandini, A., 2020. Optimization of Xylanase Production by Streptomyces costaricanus 45I-3 Using Various Substrates through Submerged Fermentation. *Microbiology Indonesia*, 14(1), pp.34–43.

Siwach, R. et al., 2024. Optimization of xylanase production by Bacillus sp. MCC2212 under solid-state fermentation using response surface methodology. *Biocatalysis and Agricultural Biotechnology*, 57, p.103085.

Six Sigma, 2024, *Design of Experiments: Plackett Burman Designs* [Online]. Available at: https://www.6sigma.us/six-sigma-in-focus/plackett-burman-designs/ [Accessed: 17 November 2025].

Sohpal, V.K., Dey, A. and Singh, A., 2010. Investigate of Process Parameters on Xylanase Enzyme Activity in Melanocarpus Albomyces Batch Culture. *World Congress on Engineering : WCE 2010*. June 2010 Newswood Ltd. : International Association of Engineers, London, pp. 1–4.

Sokač, T. et al., 2023. Standardization of 3,5-dinitrosalicylic acid (DNS) assay for measuring xylanase activity. *Croatian journal of food science and technology*, 15(2), pp.151–162.

Sriyapai, T. et al., 2011. Cloning of a thermostable xylanase from Actinomadura sp. S14 and its expression in Escherichia coli and Pichia pastoris. *Journal of Bioscience and Bioengineering*, 111(5), pp.528–536.

Su, Y. et al., 2011. Improvement of xylanase production by thermophilic fungus Thermomyces lanuginosus SDYKY-1 using response surface methodology. *New Biotechnology*, 28(1), pp.40–46.

Suleman, M., Faiz, A. ul H. and Faiz. Lariab Zahra, 2020. Optimization of Xylanase Activity in the Presence of Salts of Different Metals for the Pulping of Indigenous Non-Woody Raw Materials (Gossypium Arborium). *Journal of Bioresource Management*, 7(1), pp.01–09.

Sun, J.Y. et al., 2007. Expression of recombinant Thermomonospora fusca xylanase A in Pichia pastoris and xylooligosaccharides released from xylans by it. *Food Chemistry*, 104(3), pp.1055–1064.

Sunder, Yadav, S. and Pal, J., 2025. Optimisation of process parameters for lignocellulosic biomass degradation by Pseudomonas sp. using response surface methodology. *International Journal of Biological Macromolecules*, 309, p.142792.

Tafazzoli, K., Ghavami, M. and Khosravi-Darani, K., 2024. Investigation of impact of siderophore and process variables on production of iron enriched Saccharomyces boulardii by Plackett–Burman design. *Scientific Reports*, 14(1), p.22813.

Taibi, Z. et al., 2012. Purification and biochemical characterization of a highly thermostable xylanase from Actinomadura sp. strain Cpt20 isolated from poultry compost. *Applied Biochemistry and Biotechnology*, 166(3), pp.663–679.

Tang, K. et al., 2021. Molecular cloning and characterization of a novel xylanase from Microbacterium imperiale YD-01. *Journal of Food Biochemistry*, 45(12), p.e13988. Available at: /doi/pdf/10.1111/jfbc.13988 [Accessed: 26 May 2025].

Tarrsini, M. et al., 2020. Optimization of On-Site Xylanase Production from Aspergillus niger via Central Composite Design (CCD). *IOP Conference Series: Materials Science and Engineering*, 855(1), p.012005.

Teertstra, W.R. et al., 2017. Maturation of conidia on conidiophores of Aspergillus niger. *Fungal Genetics and Biology*, 98, pp.61–70.

Teng, C. et al., 2017. Improving special hydrolysis characterization into Talaromyces thermophilus F1208 xylanase by engineering of N-terminal extension and site-directed mutagenesis in C-terminal. *International Journal of Biological Macromolecules*, 96, pp.451–458.

Tenkanen, M. and Siika-Aho, M., 2000. An a-glucuronidase of Schizophyllum commune acting on polymeric xylan. *Journal of Biotechnology*, 78(2), pp.149–161. Available at: www.elsevier.com/locate/jbiotec.

Terrasan, C.R.F. et al., 2013. Xylanase and β-Xylosidase from Penicillium janczewskii: Production, Physico-chemical Properties, and Application of the Crude Extract to Pulp Biobleaching. *BioResources*, 8(1), pp.1292–1305.

Terrasan, C.R.F., Temer, B., Duarte, M.C.T. and Carmona, E.C., 2010. Production of xylanolytic enzymes by Penicillium janczewskii. *Bioresource Technology*, 101(11), pp.4139–4143.

Thakur, V., Kumar, Virender, Kumar, Vijay and Singh, D., 2022. Xylooligosaccharides production using multi-substrate specific xylanases secreted by a psychrotolerant Paenibacillus sp. PCH8. *Carbohydrate Polymer Technologies and Applications*, 3, p.100215.

Tsegaye, B., Balomajumder, C. and Roy, P., 2019. Microbial delignification and hydrolysis of lignocellulosic biomass to enhance biofuel production: an overview and future prospect. *Bulletin of the National Research Centre*, 43(1), p.51.

Uday, U.S.P., Choudhury, P., Bandyopadhyay, T.K. and Bhunia, B., 2016. Classification, mode of action and production strategy of xylanase and its application for biofuel production from water hyacinth. *International Journal of Biological Macromolecules*, 82, pp.1041–1054.

Ughy, B. et al., 2023. Reconsidering Dogmas about the Growth of Bacterial Populations. *Cells*, 12(10), p.1430.

Vanaja, K. and Rani, R.H.S., 2007. Design of experiments: Concept and applications of plackett burman design. *Clinical Research and Regulatory Affairs*, 24(1), pp.1–23.

Verma, D. and Satyanarayana, T., 2012. Cloning, expression and applicability of thermo-alkali-stable xylanase of Geobacillus thermoleovorans in generating xylooligosaccharides from agro-residues. *Bioresource Technology*, 107, pp.333–338.

Verma, R., Kumar, A. and Kumar, S., 2019. Synthesis and characterization of cross-linked enzyme aggregates (CLEAs) of thermostable xylanase from Geobacillus thermodenitrificans X1. *Process Biochemistry*, 80, pp.72–79.

Visagie, C.M. and Houbraken, J., 2020. Updating the taxonomy of Aspergillus in South Africa. *Studies in Mycology*, 95, pp.253–292.

Vries, R.P. de and Visser, J., 2001. Aspergillus Enzymes Involved in Degradation of Plant Cell Wall Polysaccharides . *Microbiology and Molecular Biology Reviews*, 65(4), pp.497–522.

Wagner Jr., J.R., Mount III, E.M. and Giles Jr., H.F., 2014. Design of Experiments. In: *Extrusion*. Elsevier, pp. 291–308.

Walia, A. et al., 2017. Microbial xylanases and their industrial application in pulp and paper biobleaching: a review. *3 Biotech*, 7(1), p.11.

Wang, L. et al., 2018. Application of response surface methodology to optimize the production of antimicrobial metabolites by Micromonospora Y15. *Biotechnology and Biotechnological Equipment*, 31(5), pp.1016–1025.

Wang, L. et al., 2022. Identification and characterization of a thermostable GH11 xylanase from Paenibacillus campinasensis NTU-11 and the distinct roles of its carbohydrate-binding domain and linker sequence. *Colloids and Surfaces B: Biointerfaces*, 209, p.112167.

Wang, L., Wang, Y.Y., Chen, Z.L. and Li, Y.H., 2024. Enzymatic characterization and thermostability improvement of an acidophilic endoxylanase PphXyn11 from Paenibacillus physcomitrellae XB. *Protein Expression and Purification*, 219, p.106482.

Wang, S. et al., 2025. A novel GH11 β-1,4-xylanase from Fusarium verticillioides: Its eukaryotic expression, biochemical characterization and synergistic effect with cellulase on lignocellulosic biomass degradation. *International Journal of Biological Macromolecules*, 305, p.141169.

Whitford, W.G., Lundgren, M. and Fairbank, A., 2018. Cell Culture Media in Bioprocessing. In: Jagschies, G., Lindskog, E., Łącki, K. and Galliher, P., (eds.) *Biopharmaceutical Processing: Development, Design, and Implementation of Manufacturing Processes*. Elsevier, pp. 147–162.

Willey, J.M.., Sandman, K.M.. and Wood, D.H.., 2020. *Prescott's microbiology* 11th ed., McGraw-Hill Education, New York, NY.

Wu, Q. et al., 2023. Improved thermostability, acid tolerance as well as catalytic efficiency of Streptomyces rameus L2001 GH11 xylanase by N-terminal replacement. *Enzyme and Microbial Technology*, 162, p.110143.

Xu, Y.X. et al., 2008. Improvement of xylanase production by Aspergillus niger XY-1 using response surface methodology for optimizing the medium composition. *Journal of Zhejiang University: Science B*, 9(7), pp.558–566.

Yang, J., Ma, T., Shang-guan, F. and Han, Z., 2020. Improving the catalytic activity of thermostable xylanase from Thermotoga maritima via mutagenesis of non-catalytic residues at glycone subsites. *Enzyme and Microbial Technology*, 139, p.109579.

Yang, X. et al., 2014. Two xylose-tolerant GH43 bifunctional β-xylosidase/α-arabinosidases and one GH11 xylanase from Humicola insolens and their synergy in the degradation of xylan. *Food Chemistry*, 148, pp.381–387.

Yang, Z. and Zhang, Z., 2017. Codon-optimized expression and characterization of a pH stable fungal xylanase in Pichia pastoris. *Process Biochemistry*, 53, pp.80–87.

Yates, G.T. and Smotzer, T., 2007. On the lag phase and initial decline of microbial growth curves. *Journal of Theoretical Biology*, 244(3), pp.511–517.

Zhang, J. et al., 2011. Thermostable recombinant xylanases from Nonomuraea flexuosa and Thermoascus aurantiacus show distinct properties in the hydrolysis of xylans and pretreated wheat straw. *Biotechnology for Biofuels*, 4, p.12.

Zhang, Z. et al., 2024. Review of research progress on the production of cellulase from filamentous fungi. *International Journal of Biological Macromolecules*, 277, p.134539.

Zhao, X.Q., Xu, X.N. and Chen, L.Y., 2016. Production of Enzymes from Marine Actinobacteria. In: Kwon Kim, S. and Toldrá, F., (eds.) *Advances in Food and Nutrition Research*. Academic Press Inc., pp. 137–151.

Zheng, F. et al., 2024. Expression and characterization of a novel halophilic GH10 β-1,4-xylanase from Trichoderma asperellum ND-1 and its synergism with a commercial α-L-arabinofuranosidase on arabinoxylan degradation. *International Journal of Biological Macromolecules*, 282, p.136885.

APPENDIX A

Preparation of xylose standard curve using the DNS method.

i. Preparation of xylose standard solution

A xylose stock solution of 10 mg/mL was prepared by dissolving 1 g of xylose powder into 100 mL of sodium acetate buffer. Then, the xylose stock solution was diluted into 2.0 mg/mL, 4.0 mg/mL, 6.0 mg/mL, 8.0 mg/mL and 10.0 mg/mL, using formula below:

$$M_1M_2 = M_2V_2$$

where,

M_1 = Concentration of stock solution

V_1 = Volume of stock solution

M_2 = Concentration of standard solution prepared

V_2 = Volume of standard solution

The standard xylose in different concentration was prepared based on the volume tabulated at Table A.1. After that, each of the solution were tested with cuvette (1mL) using 540 nm absorbance range setting.

Table A.1: Preparation of standard xylose solution in different concentration.

Standard xylose concentration (mg/mL)	Volume of xylose solution (µL)	Volume of distilled water (µL)	Total volume (µL)
0	0	300	300
2	30	270	300
4	60	240	300
6	90	210	300
8	120	180	300
10	150	150	300
12	180	120	300
14	210	90	300
16	240	60	300
18	270	30	300
20	300	0	300

ii. Construction of xylose standard curve

The standard xylose prepared were tested with UV-Vis spectrophotometer using 540 nm absorbance range setting. Volume of cuvette with 1 mL was used in this run test. The absorbance reading was tabulated at Table A.2 and xylose standard curve was plotted at Figure A.1.

Table A.2: Different standard xylose concentrations with respective absorbance values obtained at 540 nm.

Standard xylose concentration (mg/mL)	Absorbance at 540 nm ($A_{540\ nm}$)				
	1	2	3	Mean	SD
0	0	0	0	0.0000	0.0000
2	0.2940	0.2950	0.2930	0.2940	0.0010
4	0.6880	0.6840	0.6810	0.6843	0.0035
6	1.0290	1.0170	1.0100	1.0187	0.0096
8	1.3700	1.3570	1.3450	1.3573	0.0125
10	1.6790	1.6600	1.6460	1.6617	0.0166
12	2.0200	2.0180	2.0120	2.0167	0.0042
14	2.3010	2.2950	2.3100	2.3020	0.0075
16	2.5010	2.5710	2.5670	2.5463	0.0393
18	2.8800	2.8680	2.8680	2.8720	0.0069
20	3.0990	3.0960	3.1030	3.0993	0.0035

*SD is the standard deviation

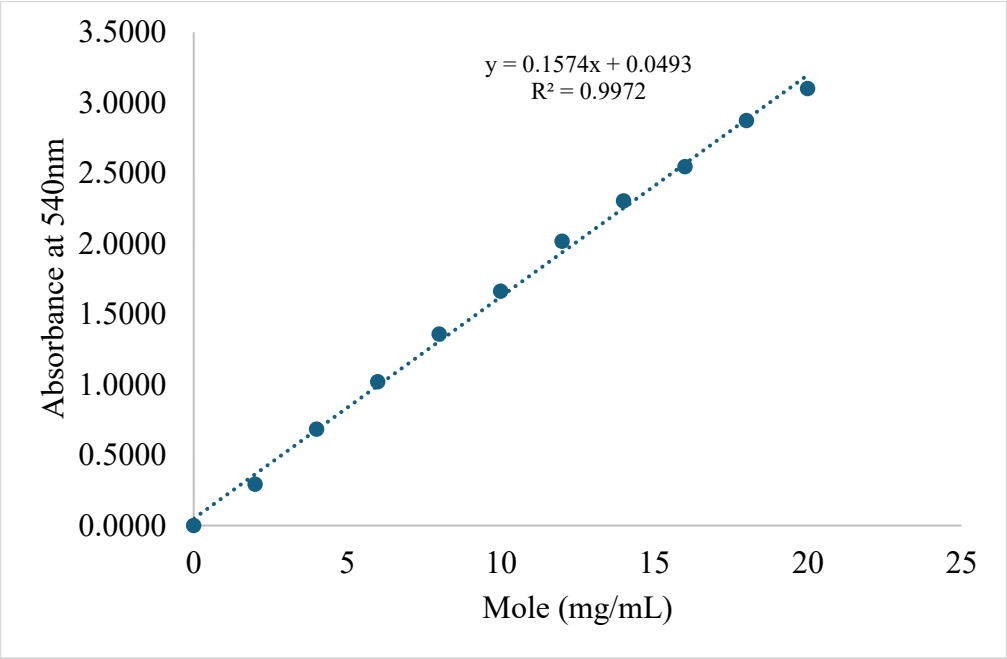

Figure A.1: Xylose standard curve

APPENDIX B

Calculation of the xylanase activity produce by the *Aspergillus niger*

i. Interpretation of xylose standard solution

Calculation of reducing sugar (xylose) production yield can be performed by substituting the absorbance value obtained from the sample to the equation of constructed xylose standard curve determined by DNS test. The equation of xylose standard curve yield was $y = 0.1574x + 0.0493$ with R^2 of 0.9972. The nearest the R^2 to 1.0 indicated the high correlation between experimental and predicted value.

Where,

y = Mean absorbance reading at 540 nm

x = Reducing sugar concentration (mg/mL)

$$x = \frac{y+0.2655}{0.3147} \qquad \text{----- (B1)}$$

ii. Calculation of enzyme activity

The xylanase activity was calculated by using the equation following:

$$Xylanase\ activity\ \left(\frac{U}{mL}\right) = \frac{xylose\ concentration\left(\frac{mg}{mL}\right)(from\ curve) \times total\ volume\ of\ reaction\ mixture\ (mL)}{reaction\ \ time\ (min) \times sample\ volume\ (mL)} \qquad \text{(B2)}$$

APPENDIX C

DETAILED DATA FOR GROWTH CURVE CONSTRUCTION

Table C.1: Growth profile data for mycelial dry cell weight (g/L)

Time (day)	Weight of mycelial dry cell (g/L)				Standard Deviation, ±
	1	2	3	Average	
0	0	0	0	0	0
1	0.0275	0.0300	0.0275	0.0283	0.0014
2	1.5525	1.8400	1.6275	1.6733	0.1491
3	2.3425	2.1500	2.0775	2.1900	0.1370
4	2.3675	2.3650	2.3425	2.3583	0.0138
5	2.4925	2.5800	2.4200	2.4975	0.0801
6	2.1075	2.1575	2.0675	2.1108	0.0451
7	1.8325	1.9900	2.0450	1.9558	0.1103

Table C.2: Growth profile for xylanase activity (U/mL)

Time (day)	Xylanase activity (U/mL)				Standard Deviation, ± (x 10^3)
	1	2	3	Average	
0	0	0	0	0	0
1	0.0120	0.0120	0.0120	0.0120	0
2	1.6002	1.6002	1.6002	1.6002	0
3	4.0600	4.0607	4.0600	4.0602	0
4	4.5660	4.5662	4.5657	4.5659	0.4388
5	5.3842	5.3842	5.3842	5.3842	0.2603
6	3.6079	3.6079	3.6081	3.6080	0
7	2.5405	2.5405	2.5413	2.5408	0.1386

APPENDIX D

Detailed Data for Plackett-Brurman Design with Biomass Determination

Table D.1: PB experimental design matrix for screening the media composition and culture condition for biomass determination.

Run	Variables											Y (g/mL)
	X1	X2	X3	X4	X5	X6	X7	X8	X9	X10	X11	Experimental
1	1 (5)	-1 (6)	1 (40)	-1 (100)	-1 (1)	-1 (1)	1 (3)	1 (0.7)	1 (1.0)	-1 (0.01)	1	0.2725 ± 0.1089
2	-1 (3)	-1 (6)	1 (40)	1 (200)	1 (3)	-1 (1)	1 (3)	1 (0.7)	-1 (0.5)	1 (0.05)	-1	0.8075 ± 0.2613
3	-1 (3)	-1 (6)	-1 (30)	-1 (100)	-1 (1)	-1 (1)	-1 (1)	-1 (0.3)	-1 (0.5)	-1 (0.01)	-1	1.2300 ± 0.3097
4	1 (5)	1 (8)	-1 (30)	1 (200)	1 (3)	-1 (1)	1 (3)	-1 (0.3)	-1 (0.5)	-1 (0.01)	1	0.7125 ± 0.3036
5	-1 (3)	1 (8)	1 (40)	-1 (100)	1 (3)	-1 (1)	-1 (1)	-1 (0.3)	1 (1.0)	1 (0.05)	1	1.7725 ± 0.1840

6	1 (5)	1 (8)	-1 (30)	1 (200)	-1 (1)	-1 (1)	-1 (1)	1 (0.7)	1 (1.0)	1 (0.05)	-1	2.2425 ± 0.3132
7	-1 (3)	-1 (6)	-1 (30)	1 (200)	1 (3)	1 (3)	-1 (1)	1 (0.7)	1 (1.0)	-1 (0.01)	1	0.7925 ± 0.2293
8	1 (5)	1 (8)	1 (40)	-1 (100)	1 (3)	1 (3)	-1 (1)	1 (0.7)	-1 (0.5)	-1 (0.01)	-1	0.1800 ± 0.0048
9	1 (5)	-1 (6)	1 (40)	1 (200)	-1 (1)	1 (3)	-1 (1)	-1 (0.3)	-1 (0.5)	1 (0.05)	1	0.8450 ± 0.2425
10	-1 (3)	1 (8)	1 (40)	1 (200)	-1 (1)	1 (3)	1 (3)	-1 (0.3)	1 (1.0)	-1 (0.01)	-1	2.0875 ± 0.2801
11	-1 (3)	1 (8)	-1 (30)	-1 (100)	-1 (1)	1 (3)	1 (3)	1 (0.7)	-1 (0.5)	1 (0.05)	1	1.6475 ± 0.0389
12	1 (5)	-1 (6)	-1 (30)	-1 (100)	1 (3)	1 (3)	1 (3)	-1 (0.3)	1 (1.0)	1 (0.05)	-1	1.5200 ± 0.0976

*The variables represent as X1 – Incubation time (day), X2 – pH, X3 - Temperature (ºC), X4 – Agitation rate (rpm), X5: Xylan (g/L), X6 – NH_4NO_3 (g/L), X7 – K_2HPO_4 (g/L), X8:$MgSO_4 \cdot 7H_2O$ (g/L), X9 – $CaCl_2$, (g/L) , X10 – $FeSO_4 \cdot 7H_2O$ (mg/L), X11- dummy, and Y - Weight of mycelial dry cell.

* Mean values with standard deviation (±SD) from three replicates.

Table D.2: Data for the Pareto Chart.

Source	Sum of Squares	Percent of contribution (%)	Standard error
Model	35.2340		0.2537
X2	9.3838	26.64	0.2537
X9	6.2515	17.74	0.2537
X5	5.1641	14.66	0.2537
X7	4.7889	13.59	0.2537
X1	4.7124	13.37	0.2537
X3	3.6796	10.44	0.2537
X6	1.2528	3.56	0.2537

* The variables represent as X2 – pH, X9 – $CaCl_2$, X5: Xylan, X7 – K_2HPO_4, X1 – Incubation time, X3 - Temperature, X6 – NH_4NO

APPENDIX E

Detailed Data for Central Composite Design with Biomass Determination and Xylanase activity

Table E.1: Central composite design matrix for biomass determination production

Run	pH	$CaCl_2$ (g/L)	Weight of mycelial dry cell (g/L)			
			1	2	3	Mean
1	0 (7)	0 (0.75)	0.5490	0.4100	0.4134	0.4575 ± 0.0793
2	+1 (8)	+1 (1.00)	1.2508	1.2647	1.2787	1.2647 ± 0.0140
3	+1 (8)	0 (0.75)	0.8746	0.8350	0.6587	0.7894 ± 0.1149
4	-1 (6)	0 (0.75)	0.4519	0.4679	0.3938	0.4379 ± 0.0390
5	0 (7)	0 (0.75)	0.8437	0.9146	0.9257	0.8947 ± 0.0445
6	-1 (6)	-1 (0.50)	0.2861	0.1247	0.2936	0.2348 ± 0.0954
7	0 (7)	+1 (1.00)	1.3451	1.3647	1.3846	1.3648 ± 0.0198
8	+1 (8)	-1 (0.50)	0.5516	0.5612	0.5363	0.5497 ± 0.0126
9	0 (7)	0 (0.75)	0.7469	0.7401	0.7536	0.7469 ± 0.0068
10	0 (7)	-1 (0.50)	0.4519	0.4679	0.5439	0.4879 ± 0.0492

11	0 (7)	0 (0.75)	0.9954	0.9549	0.9789	0.9764 ± 0.0204
12	0 (7)	0 (0.75)	0.7864	0.8257	0.7126	0.7749 ± 0.0574
13	-1 (6)	+1 (1.00)	1.4905	1.4769	1.502	1.4898 ± 0.0126

*Mean values with standard deviation (±SD) from three replicates.

Table E.2: Central composite design matrix for xylanase activity

Run	pH	$CaCl_2$ (g/L)	Weight of mycelial dry cell (g/L)			
			1	2	3	Mean
1	0 (7)	0 (0.75)	0.3369	0.3565	0.3467	0.3467 ± 0.0098
2	+1 (8)	+1 (1.00)	3.3674	3.3270	3.3456	3.3467 ± 0.0202
3	+1 (8)	0 (0.75)	0.8924	0.8864	0.8954	0.8914 ± 0.0046
4	-1 (6)	0 (0.75)	0.2467	0.2457	0.2476	0.2467 ± 0.0010
5	0 (7)	0 (0.75)	0.5517	0.5497	0.5477	0.5497 ± 0.0020
6	-1 (6)	-1 (0.50)	0.1530	0.1767	0.1740	0.1679 ± 0.0130
7	0 (7)	+1 (1.00)	3.1628	3.1648	3.1760	3.1679 ± 0.0071
8	+1 (8)	-1 (0.50)	0.7988	0.7846	0.8117	0.7984 ± 0.0136
9	0 (7)	0 (0.75)	0.6549	0.6457	0.6430	0.6479 ± 0.0062
10	0 (7)	-1 (0.50)	0.6824	0.6789	0.6782	0.6798 ± 0.0023

11	0 (7)	0 (0.75)	1.0680	1.0732	1.0648	1.0687 ± 0.0042
12	0 (7)	0 (0.75)	0.6801	0.6792	0.6803	0.6799 ± 0.0006
13	-1 (6)	+1 (1.00)	1.4725	1.4864	1.4449	1.4679 ± 0.0211

*Mean values with standard deviation (±SD) from three replicates.

APPENDIX F

Detailed Data for Validation Test with Biomass Determination and Xylanase Activity

Table F.1: Percentage error between predicted value and actual value for mycelial dry cell weight.

No.	Predicted mycelial dry cell weight (g/L)	Actual mycelia dry cell weight (g/L)				Percentage error (%)
		1	2	3	Mean	
1	1.1090	1.0179	1.1124	1.0045	1.0449 ± 0.0590	5.78

* Mean values with standard deviation (±SD) from three replicates

Table F.2: Percentage error between predicted value and actual value for xylanase activity

No.	Predicted xylanase activity (U/mL)	Actual xylanase activity (U/mL)				Percentage error (%)
		1	2	3	Mean	
1	1.553	1.5489	1.5395	1.5412	1.5432 ± 0.0050	0.63

* Mean values with standard deviation (±SD) from three replicates

Percentage error (%) was calculated by using the equation following:

$$\text{Percentage error (\%)} = \frac{|Predicted\ value - Actual\ value|}{Predicted\ value} \times 100\% \quad \text{--F2}$$